Dynamics of Complex Fluids at Liquid-Solid Interfaces

Von der Fakultät für Mathematik und Physik der Universität Stuttgart zur Erlangung der Würde eines Doktors der Naturwissenschaften (Dr. rer. nat.) genehmigte Abhandlung

Vorgelegt von

Laura Almenar Egea

aus Valencia (Spain)

Hauptberichter:	Prof. Dr. S. Dietrich
Mitberichter:	Prof. Dr. J. Main

Tag der Einreichung:	3. September 2010
Tag der mündlichen Prüfung:	12. November 2010

Institut für Theoretische und Angewandte Physik
Universität Stuttgart

Max-Planck-Institut für Metallforschung
Stuttgart

2010

Contents

Nomenclature

The following is a list of the most frequently occurring symbols used in this thesis. Symbols not defined here are defined at their first place of use.

$\mathcal{F}[\rho]$	total Helmholtz free energy functional
$\beta = 1/k_B T$	inverse thermal energy
$\mathbf{r}$	particle position in two dimensions
$u(\mathbf{r}, t)$	flow field velocity
$\rho(\mathbf{r}, t)$	probability density
$\mathbf{\Gamma}(\mathbf{r})$	position dependent mobility matrix
$\Phi(\mathbf{r})$	external potential with surface confinement
$\Psi(\lvert\mathbf{r}_i - \mathbf{r}_j\rvert)$	interaction potential between particles
$\eta(\mathbf{r}, t)$	stochastic force
$\boldsymbol{\nabla} = (\partial_x, \partial_y, \partial_z)$	
$P(\mathbf{r}, t)$	non-equilibrium probability density
W	half channel width
L	half channel length
W_i	half width of region in which particles can move
d_i	particle radio
R	circular cylinder radius
d	minimal distance between the center of mass of two particles
u_0	velocity at the channel center
$\mathbf{D}$	wall-particle distance dependent diffusivity
$\mathbf{J}$	total probability flow
$\mathbf{j}$	probability flow of each particle
Re	Reynolds number
Q	throughput
ρ_{eq}	equilibrium probability density
$\mathbf{R}(x_1 - x_2, y_1, y_2)$	particle position in three dimensions
$C(\mathbf{R})$	stationary non-equilibrium probability density
$\mathbf{U}(\mathbf{R})$	flow field velocity
$\mathbf{V}(\mathbf{R})$	total interaction potential
$\boldsymbol{\nabla}_R = (\partial_{x_1 - x_2}, \partial_{y_1}, \partial_{y_2})$	
R_h	hydrodynamic radius
R_g	gyration radius
Pe	Pèclet number
l	distance between two particles
L_x, L_y	lateral distance lengths
c	velocity of upper and down channel walls
ν	self-avoiding walk exponent

Chapter 1

Introduction

The discipline called soft condensed matter (or complex fluids) has experienced significant growth over the last decades, becoming an important field of research for the understanding of the physical properties of the above mentioned fluids. However, nowadays, there still remain some open problems in the soft condensed matter field.

Soft condensed matter displays many fascinating properties. The dynamics of complex fluids in non-equilibrium situations[1] are characterized by multiple length and time scales. These non-equilibrium processes are irreversible; i.e., the entropy increases in time such that one cannot come back to the initial state. The properties of such systems cannot be described by the equilibrium statistical mechanics only, but rather, the description should include the dynamics.

Nevertheless, under certain special conditions, the behavior of a large number of systems can be described by the formalism of the equilibrium statistical mechanics when they are in local equilibrium. Otherwise, the non-equilibrium systems occur more frequently than the equilibrium systems, but also, in many cases, they cannot be treated by the Boltzmann-Gibbs formalism. In the last 30 years, there have been notable efforts to characterize non-equilibrium systems.

This chapter is intended to provide a short review of the main topics related to the present work.

1.1 Complex fluids

This thesis is concentrated in a theoretical framework of soft condensed matter physics, which is the study of materials such as polymer solutions, liquid crystals,

[1]By non-equilibrium systems we refer both to systems held far from thermal equilibrium by an external driving force, and the complementary situation of systems relaxing towards thermal equilibrium.

surfactant solutions, colloidal suspensions, and fluids but also granular media, foams, and most biological matter. Soft condensed matter can also be found in the display of our laptop computer, in the food we eat, and the cells in our bodies. Soft condensed matter means everything which is dense on the one hand — in the sense that many particles interact with each other — but which can easily be deformed by external stresses, electromagnetic fields, and thermal fluctuations, on the other hand. The macroscopic physical properties of complex fluids, such as rheological, viscoelastic, wetting, etc., cannot be described by usual hydrodynamics equations.

Amongst the physical properties arising out of these structures and characterizing soft matter, are non-linear mechanical properties (e.g., shear thinning and shear bands), structural phase transitions and non-Newtonian flow properties. One characteristic of these complex fluids is the ability to self-assemble into complex organized structures. On the other hand, due to the softness of these fluids, fluctuations and disorder are important, and one needs a proper description to understand their behavior. The most important characteristic of complex fluids is the existence of interplay between mesoscopic length and time scales, which is one of the many obstacles for a theoretical understanding of complex fluids unpredictable. The mechanical response of these fluids depends usually on time.

As mentioned above, these fluids have to be described by the non-equilibrium statistical mechanics because they are composed of a large number of species. Understanding the nature of the structure and behavior of this wide class of materials has been a challenging and interesting field of investigation. Interesting problems associated with the dynamics of these fluids are the development of a theory and numerical tools and simulations for predicting the behavior of this kind of fluid in addition to the study of instabilities in the flow, both in its interior and at its interfaces. In the last decades, progress in the field of soft condensed matter physics has been achieved due to the development of novel experimental and theoretical methods and the increasing use of numerical simulations such as molecular dynamics, lattice Boltzmann, and stochastic rotation dynamics. A theoretical approximation is considering only one of the mesoscopic species constituting a complex fluid explicitly. In this approximate theory, the particles are submitted to effective interactions which take into account the direct interactions between them and the indirect interactions mediated by the particles of the other species.

And so then, in this thesis, our interest is in the dynamics of the two most representative kinds of complex fluids: colloidal suspensions and polymer solutions.

Colloidal suspensions

Colloids are well-defined mesoscopic particles[2] which are suspended in a fluid. These particles are larger than solvent particles, but still small enough to exhibit thermal motion (Brownian motion) [30]. Due to different length scales, the description of mesoscopic particles at non-equilibrium seems to be a difficult theoretical approach. Many fluids in our everyday life are suspensions; however, we hardly recognize them as such. Examples of suspensions are milk (fat globules in water), and blood [see **Fig. 1.2 b**], amongst others. Colloidal particles are larger than molecules and ordinary ions.

The colloids interact in a different way than the solvent molecules in a fluid: they have a slower dynamics and because of their size, they generate structures that easily move away from the equilibrium. The dynamics of this kind of particles differs from the dynamics of atoms because colloids diffuses in a suspension and they exhibit hydrodynamic interactions that affect other colloidal particles in their motion, while this interaction is hardly relevant for atoms. These hydrodynamic interactions are an important characteristic of this kind of particles, in particular when they are out of equilibrium. Another important characteristic of colloidal particles is their stability against sedimentation. This stability results from the action of Brownian motion. The last important characteristic is the size of the particles and the rigidity of the particles. The latter one is only important in concentrated suspensions but not in dilute suspensions.

This characteristic has already been studied in the last decades. Sedimentation of the particles was studied by Batchelor [8]. The role of hydrodynamic interactions were studied in the context of two spheres far from bounding walls [25], or of a single sphere in the presence of one wall [102], or of two walls [72] or between many spheres [134].

Polymer solutions

It is obvious that polymers solutions are a mixture of larger polymer chains and smaller solvent molecules, just as colloidal suspensions are. They are the best-known soft matter structures. The polymer can adopt different architectures; the simplest one is a linear chain. **Fig. 1.1** shows typical types of polymer chains: as a semiflexible molecule, as coil polymer, star polymer and brush polymer. Other special types of branched polymers include comb polymers, dendronized polymers, ladders, and dendrimers. As in the case of colloidal suspensions, there are more examples of

[2]Mesoscopic particle size varies from 10 nm up to a few μm.

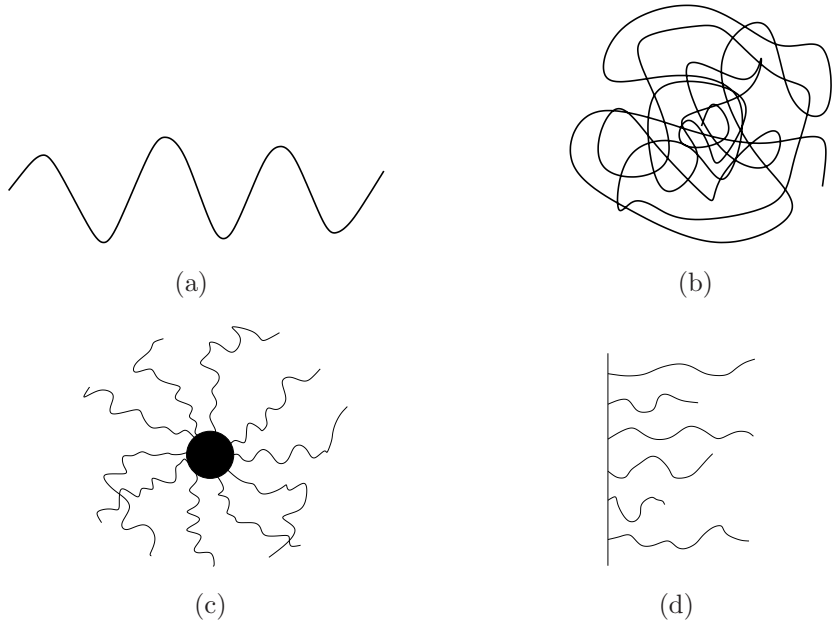

Figure 1.1: Commonly representations of polymer chains. (a) Linear chain, (b) coil polymer, (c) star polymer, and (d) brush polymer.

polymers around us in our everyday life than one may think. Biological molecules like DNA, RNA, and proteins are all polymers. Furthermore, a large fraction of objects are made with plastics which are just synthetic polymers. Now, more than ever, polymers are finding their way into new areas of application, such as light-emitting diodes, electric circuitry, computer memory, and solar cells.

The polymer solutions are, in general, highly viscous. Viscosity depends on the chemical structure of the polymer, on the interactions with the solvent, the concentrations, and on the molecular weight. Normally, a molecule of high molecular weight in a good solvent acquires an open coil conformation with a large hydrodynamic volume leading to a large viscosity of the solution. The hydrodynamic volume is the volume ocuppied by a polymer coil (the form that adopts a polymeric molecule when it is in a solution) when it is in solution. The hydrodynamic volume can change depending on how the polymer acts with the solvent and on the molecular weight of the polymer. To understand the behavior of the polymer solution, it is necessary to know the contributions of the potential energies to the free energy as well as the influence of hydrodynamic interactions on the dynamics. Besides, understanding of the polymer chains' dynamics enables us to explain and predict many properties of polymer solutions, such as diffusion coefficients, viscosity, sedimentation coefficient, and various rheological properties [32].

Polymer solutions play an important role in many commercial applications in which the polymer solutions are used to control the rheological properties as well as the stability of these commercial systems; at the same time, they are used to characterize the polymer structure through such different techniques as viscosimetry, chromatography of molecular exclusion, and light scattering, amongst other. Some examples of polymer solutions are paints, medical products, crude and processed foods.

1.2 Role of Hydrodynamic Interactions

It is well known that in the range of microscale and nanoscale, inertia plays a negligible role. In fact, the dynamics of complex fluids takes place at very low Reynolds numbers, and consequently, the viscous forces dominate over the inertial effects. Hence, complex fluids dynamics will be governed by hydrodynamic interactions (HI). But why are the hydrodynamic modes in Brownian motion important? When a particle diffuses in a viscous fluid, the above-mentioned particle disturbs the velocity field of the fluid (induces a flow field in the solvent) propagating through the solvent which will be felt by all the other particles. And thus, the motion of nearby particles will be affected, even in the absence of direct inter-particle interactions. As a result, these particles experience a force which is called hydrodynamic interaction with the original particle [46]. This hydrodynamic interaction between two particles retards the motion of the particles. However, if there is no hydrodynamic interaction, then each particle interacts with a flow field that is unaltered by the addition of other particles. Dieter Langbein [67, 68] has a couple very nice articles showing coupling effects for two spheres moving in a fluid, for various configurations of the spheres (parallel, serial, etc).

It is well known that the study of the dynamics of colloidal suspensions or polymer solutions should take into account the hydrodynamic interactions between particles, but up to now, there are still many obstacles to understanding the dynamics of complex fluids. One of these obstacles is the long-range hydrodynamic interactions between particles in dense systems. There are a number of interesting problems, where inter-particle HI may play such crucial roles such as in colloidal phase separation, aggregation, and gel formation. The role of hydrodynamic interactions in complex fluids has been studied in the past decades. Prof. Zimmerman's group [135] who studies a single polymer diffusing in a Poiseuille flow inside a channel and Prof. Winkler's group [24] who simulate a flexible polymer inside a channel. There are also studies by Nägele *et al* [97] and Zhan *et al* [133] related to the problem of hydrodynamic

interactions for a suspension of colloidal particles.

1.3 Nano- and microfluidics

When complex fluids are inside nanoscale channels where the surface-volume ratio is high, the colloids and molecules feel the walls very strongly. Consequently, depletion layers appear if repulsive forces prevent the particles from reaching the walls. This effect cannot be ignored by the particles, and therefore, it affects the motion or the transport of the particles. In other words, the behavior of the complex fluids when they are in confinement is strongly modified by the effect of the impenetrable surfaces on the particles. The behavior of these molecules is different in a microchannel, due to the greater distance between the particles and the walls in comparison with the distance between the two items in a nanochannel. The effect of the surface, roughness, Debye layer, and other factors can no longer be ignored.

In recent years, understanding of the impact of the surface on the molecules has increased. On the other hand, that phenomenon has been observed in many experiments, but up to now we do not understand it completely. There are experimental papers exploring the possibility of controlling the transport parameters of differently charged species inside nanochannels by electrokinetics [see ref. 104,125-127 of [120]]. Some of these experiments were conducted for DNA and for proteins. Adequate understanding of complex nanoscale processes and new phenomena at the nanoscale is still missing.

The transport of suspended particles within microfluidic and nanofluidic channels is of central importance to many biologically and industrially relevant processes. The dominant interest in the field is flow control, separation of molecules by size, and analysis of biological molecules. Within nanofluidics, we are able to isolate a single molecule, and that enables us to analyze the dynamics of a single particle [90].

One of the interests in the field is the necessity of finding a theory for the dynamics at molecular level to describe the "lab-on-chip" [see **Fig. 1.2 c**]. These chips have an analogy with the chips of microelectronics. The difference between them is that in lab-on-chip systems, fluids are transported through micro and nanoscale channels while in microelectronics charges are transported through nanoscale conductors. They are dominated by surface confinement and also by long-range intermolecular interactions, by thermal fluctuations, or by the size of the molecules. The efficient design of the above mentioned mechanisms needs a theory for the dynamics at the molecular level. To date, there are some first applications in the nanofluidic regime, for example, enzymatic analysis, and DNA sequencing.

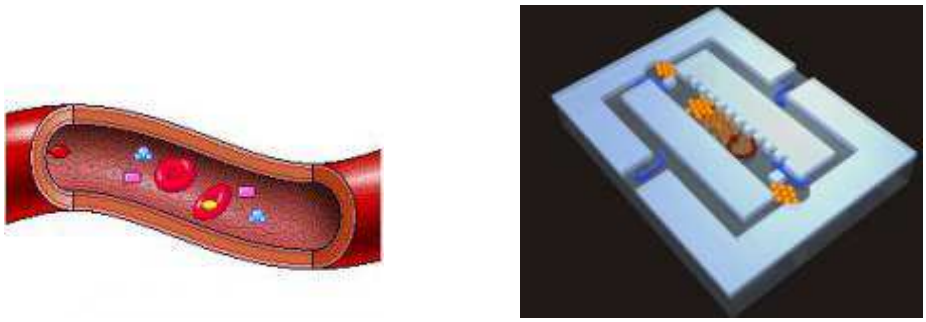

(a) (b)

Figure 1.2: a) a) Blood vessel [45]. The blood is a fluid which contains mesoscopic particles, such as polymers or colloidal particles. b) Lab-On-Chip Device [100]

Another point of interest is understanding the transport process inside the blood so as to be able to predict cancer early and the separation mechanism which can enable us to separate cancer cells from a blood sample with very few insidious cells. This difficult but fascinating field of investigation requires a narrow relation between such different fields as chemistry, physics, and biology. For this reason, development is slow. In physics, it is still necessary to develop in depth fluid mechanics in order to be capable of separating large molecules inside a fluid. One more point of interest is the understanding of diffusion transport inside the ionic channel.

Also, fluid flow on nanoscale is relevant to many other industrial processes, environmental protection, biomedical applications, and microfluidics. It has been computationally challenging: large range of scales in spatial and time domains have to be covered. Colloidal systems and Brownian motion in confined geometries have received considerable attention in the last century.

1.4 Aim of the present work

The aim of this thesis is to put the spotlight on fluid mechanics in the nano- and microscale in order to develop understanding of the separation process (the hydrodynamic chromatography mechanism) as well as the influence of both surface confinement and direct and hydrodynamic interactions on the transport of complex fluids from a theoretical point of view (by means of numerical and analytical work). When the time comes for tackling the problem of transport process both theoretically and numerically, the most difficult problems to solve come from the control of the transport process by advection and from the hydrodynamic interactions among the solid particles. The thesis is mainly focused on colloidal suspensions and polymer solutions

and studies the dynamics of suspended mesoscopic particles in small channels in the flow. This does not include the feedback of the particle motion on the solvent flow field, which was discussed in a previous work by Krüger [64, 65, 104].

In particular, this work focuses on the hydrodynamic interaction of immersed particles in a fluid and the effect of these on the fluid dynamics. The particles move due the force exerted by the fluid. We are mainly interested in the influence of hydrodynamic interactions which play a major role in the transport of suspensions through nano-channels. The separation process will be hindered by the hydrodynamic interactions. With hydrodynamic chromatography as an application in mind, we aim for a better understanding of these transport processes.

Hydrodynamic chromatography

Chromatography is a technique capable of separating and analyzing chemical species of smaller molecular mass. Hydrodynamic chromatography technique (HDC, sometimes called separation by flow) has been used experimentally for the separation of macromolecules in systems with small channels [14, 122, 124, 125]. It was conceived to reduce the time involved in measuring the size of colloids, and thus to understand better the behavior of such systems and enable to control them. In this technique, colloidal forces, tubular pinch effects, and interactions with solid walls play an important role [125]. The large molecules will not be able to approach the wall as close as smaller molecules, and thus, larger molecules will have a larger average velocity.

The basis of HDC consists of the study of a complex fluid confined between two walls (**Fig. 1.3**), where the particles are advected with a parabolic flow (Poisseuille Flow) and interact with the channel walls. This technique takes place when the suspended particles are much larger than the solvent molecules. These particles can move through the entire channel except for an excluded region near the channel walls with a thickness related to the particle radius. The small ones can move up and down. The particles tend to follow the flow streamlines. In particular, we look at the experiment conducted by Tijssen [124]. He studied the transport of polymers in a solvent through a microcapillary cylindrical tube. The idea of this experiment was to separate polymer particles (big particles) in the solvent by size. This was possible due to the fact that large particles will not be able to approach the wall as close as smaller particles because of the bigger excluded zone. Therefore, the larger particles will have a larger velocity. For this reason, it is possible to separate the bigger particle from smaller particles by hydrodynamic chromatography and to study the hydrodynamic interactions between the particle and between the particles and the wall. In his experiment, he used a microcapillary as a hydrodynamic chromatography

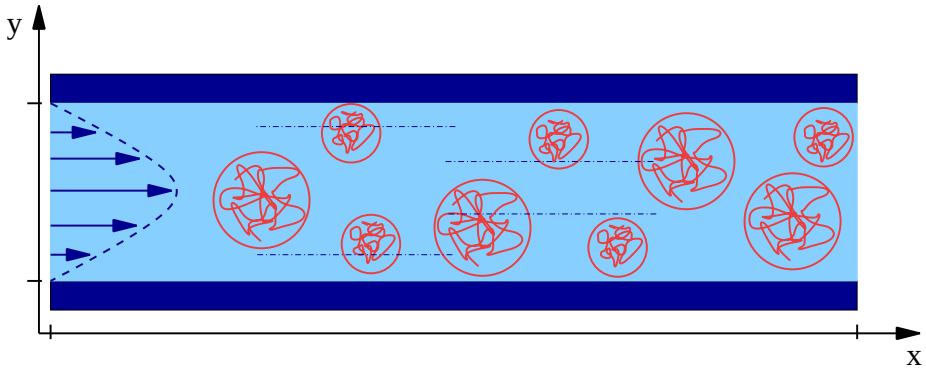

Figure 1.3: Fundaments of the hydrodynamic chromatography mechanism.

device (see **Fig. 1.4 a**).

The microcapillary is filled with the solvent, and at some moment, the polymers particles are injected. **Fig. 1.4 b** shows the separation effect of the particle and wall interaction for three different column radii. Each peak corresponds to polymers of a certain size or to the solvent. The first peak on the right corresponds to toluene particles and the other peaks correspond to the polystyrenes particles of different molecular weight. The peaks are the signal of the individual components, well separated, that are detected by the detector.

Despite many attempts in the past years to explain the hydrodynamic properties, they remain unexplained in some systems, for example, in colloidal systems. Previously experimental and theoretical studies are based on the study of the dynamics of one single spherical particle in the presence of one or two walls [35] or for two spherical particles far from bounding or near a flat plate [36]. The theory of Brownian motion is used as an example of non-equilibrium dynamics which is still close to thermal equilibrium. Since the transport of an isolated particle has been studied experimentally previously and does not introduce any new aspect, we want to take a step forward in the understanding of the transport process. Therefore, we concentrate only on the study of a two dimensional system of two particles at non-equilibrium, taking into account the hydrodynamic interactions. This simplified model can give us an idea of the behavior of the general case of many suspended particles (a concentrate solution).

This thesis is organized as follows. In the second chapter of this thesis, we will introduce the dynamical density functional theory, and we will give some reasons for the failure of this theory of the transport processes. We will also introduce the model used during all this work to understand the influence of interactions on the transport process. In chapter 3, we will discuss the influence of the direct interactions on the

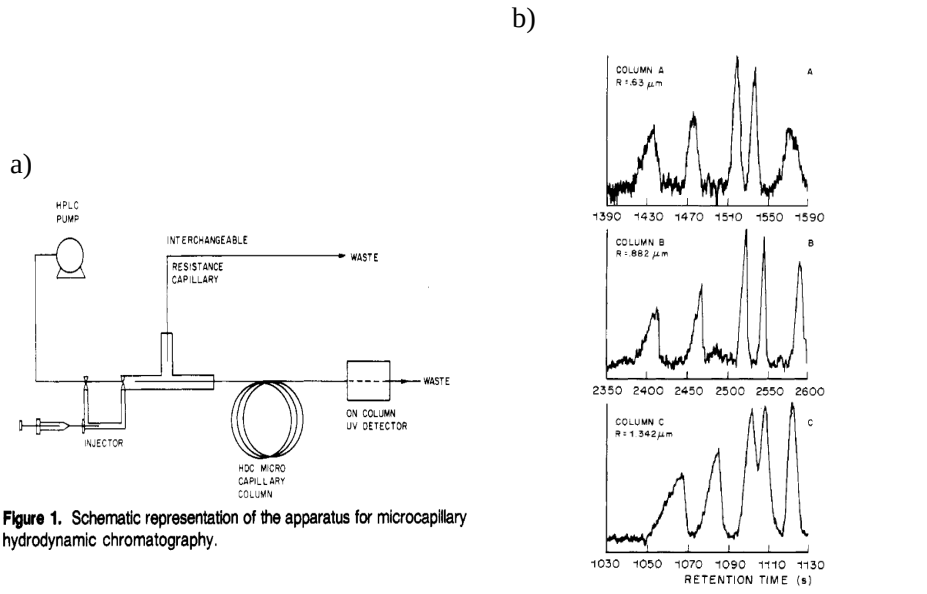

Figure 1. Schematic representation of the apparatus for microcapillary hydrodynamic chromatography.

Figure 7. Comparison of the separations effected using three different column radii (R) for a test mixture containing toluene, PS 68K, 127K, 411K, and 775K (from right to left) in concentrations of 1 mg/mL each in THF. Column dimensions are shown in Table III. The injection time for all three chromatograms was 5 s. Inlet pressures are as follows: column A, 40 bar; column B, 160 bar; and column C, 200 bar.

Figure 1.4: Microcapillary hydrodynamic chromatography device. a) The microcapillary is filled with the solvent and at some moment, the polymer particles are injected. b) Each peak corresponds to a type of polymer particles. The first peak on the right corresponds to the toluene particle and the rest correspond to the polystyrenes particles for different molecular weight. [125]

particles distribution along the channel as well as on the flow. In chapter 4 we will discuss the influence of hydrodynamic interactions. We will obtain the diffusion tensor including these interactions. In chapter 5, we will investigate a more real system, the polymer distribution along the channel, as well as the flow for each polymer in a dilute solution. In particular, we will discuss soft particles in a good solvent. Finally, in chapter 6, we conclude and give an outlook to possible future work.

The results contained in this thesis have been published or are planned to be published in the following articles:

- L. Almenar and M. Rauscher, *Dynamics of Colloids in confined Geometries*, J. Phys.: Condens. Matter, in print (2010)
- L. Almenar and M. Rauscher, *Limits of DDFT for sheared suspensions*, in preparation.

Chapter 2

Dynamics of suspended particles in confined geometries

The behavior of a confined fluid can be different in many aspects from the behavior of a free fluid, i.e., in the absence of walls. First of all, the confinement induces inhomogeneities in the density. The presence of walls, which not only changes the fluid properties of equilibrium, but also affects its behavior dependent on time, like diffusion. Consequently, the behavior of a fluid that moves through microchannels and nanochannels, as much in systems in equilibrium as in systems out of equilibrium, has become the subject of both experimental and theoretical studies and has wide relevance in many biological and industrial processes.

The transport of suspended particles in confined geometries has been studied extensively in the last century, because the transport of suspended particles within microfluidic and nanofluidic channels is of central importance to many biologically and industrially relevant processes. Up to now, there have been experimental and theoretical studies based on the study of the dynamics for one single sphere in the presence of one wall [102] or two walls [40, 72, 73]; for two spheres far from the wall [25, 89]; for a hard-sphere system between parallel hard walls [6] or anisotropic particles confined between two soft walls [110]. The properties of interest are the self-diffusion coefficient and the viscosity. Up to now the behavior of such systems at non-equilibrium is not well understood — both in bulk and in confinement — in spite of many previous investigations both experimental and theoretical. In these works, various applied theories are used to describe the system. Consequently, the question of which theory can best describe this kind of system remains controversial.

Due to the massive effort devoted to the understanding of systems at thermodynamic equilibrium, new techniques were developed in the 70's. The density functional theory (DFT) has been used in recent years to understand the static proper-

ties of many particle systems and inhomogeneous classical fluids in equilibrium. The DFT establishes that the grand canonical functional $\Omega[\rho] = \mathcal{F}[\rho] - \int \mu\rho dV$ (with the Helmholtz free energy functional $\mathcal{F}[\rho]$) is mininized by the equilibrium density distribution. This theory has been applied successfully in the case of anisotropic fluids, the structure of confined liquids, wetting, and fluid-fluid interfaces, to name a few. A good agreement between the theory and the simulation results has been demonstrated (For a review see [132]). Due to the capability of the DFT to describe such systems, there have been attempts to extend the theory to understand the dynamics of the above systems which are dependent on time, out of equilibrium. In recent years, a new theory, the dynamical density functional theory (DDFT), was proposed by Marconi and Tarazona [83, 84] to study the dynamics of colloidal particles dispersed in a molecular solvent for non equilibrium as an extension of the classical DFT to phenomena dependent on time. The foundations of the DDF theory are presented in the section 2.1. However, this theory has not been successfully used to describe some systems; the reasons for this failure are presented in the section 2.2. Also, in the section 2.3, a specific system that cannot be described by the dynamical density functional theory is presented.

2.1 Foundations of dynamical density functional theory

The basis of the DDFT is the assumption of local equilibrium, i.e., that the two particle correlations in the time-dependent systems (out of equilibrium) are well described by the correlation of equivalent systems; in which the instantaneous density field $\rho(\mathbf{r}, t)$ of the dynamical system is equal to that of the one-particle density in equilibrium $\rho_{eq}(\mathbf{r})$, i.e., $\rho^{(2)}(\mathbf{r}, \mathbf{r}', t) \approx \rho^{(2)}_{eq}(\mathbf{r}, \mathbf{r}')$. This assumption is possible in the case of overdamped Brownian particles for which the momentum degrees of freedom relax faster than the velocity, allowing the DDFT formalism to be applicable. For a system of N interacting Brownian particles advected in a solvent with velocity $\mathbf{u}(\mathbf{r}, t)$, one can write the time evolution of the ensemble averaged one body density correlation function as a functional of the density under the local equilibrium approximation [104],

$$\frac{\partial \rho(\mathbf{r}, t)}{\partial t} + \boldsymbol{\nabla} \cdot [\mathbf{u}(\mathbf{r}, t)\, \rho(\mathbf{r}, t)] = \boldsymbol{\nabla} \cdot \left[\Gamma \rho(\mathbf{r}, t)\, \boldsymbol{\nabla} \left. \frac{\delta \mathcal{F}[\rho]}{\delta \rho} \right|_{\rho(\mathbf{r},t)} \right] \tag{2.1}$$

with Γ as the mobility coefficient, and $\mu = \frac{\delta \mathcal{F}[\rho]}{\delta \rho}$ as the local chemical potential, which is not constant throughout the system (as it would be in equilibrium) and the total

Helmholtz free energy functional

$$\mathcal{F}[\rho] = k_B T \int d\mathbf{r}\rho(\mathbf{r}) \left\{ \ln \left[\rho(\mathbf{r})\lambda^3 \right] - 1 \right\} + \int dr\rho(\mathbf{r})\Phi(\mathbf{r}) + \Delta\mathcal{F}[\rho] \tag{2.2}$$

with λ as the thermal de Broglie wavelength. The Helmholtz free energy functional is the sum of three terms: the exact ideal gas entropy, the external potential contribution, and the third one includes the effects of interactions and correlations between the particles and is called excess free energy $\Delta\mathcal{F}$. Eq. (2.1) governs the transport of the particles at non-equilibrium and has the form of a continuity equation $\partial_t \rho(\mathbf{r}, t) + \boldsymbol{\nabla}\mathbf{j} = 0$. It is a generalized convection diffusion equation. The drift term describes the advection of the particles. Within this theory, the solvent flow field is independent of the particle positions and the hydrodynamic interactions among the particles are neglected. For a simple system of non interacting Brownian particles, the DDFT is exact and it reduces to a simple one-particle drift-diffusion equation. For the time being, the Helmholtz free energy functional is only known analytically for two systems — non-interacting particles and hard rods in one space dimension. In practice one can only obtain an approximation to the exact functional employing the mean field or random-phase approximation and the Rosenfeld Fundamental Measure Theory for hard spheres [113, 114]. DDFT is not applicable to situations in which hydrodynamic modes are relevant because there is no such functional available even for non-interacting particles. However, a classical version of the quantum mechanical proof of existence of DDFT by Runge and Gross [116] exists, which also includes hydrodynamic modes, see [23]. In the last few years a new version of the DDFT including hydrodynamic interactions was developed by Löwen *et al* [109] by adding two more terms corresponding to the correlations induced by the hydrodynamic interactions.

The DDFT has been applied satisfactorily for 1D hard-rod system employing the exact functional and approximated density functional [83, 84], to spinodal decomposition in colloidal fluids (which exhibits liquid-gas phase separation or more generally fluid-fluid phase separation) [5], for driving colloidal particles in polymer solutions [95], for anisotropic particles in stationary external potential [38] and with rotational dynamics [110], for a simple system of mutually non-interacting spherical Brownian particles [65], for driven systems with oscillating external potentials [104], and for mixtures [6]. All of the above works, however, have neglected the hydrodynamic interactions and an excellent agreement between the DDFT and the simulations results was found. More recently, the hydrodynamic interaction in the DDFT has been considered. It can be included by replacing the mobility Γ in Eq. (2.1) by a space dependent and symmetric mobility tensor $\boldsymbol{\Gamma}(\mathbf{r}_i)$ [108, 109] or by treating the

HI in a mean field manner [115]. The inertia effects of the particles [86,87] have also been considered. Tarazona and Marconi [86] believe that the use of the DDFT is justified when the currents are of diffusive character, while in the cases where convective terms are present, it is necessary to include extra terms which describe the transport of momentum and energy. Melchionna [82] found that the DDFT can only deal with colloidal fluids and is not apt to describe the hydrodynamic behavior of a molecular fluid.

To summarize, the DDF theory is well suited to describe mixtures of point particles with direct pairs or many body interactions and advected in a solvent. There are still open questions relating to the DDFT, such as how to apply the DDFT when fluctuations and hydrodynamic interactions play a role in the transport of suspended particles, and how to threat active particles. Up to now, there is no consensus in which functional — approximate or exact — should be used [2]. The advantages of the DDF formalism is based on a closed equation for time evolution of $\rho(\mathbf{r}, t)$.

2.2 Limits and problems of DDFT when hydrodynamics modes are considered

Despite these studies, the present work shows how the DDFT fails to describe the stationary transport properties of Brownian particles in a channel advected by a flowing solvent. In the later chapters, the above mentioned affirmation will be demonstrated, but for now we will give the arguments on which this failure is based.

The case considered in this work is a two dimensional non-equilibrium steady state[1] $\partial_t \rho(\mathbf{r}, t) = 0$, where there exists a translation invariance along the x-axis, the velocity field depends only on the y-coordinate perpendicular to the channel boundaries and it is unidirectional in the x-direction parallel to the channel boundaries. Moreover the mobility depends on the y-direction. By simmetry, the steady state of Eq. (2.1) is solved by the equilibrium solution only $\rho = \rho_{eq}$ for which $\frac{\delta \mathcal{F}[\rho]}{\delta \rho}\Big|_{\rho_{eq}} = const.$,

$$0 = \frac{\partial}{\partial y} \cdot \Gamma_{yy}(y) \left[\rho(y) \frac{\partial}{\partial y} \frac{\delta \mathcal{F}[\rho]}{\delta \rho}\Big|_{\rho(\mathbf{r},t)} \right] \tag{2.3}$$

Therefore within the DDF formalism, the convection term in Eq. (2.1) which generates the non-equilibrium is equal to zero and then the effects of the forces that move a fluid vanishes. Thus, the characteristics of the particle dynamic are not described

[1] Non-equilibrium steady states are characterized by the presence of a constant current of particles. This behavior is due to the dissipative nature of the system.

by the DDF theory, although they are present in the system. Within the DDFT for this kind of system, the density profile is not changed by the flow. It is well-known that for a non-equilibrium system, the properties of this kind of systems are not only dominated by the statics but also by the dynamics [81]. Consequently, the system is not accurately described and a new formalism for that kind of system is necessary. Therefore, hydrodynamic instability is not well described by the DDF theory.

Independent of the functional used, dynamic density functional theory fails to capture three key features of the transport of advected Brownian particles in a narrow channel: the change of the density distribution across the channel induced by the solvent, the non-linear dependency of the throughputs on the solvent flow velocity, and the fact that the throughputs have to be equal for particles which cannot pass each other. Although it will be further demonstrated throughout this work, this chapter will give a brief overview of the reasons for this failure.

As mentioned above in Section 2.1, the DDFT formalism is settled by the local equilibrium approximation, by the use of an approximate free energy functional and by not taking into account hydrodynamic interactions. The density distribution in the DDFT is considered as a grand canonical ensemble where the particles number can fluctuate keeping the chemical potential μ constant. Equilibrium density functional theory is valid in the grand canonical ensemble. Closed systems with a small number of particles, which can only be changed through the system boundaries in the absence of chemical reactions, are described by the canonical ensemble. The considered system is a closed system with a fixed number of particles, therefore one needs in the DDFT formalism new functionals governed by the canonical ensemble. This was already observed in [83, 84]; they found small discrepancies between the DDFT results compared with the Brownian dynamic results, which they attribute to the error of taking the grand canonical functional in the DDFT.

When a system is in a steady state at non-equilibrium, spatial long range correlations develop — this is a universal characteristic of non-equilibrium systems [93]. It has also been demonstrated that steady state systems at non-equilibrium tend to develop long-ranged correlations even if the correlations in the equivalent equilibrium system are short ranged [29, 117, 121]. In this context long ranged means long as compared to the characteristic microscopic length scales, usually the particle size or the range of the intermolecular interactions. Therefore, the local equilibrium approximation is not valid in non-equilibrium steady state systems.

And on the other hand the DDF formalism in Eq. (2.1) is not applicable when hydrodynamic modes are relevant for the above reason and when two or more particles move in a viscous fluid, the hydrodynamic interactions govern the dynamics of col-

loidal suspensions and the transport process depends on the advective and diffusive terms. However, it is well known that the transport of suspended particles cannot be explained without taking the hydrodynamic interactions into account [30], because the effects of the solvent dominate the behavior of two or more colloidal particles, due to their long-range nature.

Due to all these reasons explained above, we present in this thesis a simple system in which DDFT fails to describe some aspects of the transport properties but which we can treat directly and efficiently: Two Brownian particles in a 2D channel advected by a flowing solvent.

2.3 Model system

Suspended particles in confined geometries interact with other particles or with container walls in many ways. When an object moves in a fluid, forces exist between the fluid and the object that depend on the velocity. The forces between the colloidal particles are due to the large quantity of surface that exists in these systems. This surface has associated energy greater than the thermal energy k_BT, therefore the interactions between colloidal particles are very important. In a moving fluid, the pressure will be not constant in all the system and in some points there would be maxima or minima, depending on the velocity at each point of the system.

Colloidal particle dynamics is determined by the direct particle interactions, the effect of the solvent that transmits hydrodynamic forces between the suspended particles, the so-called hydrodynamic interactions through the solvent, and electrical interactions. The last one appears when the colloidal particles are charged. Many colloidal particles present a charge, but the analysis will be very complicated due to the solvent charge. However, for high enough salt concentration, the range of the screened electrostatic interactions is small as compared to the particle size. In two dimensions, hydrodynamics is ill defined: Hydrodynamic interactions do not go to zero at large distances. However, we can mimick some aspects of 3D hydrodynamic interactions, in particular the reduction of the mobility in the vicinity of channel walls in a phenomenological way even in 2D systems.

In this work we concentrate only in the basic mechanism of the influence of both direct and hydrodynamic interactions on the particle separation in channel flows. In particular, we study the dynamic behavior of the transport of suspended particles in confined geometries in two dimensions on the separation process. We assume low Reynolds number ($Re << 1$) to be consistent with nanoscale parameters, hence it is assumed that the fluid is so viscous that the effects of inertia can be neglected,

therefore the dynamics of the particles are overdamped and Brownian. With hydrodynamic chromatography as an application in mind, we aim for a better understanding of these transport processes. The separation of particles of different size diffusing through a fluid in stationary state is possible with this technique. The separation of the particles is achieved because the larger particles are confined to the channel center where the flow velocity is larger, while the small particles spend more time at the channel walls where the flow is slower. Therefore, the larger particles will travel faster through the channel, allowing us to separate the larger particles from the smaller. We assume as the length scale the scale of the suspended particles and the time scale of the order of the diffusion time scale where the effects of hydrodynamic interactions are most prominent.

The dynamics of the suspended particles can be modeled by the Langevin equation of an ensemble of N advected interacting particles in the overdamped limit:

$$\frac{\partial \mathbf{r}_i}{\partial t} = \mathbf{u}(\mathbf{r_i}) - \mathbf{\Gamma} \cdot \boldsymbol{\nabla}_i \left[\Phi_i(\mathbf{r}_i) + \sum_{j=1}^{N} \Psi(|\mathbf{r}_i - \mathbf{r}_j|) \right] + \boldsymbol{\eta}_i(\mathbf{r}_i, t) \tag{2.4}$$

with $\boldsymbol{\nabla}_i = (\partial_{x_i}, \partial_{y_i})$. Being $\mathbf{\Gamma}$ the position dependent mobility matrix, $\Phi_i(\mathbf{r}_i)$ the external potential of each particle with channel walls, $\Psi(|\mathbf{r}_i - \mathbf{r}_j|)$ the interaction potential between the particles and $\boldsymbol{\eta}_i(\mathbf{r}_i, t)$ the stochastic force. This equation describes the transport of Brownian particles in a mesoscopic way and is governed by the sum of direct and stochastic forces.

One is typically not interested in the position of all individual particles but rather in the probability of finding any particle at a certain position $\mathbf{r}$ at time t. The corresponding Fokker-Planck (FP) equation to the above Langevin Eq. (2.4) for the non-equilibrium probability density $P(\mathbf{r}_i, t)$ for finding the particles at time t at positions $\mathbf{r}_i$ [104, 112] is

$$\frac{\partial P(\mathbf{r}_i, t)}{\partial t} = -\sum_{i=1}^{N} \boldsymbol{\nabla}_i \left[\mathbf{\Gamma} \left(\frac{u(\mathbf{r}_i)}{\mathbf{\Gamma}} - \boldsymbol{\nabla}_i \Phi(\mathbf{r}_i) - \sum_{j=1}^{N} \Psi(|\mathbf{r}_i - \mathbf{r}_j|) - k_B T \boldsymbol{\nabla}_i \right) P(\mathbf{r}_i, t) \right] \tag{2.5}$$

By using the Smoluchowski equation the description of the complex fluid is reduced to the dynamics of a deterministic function of the position coordinates of the colloids.

In describing hydrodynamic interaction between Brownian particles, both translational and rotational motions are of importance, since both induce a fluid flow velocity that affects other particles in their motion. In 3D the particles may either translate or rotate. It is evident that both motions exhibit symmetry concerning the xz plane. The velocity gradient can induce the large particles feeling extremely different velocities at opposite sides. The difference of these velocities induce that

the particle rotate. Through a spherical isotropic body which exhibits the same resistance to translational motion no matter what orientation it has relative to a uniformly moving fluid, it will not rotate if suspended freely in any orientation in a uniformly fluid [47]. Reichert [105] found that longitudinal translations and the rotations about the axis do not couple to each other because of the different parities of translations and rotations. If the particles are spheres, it is possible to analyze the translational motion without considering the rotational motion. In this case, the hydrodynamic torques are equal to the total torques and equal to zero on the Brownian time scale [30]. Therefore, it is possible to describe completely the dynamics of the particles considering only the translational motion.

The evaluation of the transport of N particles in narrow channels is more complex than for two particles. Up to know, there are only computer simulations for systems of N particles [97] or experimental works for only one particle between two walls [40, 72] considering in both cases hydrodynamic interactions, but there are no analytical works due to the unavailability of a solution for the FP Eq. (2.5). Since we are looking for non-equilibrium steady state situations and analytical steady state solutions of the FP Eq. (2.5) are not available due to the interactions among the particles. In this work we concentrate on the study of a simplified toy model system of a mixture of two colloidal suspended particles of different size. The particles diffuse through a two-dimensional narrow channel of width $2W$ with the channel walls located in the planes $y = -W$ and $y = W$ as indicated in **Fig. 2.1** and length $2L$ with periodic boundary conditions in x-direction. The channel walls are planar, fixed and impermeable. The particles are at position $\mathbf{r}_1(x_1, y_1)$ and $\mathbf{r}_2(x_2, y_2)$ respectively. The distance between the particles is considered to be sufficiently close to allow the particles to interact. The particles are considered as uncharged particles. The no-slip boundary conditions are satisfied on the walls and the particles surfaces, that is, the velocity flow field would be zero for whatever surface limits the fluid motion.

The behavior of the suspended particles will be modified by the channel walls in contrast to the case without confinement and will be affected by the presence of boundary conditions. The particles will be repelled by the walls, creating a zone which the particles cannot enter — the width of this region is related to the particle radius. In our model, the width of the region in which the particles can move through the channel will be denoted by $2W_1$ and $2W_2$ respectively; and the thickness of the forbidden region for each particle near the wall is denoted by $d_1 = W - W_1$ and $d_2 = W - W_2$ respectively, see **Fig. 2.1**. The accessible volume of the small particle is limited by the large particle due to the excluded zone of the large particle. Both particles cannot overlap and the excluded zone between the particles consist of a

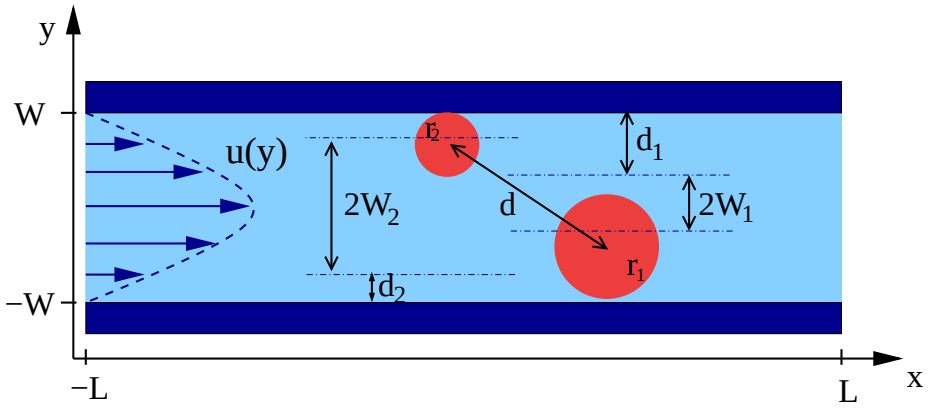

Figure 2.1: Two particles of different size at positions r_1 and r_2 in a channel of width $2W$ and length $2L$, which is assumed to be longer than any other length in the system but finite; the width of the region where each particle can move through the channel is denoted by $2W_1$ and $2W_2$; and the forbidden region for each particle near the wall is denoted by $d_1 = W - W_1$ and $d_2 = W - W_2$. Both particles cannot overlap: their minimum distance is d.

sphere of radius $d = d_1 + d_2$. The large particle is restricted to the channel center, where the solvent velocity is higher than at the channel walls.

The flow field that crosses the system is at non-equilibrium. As the colloidal particles are much larger than the solvent particles, the fluid can be considered to be continuous on the length scale of the suspended particles. The effect of the collisions between the solvent particles and the colloids is summarized in the noise term η_i in Eq. (2.4) which gives rise to the last term on the right hand side of Eq. (2.5). The drag due to the solvent flow around the particles is summarized in the mobility coefficient. The particles are advected with a parabolic Poisseuille velocity profile $u(y) = u(y)\mathbf{e}_x$ with

$$u_x(y) = u_0(W^2 - y^2)/W^2 \tag{2.6}$$

and u_0 the velocity at the channel center, see **Fig. 2.2**. The flow depends only on the y coordinate, i.e., it increases (decreases) with position in the y-direction and it is unidirectional along the x-direction. Due to the considered Poiseuille flow, the big particles should move faster than the smaller ones.

In a general case, the particles can interact both directly and hydrodynamically with the channel walls and among each other. The interaction with the channel walls is created by the surface and depends only in the y-direction. One can model the dynamics for the transport of an ensemble of two advected interacting particles through a system of two Langevin equations corresponding to each particle in the

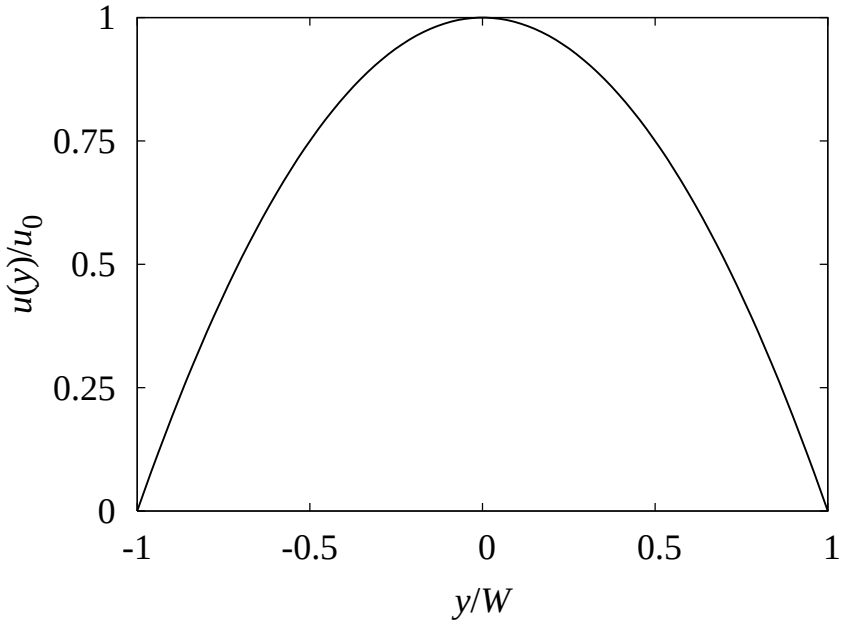

Figure 2.2: Velocity profile $u(y)$ for a fluid flow between two planes in a two dimensional channel normalized by u_0.

overdamped limit:

$$\partial_t \mathbf{r}_1 = \mathbf{u}(y_1) - \mathbf{\Gamma}_1(\mathbf{r}_1) \cdot \boldsymbol{\nabla}_1 \left[\Phi_1(y_1) + \Psi(|\mathbf{r}_1 - \mathbf{r}_2|)\right] + \boldsymbol{\eta}_1(\mathbf{r}_1, t) \tag{2.7a}$$

$$\partial_t \mathbf{r}_2 = \mathbf{u}(y_2) - \mathbf{\Gamma}_2(\mathbf{r}_2) \cdot \boldsymbol{\nabla}_2 \left[\Phi_2(y_2) + \Psi(|\mathbf{r}_1 - \mathbf{r}_2|)\right] + \boldsymbol{\eta}_2(\mathbf{r}_2, t) \tag{2.7b}$$

with $\boldsymbol{\nabla}_1 = (\partial_{x_1}, \partial_{y_1})$ and $\boldsymbol{\nabla}_2 = (\partial_{x_2}, \partial_{y_2})$, respectively. The term between the square brackets corresponds to the colloids and the noise is due to the chaotic random motion of the solvent molecules and represents the fluctuations. The stochastic force has zero mean $\langle \boldsymbol{\eta}_i(\mathbf{r}_i, t) \rangle = 0$ and the correlator is chosen such that the fluctuation dissipation theorem is observed, i.e.,

$$\langle \eta_i(\mathbf{r}_i, t)\, \eta_j(\mathbf{r}_j, t') \rangle = 2\, k_B\, T\, \Gamma_{ij}(\mathbf{r}_i)\, \delta(t - t') \delta_{if} \tag{2.8}$$

with the thermal energy $k_B\, T$.

The thermal noise in Eq. (2.4) is multiplicative in the sense that the noise $\boldsymbol{\eta}_i$ is multiplied by the fluctuating variable $\mathbf{r}_i$, see the correlator in Eq. (2.8). This usually raises the question about the calculus to be used (i.e., Stratonovich or Ito calculus). Here, we know that the calculus has to be chosen such that for $\boldsymbol{u} = 0$, the equilibrium solution of the Fokker-Planck equation corresponding to Eq. (2.4) must be

$$P_{eq}(x_1 - x_2, y_1, y_2) = \mathcal{Z}^{-1}\, e^{-\beta \left[\Phi_1(y_1) + \Phi_2(y_2) + \Psi\left(\sqrt{(x_1 - x_2)^2 + (y_1 - y_2)^2}\right)\right]} \tag{2.9}$$

with $\beta = (k_B\,T)^{-1}$ the inverse thermal energy and the canonical partition function

$$\mathcal{Z} = \int_{-W}^{W}\int_{-L}^{L} e^{-\beta\left[\Phi_1(y_1)+\Phi_2(y_2)+\Psi\left(\sqrt{(x_1-x_2)^2+(y_1-y_2)^2}\right)\right]}\,\frac{dx_1\,dx_2\,dy_1\,dy_2}{\lambda_1^2\,\lambda_2^2}. \tag{2.10}$$

$\lambda_{1/2}$ is the thermal wavelength of each particle and it is mainly used to make $\mathcal{Z}$ dimensionless. Formally, the partition sum diverges for $L \to \infty$, but all thermodynamic quantities remain well defined.

The probability $P(\mathbf{r}_i, t)$ to find particle one at position $\mathbf{r}_1$ and particle two at position $\mathbf{r}_2$ (i.e., the correlation function) for non-equilibrium is described by the Fokker-Planck equation

$$\begin{aligned}\partial_t P + \boldsymbol{\nabla}_1[\mathbf{u}(r_1)\cdot P] + \boldsymbol{\nabla}_2[\mathbf{u}(r_2)\cdot P] = \\ \boldsymbol{\Gamma}_1(r_1)\left[\boldsymbol{\nabla}_1\Phi(\mathbf{r}_1) + \boldsymbol{\nabla}_1\Psi(|\mathbf{r}_1-\mathbf{r}_2|) + k_BT\boldsymbol{\nabla}_1\right]P \\ + \boldsymbol{\Gamma}_2(r_2)\left[\boldsymbol{\nabla}_2\Phi(\mathbf{r}_2) + \boldsymbol{\nabla}_2\Psi(|\mathbf{r}_1-\mathbf{r}_2|) + k_BT\boldsymbol{\nabla}_2\right]P\end{aligned} \tag{2.11}$$

where the hydrodynamic interactions between the particles and the wall are included as a wall-particle distance dependent diffusivity $\mathbf{D}_i(y_i) = k_BT\boldsymbol{\Gamma}_i$. Particle-wall interactions are parameterized by $\Phi_1(y_1)$ and $\Phi_2(y_2)$, respectively and the direct interaction between the particles by $\Psi(|\mathbf{r}_1 - \mathbf{r}_2|)$. The probability density depends on the particle position inside the channel. Since the diffusion tensor $\mathbf{D}_i$ depends only in the y-direction, the system is translationally invariant along the x-axis and the mobility matrices and $\mathbf{D}_i$ are diagonal.

For interacting particles in the non-equilibrium case, the probability $P(\mathbf{r}_i, t)$ to find particle one at position r_1 and particle two at position r_2 (i.e., the correlation function) is a function that depends on four space variables x_1, x_2, y_1, y_2 and one temporal variable (time). In other words, the Fokker-Planck equation, also known as the Smoluchowski equation, is an equation of four spatial dimensions. This equation can only be solved analytically if the particles do not interact or for the equilibrium case, otherwise it is very difficult to solve due to the lack of possibility to separate the variables. The Fokker-Planck equation can be written as a continuity equation for the non-equilibrium probability density $\partial_t P(\mathbf{r}_i, t) + \boldsymbol{\nabla}\cdot\mathbf{J}(\mathbf{r}_i, t) = 0$ where $\mathbf{J} = \mathbf{j}_1 + \mathbf{j}_2$ is the total probability flow that is the sum of the probability flow of each particle given by

$$\mathbf{j}_{1/2}(\mathbf{r}_i, t) = \mathbf{u}(\mathbf{r}_{1/2})P - \boldsymbol{\Gamma}_{1/2}\left[\boldsymbol{\nabla}_{1/2}\Phi(\mathbf{r}_{1/2}) + \boldsymbol{\nabla}_{1/2}\Psi(|\mathbf{r}_1-\mathbf{r}_2|) + k_BT\boldsymbol{\nabla}_{1/2}\right]P \tag{2.12}$$

From now on, we are focusing on stationary, $\partial_t P = 0$, and translational invariant solutions of Eq. 2.11, i.e., solutions of the form $P(x_1 - x_2, y_1, y_2)$, from which we can

calculate the throughput of particle one and two as a function of u_0. With this ansatz in Eq. 2.11, we get with $\xi = x_1 - x_2$:

$$\begin{aligned}\partial_\xi \left[(u(y_1) - u(y_2))\ P\right] = \partial_\xi\ &\{[D_{1xx}(y_1) + D_{2xx}(y_2)]\ (\partial_\xi P + \beta\, P\, \partial_\xi \Psi)\} \\ &+ \partial_{y_1}\ \{D_{1yy}(y_1)\ [\partial_{y_1} P + \beta\, P\, \partial_{y_1}\,(\Phi_1 + \Psi)]\} \\ &+ \partial_{y_2}\ \{D_{2yy}(y_2)\ [\partial_{y_2} P + \beta\, P\, \partial_{y_2}\,(\Phi_2 + \Psi)]\} \quad (2.13)\end{aligned}$$

Fourier transformation with respect to ξ cannot be used to solve the equation since Ψ explicitly depends on ξ. The velocities $\mathbf{u}(y_1)$ and $\mathbf{u}(y_2)$ have to be parallel to the channel walls in order to allow for translationally invariant stationary solutions.

In this thesis, we are interested in the variation of the throughput of particle one and two through the channel, which are given by the integral of the particle current through a plane perpendicular to the channel. The coordinates of the other particle has to be integrated out. The correlation function $P(\xi, y_1, y_2)$ actually depends on ξ and both the advective and diffusive currents have to be taken into account, leaving

$$\begin{aligned}Q_{1/2} = \int_{-L}^{L}\iint_{W}^{W} \Big\{ & u(y_{1/2})\, P(\xi, y_1, y_2) \\ \mp\, & D_{1/2xx}(y_{1/2})\ \left[\partial_\xi P(\xi, y_1, y_2) + \beta\, P(\xi, y_1, y_2) \partial_\xi \Psi\left(\sqrt{\xi^2 + (y_1 - y_2)^2}\right)\right] \Big\}\, dy_1\, dy_2\, d\xi\end{aligned} \quad (2.14)$$

2.3.1 Non-interacting particles

Now we are looking at the case of non-interacting Brownian particles, that is, Brownian particles which do not interact with each other in any way. This is the case for very dilute dispersions. In this case, the particles are so far from each other that they are not affected by the presence of other particle. If the particles do not interact with each other, i.e., if the interaction potential Ψ is equal to zero, the solution of Eq. (2.11) factorizes and it is independent of ξ. For this kind of system, the equilibrium solution of Eq. (2.11) with $u_0 = 0$ is given by the canonical distribution function

$$P_{\mathrm{eq}}(\mathbf{r}_1, \mathbf{r}_2) = \mathcal{Z}_{1/2}^{-1}\, \exp\left\{-\beta\ [\Phi_1(\mathbf{r}_1) + \Phi_2(\mathbf{r}_2)]\right\} \quad (2.15)$$

with the partition sum $\mathcal{Z}$. P_{eq} is independent of the lateral positions x_1 and x_2. The density distribution of each particle is

$$\rho_{\mathrm{eq}_{1/2}}(\mathbf{r}_{1/2}) = \int P_{\mathrm{eq}}(\mathbf{r}_1, \mathbf{r}_2) d^3 r_{2/1} \quad (2.16)$$

which only depend on y_1 and y_2, respectively. That means that the $\rho_{\mathrm{eq}_{1/2}}$ is independent of the other particle position and of the diffusion tensor. The hydrodynamic

interactions, the dynamic forces, have no effect on the static equilibrium properties. The particle distributions give a complete but compact description of the fluid structure.

In this case, the equilibrium probability density decomposes into a product of two equilibrium probability densities of particle one and two, $\rho_{eq}(\xi, y_1, y_2) = \rho_{\mathrm{eq}_1}(y_1)\,\rho_{\mathrm{eq}_2}(y_2)$, which are defined by

$$\rho_{\mathrm{eq}_{1/2}} = \mathcal{Z}_{1/2}^{-1}\,\exp\left[-\beta\,\Phi_{1/2}\right] \tag{2.17}$$

with

$$\mathcal{Z}_{1/2} = \frac{2L}{\lambda_{1/2}^2}\int_{-W}^{W}\exp[-\beta\,\Phi_{1/2}(y)]\,dy \tag{2.18}$$

denoting the individual partition sum of particle one and two, respectively.

The flux caused by the flow is equal to the flux given by the equilibrium density, which implies that the throughput will be the integration of J in y-direction. The throughput of each type of particle is then given by

$$Q_{1/2} = \int_{-W}^{W} u(y)\,\rho_{\mathrm{eq}_{1/2}}(y)\,d_y. \tag{2.19}$$

If the particles are repelled strongly from the channel walls, the equilibrium distribution reaches its maximum at the channel center where the flow velocity is maximal. If the particles are repelled less strongly, or if they are even attracted to the channels walls, $\rho_{\mathrm{eq}_{1/2}}$ will not have a pronounced peak at the channel center and the resulting throughput will be smaller. This is the basic idea underlying hydrodynamic chromatography.

2.3.2 Interacting particles

If the particles interact with each other, then we can interpret the two particle two-dimension systems described in section 2.3 like a three dimension one particle system.

In a stationary problem, the system has translational invariance along the channel; one can reduce the system to a three dimensional static problem, i.e., to a three dimensional channel of length $2L$ which is aligned with the ξ-axis with the stationary correlation function $P(x_1 - x_2, y_1, y_2) = C(\mathbf{R})$, which is the solution of Eq. (2.13). This function is reduced to a three space variable problem and it is the probability to find a particle at position $\mathbf{R} = (\xi, y_1, y_2) = (X, Y, Z)$. That simplifies Eq. (2.13) which can be written as an advection-diffusion equation of the form

$$\boldsymbol{\nabla}_{\mathbf{R}} \cdot (\mathbf{U}(\mathbf{R})C(\mathbf{R})) = \boldsymbol{\nabla}_{\mathbf{R}} \cdot \{\mathbf{D}(Y, Z) \cdot [\boldsymbol{\nabla}_{\mathbf{R}} C(\mathbf{R}) + \beta\, C(\mathbf{R})\, \boldsymbol{\nabla}_{\mathbf{R}} V(\mathbf{R})]\} \tag{2.20}$$

with $\boldsymbol{\nabla}_{\mathbf{R}} = (\partial_X, \partial_Y, \partial_Z)$, the flow field velocity in the channel $\mathbf{U} = (U(Y,Z), 0, 0) = (u(Y) - u(Z), 0, 0)$ [see **Fig. 2.3**]; note: $\partial_{x1} = \partial_X$ and $\partial_{x2} = -\partial_X$, $V(\mathbf{R}) = \Phi_1(Y) + \Phi_2(Z) + \Psi\left[\sqrt{X^2 + (Y-Z)^2}\right]$ the interaction potential between the particles and with the channel walls. The 3×3 diagonal diffusion tensor can be writen as

$$\mathbf{D}(Y,Z) = \begin{pmatrix} D_{1xx}(Y) + D_{2xx}(Z) & 0 & 0 \\ 0 & D_{1yy}(Y) & 0 \\ 0 & 0 & D_{2yy}(Z) \end{pmatrix} \tag{2.21}$$

which contain the effects induced by the invisible solvent onto the dynamics of the observed particles, known as hydrodynamic interactions. $\mathbf{D}_i$ is the single particle diffusion coefficient [47] related to the Temperature T, the Boltzmann constant k_B and the single particle mobility $\boldsymbol{\Gamma}_i$ by the Einstein's relation, that is, $\mathbf{D}_i = k_B T \boldsymbol{\Gamma}_i$. The diffusion tend to homogenize concentrations. (Theoretically, but this cannot happen due to other factors like the solvent flow). Therefore, the flow velocity profile of Eq. (2.6) will be given in the 3D problem as

$$U_X(Y,Z) = u_0(1 - Y^2/W^2) - (1 - Z^2/W^2) \tag{2.22}$$

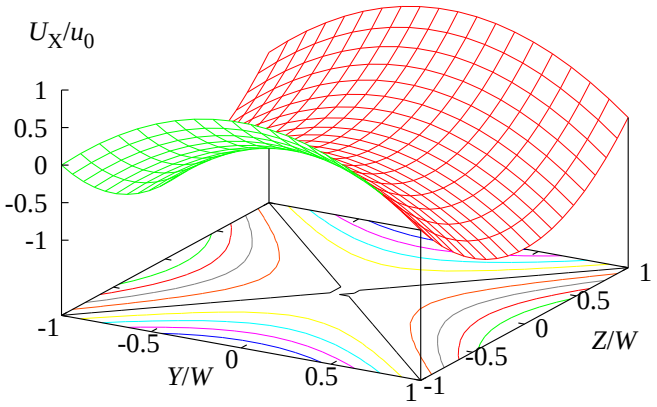

Figure 2.3: Effective flow profile $U_X(\mathbf{R})$ in the three-dimensional channel as a function of $Y = y_1$ and $Z = y_2$ for the parabolic flow profile in the two-dimensional channel shown in **Fig. 2.2**. A contour plot with 9 levels from $U_X/u_0 = -0.8$ to 0.8 is also shown on the base plane. The flow is clearly not rotation free and therefore not a potential flow.

Eq. (2.20) is a differential equation that describes how the distribution function $C(\mathbf{R})$ changes with respect to the position of the particles in the fluid.

If the forbidden zones of both particles are not equal, $d_1 \neq d_2$, the particles will explore a part of the channel with a net flow, although there is no net solvent flow through the channel ($\int_{-W}^{W} \int_{-W}^{W} U(Y, Z)\, dY\, dZ = 0$). This will break the point symmetry of the solution with respect to the origin of the coordinate system and therefore will lead to a difference of throughput of particle one and two even in the case that there is no interaction between them $\Psi = 0$, as discussed in the previous subsection.

In this section the mathematical description for a general case has been presented. Since we are interested in studying the behavior of both ideal and soft particles, in chapter 3 the idealized case of hard spheres particles will be considered and neglecting the hydrodynamic interactions. It will be seen how the DDFT fails to describe the above system. Chapter 4 will take into account the hydrodynamic interactions with the channel walls and discuss the relevance of the hydrodynamic interactions among the particles. And in Chapter 5 a more realistic case will be considered. The particles, instead of hard-spheres as soft particles in a good solvent, will be treated.

Chapter 3

Hard spheres particles

As mentioned in section 2.3, there are two types of interparticle interactions treated in this thesis that affect the transport process. The first one, the direct interaction caused by surface interactions is characterized by interaction potentials. They become significant when the particles are close to each other or close to walls usually when the clearance between particle surfaces is much smaller than the linear size of the particles [118]. The second type of interaction considered, the hydrodynamic interaction is dominant in dilute bulk systems.

Having presented the model to study the dynamics of two suspended particles diffusing through a narrow channel in the last section of the previous chapter, now we will proceed to describe the same system for the particular case of spherical particles with the first type of interaction and neglecting the second type. The hydrodynamic interactions will be treated in the next chapter 4. For hard spheres one can separate the effects due to hydrodynamic interactions from those due to direct interactions. A more realistic system will be considered in Chapter 5 in which particles will be treated like soft particles interacting via a Gaussian potential.

The aim of this chapter is to assess the influence of the direct interactions on the particle dynamics by calculating various dynamical properties and pointing to interesting features of the separation process using the described model in Section 2.3 for the case of hard spheres interaction. Additionally, we present the results which demonstrate the failure of the DDFT to describe such kind of systems.

By comparison with macroscopic channels, in micro and nanochannels the influence of the surface and the particle size on the fluid transport cannot be neglected and needs to be understood in detail [55]. The walls or the presence of other particles induce a strong resistance of the particles to the flow and modify the rheological behavior due to the interaction with the walls or between them. The presence of the walls limits the particle motion. To enhance this understanding, we study the influ-

ence of the interactions among the particles and among the walls of the confinement.

Hard spheres do not exist in nature, although to all the effects in many cases, colloidal particles behave as hard spheres. It is an academic model used both theoretically and experimentally. In general, all the particles that can form a fluid interact with a strong repulsion at short distance. This repulsion does not generate an excluded volume strictly speaking, but the energy cost of bringing the particles nearer is so high that in practice it is very improbable.

In reality, the particles may or may not be hard-spheres. Other characteristics of the particles can also influence in the interaction among the particles and between the particles and the walls. For example, if the particles are polymers [see **Fig. 3.1 b**], it is very difficult to define the radius of the particle. Depending on the situation one has to consider the gyration radius of the polymers R_g or the hydrodynamic radius R_h which is smaller than the gyration radius. The polymer can also interact with the walls and with other polymers. In the last case; their polymer chains can interlace and for confined polymers, they will be reflected by the walls due to the fact that they are not hard spheres. However, if the polymer is in a bad-solvent the chain collapses and cannot fluctuate and can behave in some effects as a sphere.

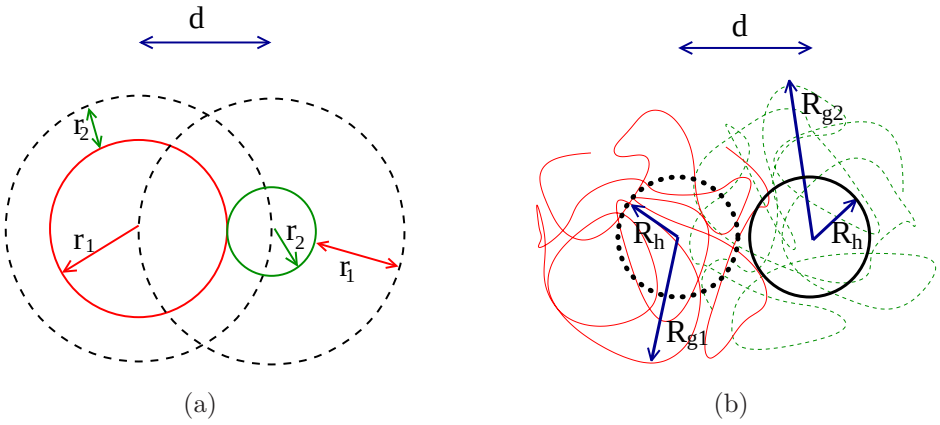

Figure 3.1: a) Two hard spheres of radius r_1 and r_2 separated a distance $d = r_1 + r_2$ between their centers. The dashed lines correspond to the excluded zone around each sphere. The center of mass of the other sphere cannot penetrate in these regions. b) Two soft particles separated a distance d being R_{gi} the gyration radius and R_h the hydrodynamic radius. The particles can overlap; the center of mass can penetrate And there is no excluded zone.

Other kinds of real particles are small colloids which can be charged positively or negatively. Their interaction depends on the charge of each particle. The particles can keep enough isolated to prevent the effects of aggregation or flocculation due to

the long-range repulsion produced by the charges. As the particles are charged, these present a surface charge density which induces the appearance of a double layer at the particle surface and consequently an increase in the exclusion diameter of the particle. Therefore, the accessible volume is affected by this change. The screening by the solvent is an important factor determining colloidal interactions. When the particles are charged, the electrostatic potential has to be taken into account in the Fokker-Planck Eq. (2.11). The effect of charged particles will show in the density distribution of each particle due to the electrostatic force that causes the particles to be repelled from each other.

Hard spheres are widely used as model particles in the statistical mechanical theory of fluids and solids. First, the hard sphere model will be described which has represented a very important role in the development of the theory of liquids and solids, and now also plays an important role in the theory of colloidal systems. The fundamental concepts of this model are the excluded and accessible volume. Hard spheres are defined simply as impenetrable spheres that cannot overlap in space [see **Fig. 3.1 a**] and have a smooth surface. Due to that, the spheres have an exclusion zone around the sphere of radius $d = r_i + r_j$, being $r_{i,j}$ the radius of each sphere. Inside the exclusion zone there cannot be any center of mass of other spheres, otherwise the particles overlap. The spheres can only approximate up to a distance greater than or equal to $d = r_i + r_j$.

They mimic the extremely strong repulsion that hard particles experience at very close distances. Hard sphere systems are studied analytically, using molecular dynamics simulations, and also experimentally with certain colloidal model systems.

Hard spheres particles interact as if they were billiar balls. They bounce off each other when they are a certain distance apart, otherwise they do not interact [44]. The interaction potential for a pair of hard spheres particles is

$$\Psi = \begin{cases} 0 & \text{for} \quad d > r_i + r_j \\ \infty & \text{for} \quad d < r_i + r_j \end{cases} \tag{3.1}$$

This functional form of Ψ says the following: when the distance is greater than d, there is *no* force acting on the particles, i.e., there is no interaction, and as soon as the distance is d, an infinitely large force arises to push the particles in another direction to avoid overlap, the particles are repelled with a intensity ∞ at contact. This is forbidden for any configuration in which there are two or more particles overlapping.

In this chapter, the simplest case will be considered: the particles behave like uncharged hard spheres and cannot overlap, and so these particles interact with a hard interaction (of exclusion). At this stage, the hydrodynamic interactions are

neglected. From here on the excluded volume will also be referred to as a forbidden zone.

3.1 Effects of confining walls on the transport of colloids

A suspension of hard spheres of radius r_i that move along a pipe behaves as if there was a layer free of particles in the immediate neighborhood of the wall; the thickness of the above mentioned layer is d_i. The walls exert on the particles a force that prevents the particle from reaching the wall. The particles will move only due to the Brownian motion, the advection due to the solvent flow field and the external forces (interactions forces) which constitute a decisive factor on the properties of the colloidal dispersions, including the rheological behavior. The particles interact directly only at contact. The interaction with the walls will be relevant when the particles are close to the walls.

Since the particles are considered as hard spheres, the interaction among the particles and between the particles and the channel walls (so-called depletion interactions) are assumed as hard core interaction Eq. (3.1). Therefore, the interactions of particle one and two in the two-dimensional channel [see **Fig. 2.1**] with the walls and with each other are of the form

$$\Phi_{1/2}(y_{1/2}) = \begin{cases} 0 & \text{for} \quad -W_{1/2} < y_{1/2} < W_{1/2} \\ \infty & \text{else} \end{cases} \tag{3.2a}$$

$$\Psi(r) = \begin{cases} 0 & \text{for} \quad r > d \\ \infty & \text{else} \end{cases} \tag{3.2b}$$

such that particle one and two can approach the channels walls only up to a distance $d_1 = W - W_1$ and $d_2 = W - W_2$ corresponding to the wall interaction radius of each particle, respectively, and they can approach each other up to a distance d (for solid particles and in the case of additive interactions $d = d_1 + d_2$).

The accessible volume for the effective 3D diffusion for both particles in the channel will be given by the interaction potential among the particles that becomes infinity for two touching particles, which corresponds in **Fig. 3.2** to the elliptical cylindrical volume with radii d and $R = d \cdot \cos 45°$ and by the direct interaction with the walls which corresponds with the vertical and horizontal confinement. In the **Fig. 3.2 a**, the outer box represents the channel walls, the inner box the surface forbidden zone due to hard particle-wall interaction and the cylinder the surface of the forbidden

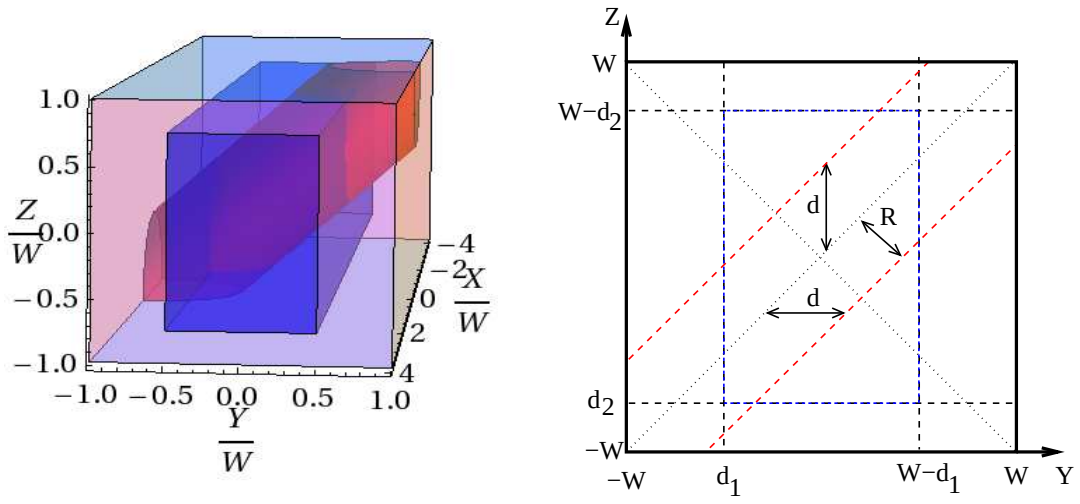

(a) (b)

Figure 3.2: a) Three-dimensional representation of the domain in which Eq. ((3.4)) is solved. The walls in Y and Z-direction of the rectangular channel (inside rectangle) are defined by the potentials Φ_1 and Φ_2, respectively, and the surface of the elliptic cylinder by the potential Ψ. For $d < d_1 + d_2$ the effective particles can bypass the cylinder. b) Front view of a).

zone due to hard particle-particle interaction. Consequently, the accessible volume will be the volume within the inner box without the volume occupied by the cylinder.

In the 3D problem, the hard core interaction with the channel walls and among the colloids leads to no-flux boundary conditions at the surface of the forbidden zone, i.e., the interaction potentials Ψ, Φ_1 and Φ_2 are replaced by a no-flux boundary condition at the cylinder surface $X^2 + (Y - Z)^2 = d^2$ and at $Y = \pm W_1$ and $Z = \pm W_2$ shown in **Fig. 3.2 a** . The no-flux boundary condition is

$$\hat{\mathbf{n}} \cdot (\mathbf{U}C(\mathbf{R}) - \mathbf{D}\boldsymbol{\nabla}_R C) = 0 \tag{3.3}$$

with the normal vector $\hat{\mathbf{n}}$ on the domain boundary and is applied on all the domain boundaries except for both channel end planes $X = \pm L$ where periodic conditions are applied. Within this domain the potentials are zero and Eq. (2.20) reduces to

$$U(\mathbf{R})\, C(\mathbf{R}) = \boldsymbol{\nabla}_{\mathbf{R}} \mathbf{D}(Y, Z) \boldsymbol{\nabla}_{\mathbf{R}} C(\mathbf{R}) \tag{3.4}$$

At this stage, the perturbation of the solvent flow field by the colloidal particles, i.e., hydrodynamic interactions are not taken into account. In principle, without hydrodynamic interactions, each particle interacts with the flow field which is unaltered by the other particles. This means that the particles do not feel each other unless

they touch each other and interact directly. For the case focused on in this chapter, neglect of HI, the particles move with a certain velocity through the channel due to the repulsion force and the periodic boundary conditions. When the hydrodynamic interactions are neglected, the diffusion coefficients $\$D_{ixx}$ and D_{iyy} in Eq. (2.21) are isotropic and homogeneous and can be replaced by D_{i0}, with which is the Stokes-Einstein diffusion coefficient [30]. For simplicity we assume the diffusion coefficients of the two particles to be equal $D_{i0} = D_{10} = D_{20} = D$.

The flux of particle one or two through the channel from Eq. (2.14) is then given by the integration over the accessible volume Ω to the effective particle (see **Fig. 3.2**) of the flow velocity by the density probability plus or minus the diffusion coefficient multiplied by the partial derivative of $C(\mathbf{R})$ with respect to X, i.e.,

$$Q_{1/2} = \iint\limits_{\Omega} \left[u(y_{1/2})\, P(\xi, y_1, y_2) \mp D_{1/2xx}(y_{1/2})\, \partial_\xi P(\xi, y_1, y_2)\right]\, dy_1\, dy_2\, d\xi. \tag{3.5}$$

and in the 3d stationary problem for hard spheres,

$$Q_1(X, Y, Z) = \int \left[U(Y)C(R) - D_1 \partial_X C(R)\right] dX dY dZ \tag{3.6a}$$

$$Q_2(X, Y, Z) = \int \left[U(Z)C(R) + D_2 \partial_X C(R)\right] dX dY dZ \tag{3.6b}$$

The differences in sign of the diffusion terms originates in $\partial_{x_{1/2}} = \pm\partial_X$.

3.1.1 Hard core interaction among particles

Let us examine the geometric form for the surface which replaces the particle-particle interaction potential Ψ. It is given by the equation $d^2 = X^2 + (Y-Z)^2$ which describes an elliptic cylinder[1] with the cylinder axis given by $(0, l, l)$, $l \in \Re$. Each cut of this cylinder by the $X-Y$-plane or by the $X-Z$-plane is a circle with radius d. Therefore cutting the cylinder with a plane normal to its axis gives an ellipse with half axes $a = 2R = 2d/\sqrt{2}$ in the $Y-Z$-plane and $b = 2d$ in the direction of the X-axis. With the cylinder axis given by $(0, l, l)$, $l \in \Re$. Each cut of this cylinder by the $X-Y$-plane or by the $X-Z$-plane is a circle with radius d. Therefore cutting the cylinder with a plane normal to its axis gives an ellipse with half axes $a = R = d/\sqrt{2}$ in the $Y-Z$-plane and $b = d$ in the direction of the X-axis. For technical reasons, we approximate the interaction potential among the particles as a circular cylinder of radius $d/\sqrt{2}$, which has the same width in the $Y-Z$-plane as the elliptical cylinder, but which is by a factor $\sqrt{2}$ thinner in X-direction.

[1] This equation has the form of a quadric equation and in particular is an elliptic cylinder equation of the form $a^{-2}x^2 + b^{-2}y^2 = 1$ with $a^{-2} = b^{-2} = d$, $x^2 = X^2$ and $y^2 = (Y-Z)^2$ as shown in **Fig. 3.2**.

Before continuing, we want to check whether the above approximation is applicable. Since for non-interacting particles we are not able to calculate the flux analytically due to the interaction, we make use of a finite element program, COMSOL [1], to solve Eq. (3.5) numerically. We compare the throughput Q_i of each particle through the channel using both parameterizations to see which is the error of using the circular cylinder approximation instead of the real interaction potential among the particles, i.e., the elliptic cylinder.

In the COMSOL software, we use the steady-state convection and diffusion mode. The geometry used is the accessible volume shown in **Fig. 3.2** for the elliptic cylinder case, and the same for the circular cylinder case but now used to consider the radius of the cylinder R. We input the starting condition $C = 1$, the flow velocity $U_X(Y, Z)$ and the diffusion tensor considering the diffusion coefficient of each particle equal $D_{iX} = D_{1X} = D_{2X} = D$ and imposing no-flux boundary conditions in all the domain except in the two channel ends where periodic conditions are imposed to allow the motion of the particles.

For the circular cylinder case, we performed calculations for a cylinder radius $R = 0.5W$ varying the sizes of both particles through the excluded zones d_i from $0W$ to $0.8W$. We solve the Eq. (3.4) for the concentration C and integrating through the entire domain we obtain the throughput for each particle according to Eq. (3.6).

In the case that the interaction potential is treated as an elliptic cylinder, we perform the following calculations. We compare the throughputs Q_1 and Q_2 for an elliptic cylinder with semiaxes $a = 0.5W$ $b = 0.7W$; and a circular cylinder of radius $a/2 = b/2 = 0.7W$.

For a smaller a the space for the particles to bypass the cylinder is bigger, but for larger values of a this space will be very small or nonexistent (case of fixed $b = 0.5W$). Therefore, we fix $a = 0.5W$ and then we vary b. The results for the elliptic cylinder is collected in **Table 3.1** together with the measured values for the circular cylinder case. One can see that the throughputs for circular and elliptic cylinders differ only in the third digit, i.e., the error is $\pm 0.002D/W^2$ or 0.3%.

Since the error on the throughputs $Q_i(d)$ of taking into account the interaction potential among the particles as a cylinder is very small, henceforth in this thesis we will work with it instead of the elliptic cylinder for technical reasons.

3.1.2 Influence of direct interactions

Why is it important to understand the interactions among the particles and among the confinement? The understanding of the influence of the direct interactions can help us to get a picture of the structural properties of the system and also of the

Table 3.1: Comparison of Q_i for both circular cylinder with radius $a/2 = b/2 = 0.7W$ and elliptic cylinder with semiaxes $a = 0.5W\, b = 0.7W$ corresponding to the interaction potential among the particles.

		$a = b = 0.7W$		$a = 0.5W\, b = 0.7W$	
W_1/W	W_2/W	$Q_1[D/W^2]$	$Q_2[D/W^2]$	$Q_1[D/W^2]$	$Q_2[D/W^2]$
0.5	1	0.952	0.943	0.951	0.943
0.5	1.5	0.961	0.826	0.959	0.826
1	1.5	0.909	0.817	0.908	0.816
1	2	0.909	0.666	0.908	0.663
2	2	0.664	0.664	0.663	0.663

dynamics of colloidal suspensions. The colloidal particles are subjected to forces both of attraction and of repulsion; these forces are due to the confinement and the large quantity of surface that exist in this kind of system. The importance of these forces is related to the particle size and to the separation of the particles to the confinement.

To assess the influence on the motion of the particles size on rheological properties, we determine the fluxes of the two particles through the channel by solving the effective 3D problem. The effective 3D diffusion problem can be solved analytically in the absence of flow ($u_0 = 0$, the equilibrium case) or for non-interacting systems ($R = 0W$ with $R = d \cdot \cos 45°$ being the cylinder radius). Analytically for non-interacting particles ($\psi = 0$), the concentration $C(\mathbf{R})$ is equal to $C(\mathbf{R}) = 1/(16W_1W_2L^2) = const$ for $|y_{1/2}| < W_{1/2}$ and to zero else. Eq. (3.6) reduces only to the first term of the integral and then the fluxes become:

$$Q_{1/2} = \frac{u_0}{2L}\left[1 - \frac{1}{3}\left(\frac{W_{1/2}}{W}\right)^2\right] \tag{3.7}$$

The smaller $W_{1/2}$ the larger is the flux $Q_{1/2}$.

However for interacting particles, we are not able to calculate the flux analytically due to the interaction; therefore we make use of COMSOL to solve Eq. (3.5) numerically for the concentration C. The geometry used is only the accessible volume shown in **Fig. 3.2** using the interaction potential among the particles as circular cylinder of radius R as in section 3.1.1. The distance d between both center of mass is related with the cylinder radius of the interaction potential ψ as $d = R/\cos 45° = R\sqrt{2}$. We allow d_i and d for vary independently. We performed simulations for a cylinder

radius $R = 0.5W$, i.e., $d = \sqrt{2}/2W$ varying the sizes of both particles through the excluded zones d_i from $0W$ to $0.8W$.

In the symmetric case $W_1 = W_2\,(d_1 = d_2)$, the solution $C(X, Y, Z)$ of Eq. (3.4) is point symmetric with respect to the origin **Fig. 3.3 a**, but for $W_1 < W_2\,(d_1 > d_2)$ **Fig. 3.3 b**, the solution is asymmetric with C larger at the left hand side of the cylinder ($X < 0$) than at the right hand side of the cylinder ($X > 0$).

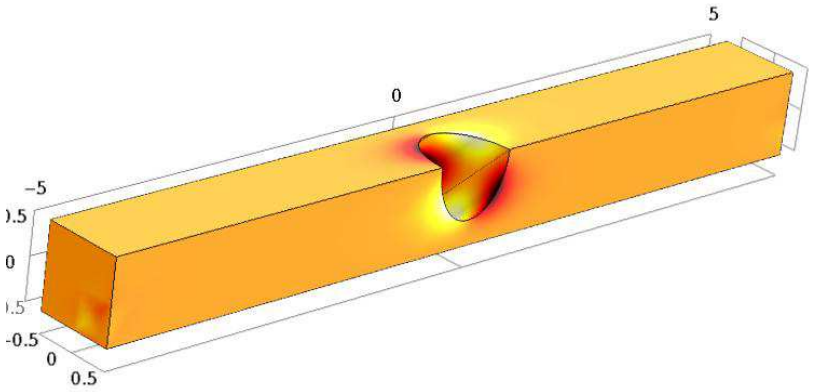

(a)

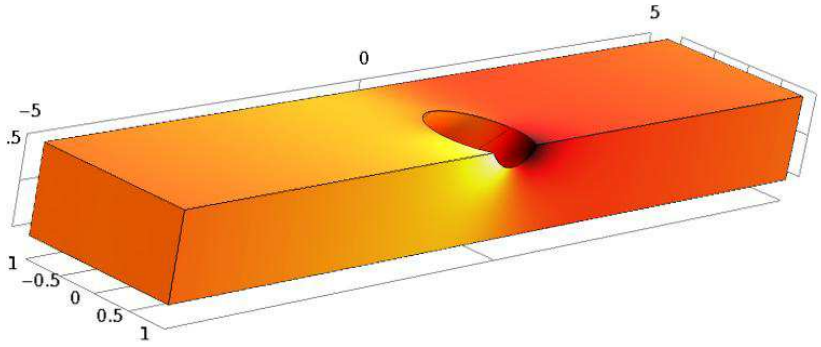

(b)

Figure 3.3: Stationary solution C(X,Y,Z) of Eq. (3.4) for $Pe = \frac{u_0 W}{D} = 1$ and $L = 5W$ for two cases. a) Symmetric case $W_1 = W_2 = 0.5W\,(d_1 = d_2)$. The color scale encode the value of C ranging from a minimum value (dark red) to a maximum value (bright yellow); b) Particle of different size $W_1 < W_2\,(d_1 > d_2)$ with $W_1 = 0.5W$ and $W_2 = W$ The color scale encode the value of C ranging from a minimum value (dark red) to a maximum value (bright yellow).

Fig. 3.4 shows the absolute flux for $d = \sqrt{2}/2W$ $(R = 0.5W)$ for different thickness of the forbidden zone d_1 and d_2 from $0W$ to $0.8W$, i.e., for different particles size. The values of $Q_i(d)$ are obtained intergrating through the entire domain for each

particles according to Eq. (3.6) and they are normalized by the value for the non-interacting case $Q_{1/2}$ in Eq. (3.7). One can see from **Fig. 3.4** that for $d_1 < d_2$, the

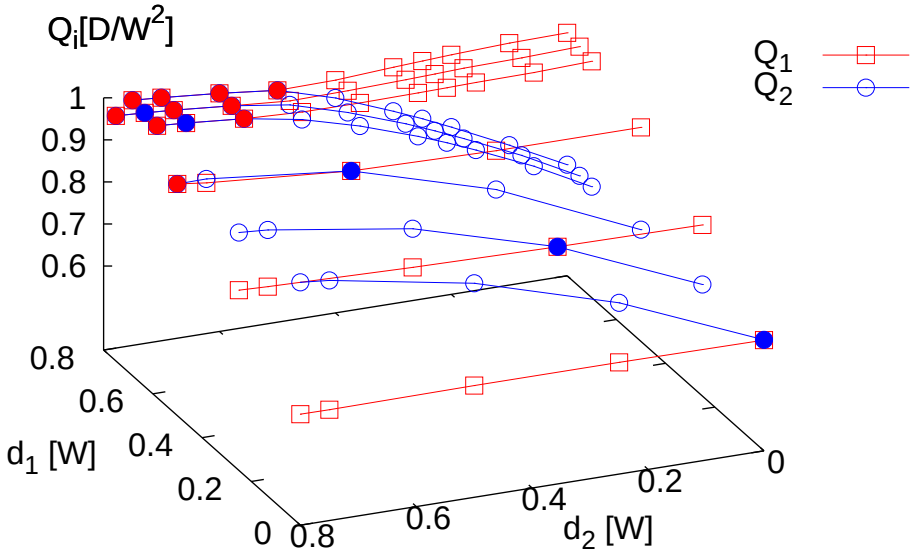

Figure 3.4: Absolute flux in 3D for both particles for a cylinder radius $R = 0.5$ ($d = R/\cos 45°$) for different thickness of the forbidden zone d_1 and d_2. • Both particles travel together. The behavior is symmetric for $d_1 = d_2$. • The particles cannot pass $d_1 + d_2 + d > W$.

flux of the first particle Q_1 increases with d_1 in contrast to the flux of the second particle Q_2 that decreases. And for $d_1 > d_2$, the flux of the first particle Q_1 decreases in contrast to the flux of the second particle Q_2 that increases as expected. In the case that both particles have equal size $d_1 = d_2$, then both fluxes are equal $Q_1 = Q_2$ and increase when the size of the forbidden zones d_i increases, i.e., when the size of the particles increases. Therefore, the two particles travel together. If the particles cannot pass each other because they are to big, they have equal flux as expected. This is due to the periodic boundary conditions.

To see the influence of the interactions on the throughput, we also compare the flux for two different cases of the separation distance $d = \sqrt{2}/2W$ ($R = 0.5W$) and $d = \sqrt{2}W$ ($R = W$), but now we fix the size of one particle $d_1 = 0.25W$ ($W_1 = 0.75W$) and we vary the size of the second particle. The results are shown in **Fig. 3.5**. We notice that the throughput of the larger particle is increased and of the smaller particles is reduced when the interaction between the particles is considered. We

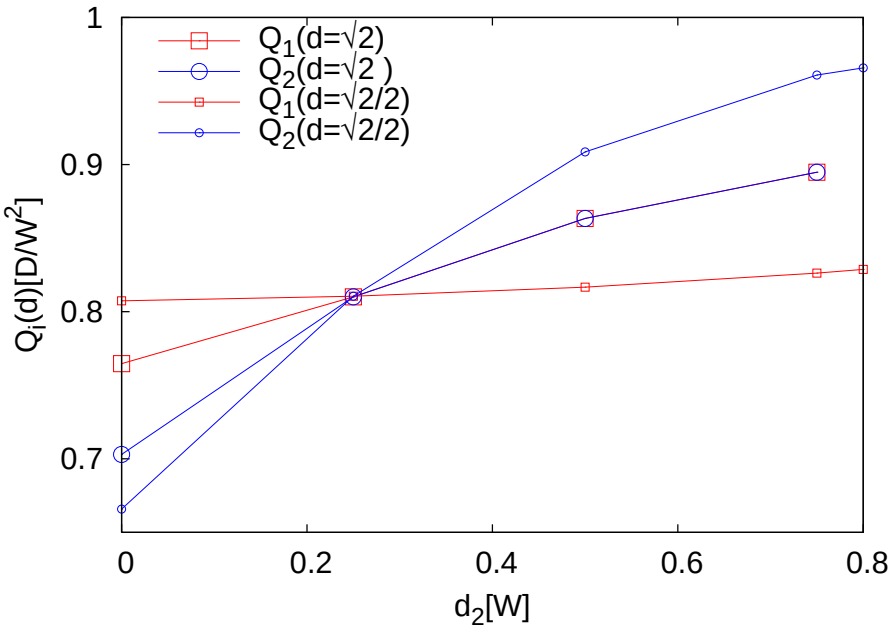

Figure 3.5: Comparison of the relative flux for both cylinder radius $R = 0.5W$ and $R = W$ ($d = R/\cos 45°$) for a fixed $d_1 = 0.25W$ and variable d_2.

observe that the fluxes become more similar for increasing R and equal in the limit that the particles cannot pass each other, which is the case for $d = \sqrt{2}W$ ($R = W$) and $d_2 > 0.34W$.

3.1.3 Distribution of particles

The interactions between the particles also affects the particle distribution across the channel. For an N particle system, it is well known that the small particles can nestle between the interstices of the large particles. The size relation between the small and large particles is also important. Consequently the interactions are an important issue in the transport of colloidal particles.

To understand the hydrodynamic chromatography method, we need to know how the particles are distributed across the channel, i.e., we have to look at the fluid density for each particle. If one particle is close to one wall and the other particle is close to the other wall, they have more space to move horizontally without colliding than if they are both at the center. Therefore we expect the density to increase near the walls.

The density profiles are defined according to Eq. (2.16) for the 3D problem as

follows:

$$\rho_1(Z) = \int C(X,Y,Z)\, dX\, dY \tag{3.8a}$$

$$\rho_2(Y) = \int C(X,Y,Z)\, dX\, dZ \tag{3.8b}$$

In equilibrium, $u_0 = 0$, the density profiles $\rho_{eq_{1/2}}$ can be calculated analytically using geometric considerations. Apart from a normalizing prefactor, $\rho_{eq_1}(y_1)$ and $\rho_{eq_2}(y_2)$ are given by the area of the cut of the accessible volume in **Fig. 3.2 b** by the plane $Y = y_1$ and $Z = y_2$, respectively. This area is given by the area of a rectangle of length L and width W_1 and W_2, respectively, minus the intersection of the rectangle and a circle of radius d centered at $Z = y_1$ and $Y = y_2$, respectively. In order to calculate the area of the cut, we calculate the area of the part of the circle of radius d outside of the rectangle (the area of a circular segment) with width $W_i = W - d_{1/2}$

$$A(Y, W_i, d) = \begin{cases} a_p(Y, W_i, d) & \text{for } |W - i - y| < d; \\ \pi d^2 & \text{for } y > W_i + d; \\ 0 & \text{for } y < W_i - d. \end{cases} \tag{3.9}$$

with

$$a_p(Y, W_i, d) = \cos^{-1}\left[\frac{W_i - Y}{d}\right] d^2 - \sin\left(\cos^{-1}\left[\frac{W_i - Y}{d}\right]\right)(W_i - Y)d \tag{3.10}$$

Therefore, the density profile $\rho_{eq}(Y, W_i, d, L)$ will be given by the total area of a rectangle ($W_i L$) minus the area of the circle of radius d, i.e., $d^2\pi$, minus the area of the circular segment above the rectangle which is $A(Y, W_i, d)$ minus the area of the circular segment below the rectangle, i.e., $A(-Y, W_i, d)$:

$$\rho_{eq}(Y, W_i, d, L) = 4W_i L - \frac{d^2\pi - [A(Y, W_i, d) + A(-Y, W_i, d)]}{\sqrt{2}} \tag{3.11}$$

For non-interacting particles ($\Phi = 0$), the expression in Eq.(2.17) reduces to a constant density $\rho_{\mathrm{eq}_{1/2}} = 1/(4W_{1/2}L)$.

Within the framework of (dynamic or equilibrium) density functional theory the equilibrium density distributions for each particle are given by the stationary points of the grand canonical functional

$$\Omega[\rho_1, \rho_2] = \mathcal{F}[\rho_1, \rho_2] - \int \left[\mu_1\, \rho_1(\mathbf{r}) + \mu_2\, \rho_2(\mathbf{r})\right]\, d^2r, \tag{3.12}$$

with the chemical potentials $\mu_{1/2}$ of particle type 1 and 2. These are chosen such that ρ_1 and ρ_2 are normalized to one. The corresponding Euler-Lagrange equations are

$\delta\mathcal{F}/\delta\rho_\ell = \mu_\ell$. As a consequence, the values obtained for the densities depend on the particular choice of the functional $\mathcal{F}$. Simple functionals which are quadratic in $\rho_{1/2}$ (i.e., the random phase approximation) do not yield the exact density distributions in Eq. (3.11).

In this case, we study the density profiles for each particle through the channel again using COMSOL. The density is normalized such that there is one particle of each type in the system. On increasing the flow, the parabolic form of the Poiseuille flow will increase, consequently affecting the particles' velocity as well as their distribution in the channel.

We solve Eq.(3.4) numerically using COMSOL as described above. We evaluate the density distribution profiles of particle 1 and 2 averaging along the X direction and the Y or Z direction of the variable C defined on some 3-dimensional domain in the yz-plane by calculating the integrals in Eq. (3.8), respectively. The data was later normalized and directly compared with the analytical equilibrium results. The analysis was realized for a set of parameters for which the particles can still pass each other and for which the particles cannot pass each other and for flow velocities u_0 up to $50D/W$ corresponding to Peclet numbers $Pe = u_0W/D$ up to 50. For $Pe < 1$ it is expected that the Brownian motion dominates the motion of the particles, i.e., the right hand side of Eq. (3.4) dominates. For bigger Pe the motion will be dominated by the advection, i.e., the left hand side of Eq. (3.4) dominates. In other words, the Peclet number indicates the amount of diffusion; for low Pe numbers, the diffusion is faster than the convection. For higher values, the diffusion is slower, i.e., their relative motion is therefore reduced.

The three different considered cases are: a) one big particle $W_1 = 0.25W$ with a small particle $W_2 = 0.5W$ for a channel length $L = W$ and a distance of both center of mass $d = 0.7W$ (particles can pass each other); b) for a symmetric case with two equal and small particles $W_1 = W_2 = W$, a channel length of $L = 5W$, and the same d as in the first case; and c) one big particle $W_1 = 0.25W$ and one small particle $W_2 = W$ with the same channel length as case b) but with $d = 1.4W$ which corresponds to the case that the particles cannot pass each other.

The behavior of $\rho_i(y)$ inside the channel are shown in **Fig. 3.6** for flow velocities u_0 up to $50D/W$ corresponding to Peclet numbers $Pe = u_0W/D$ up to 50. It is observed that the flux also changes the distribution of the particles across the channel. In **Fig. 3.6 a**, one observes that in equilibrium the smaller particle is more likely to be found near the channel wall and the big particle is almost homogeneously distributed across the channel center. In this case, the numerical data agrees with the analytical prediction. For a flowing solvent, we observe that the big particle moves even further

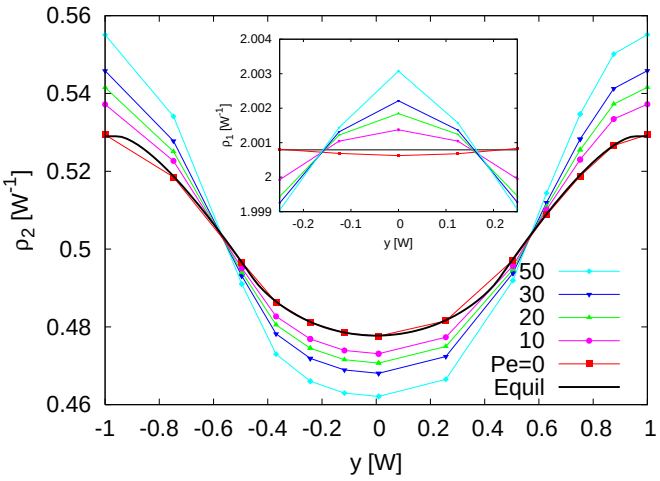

(a)

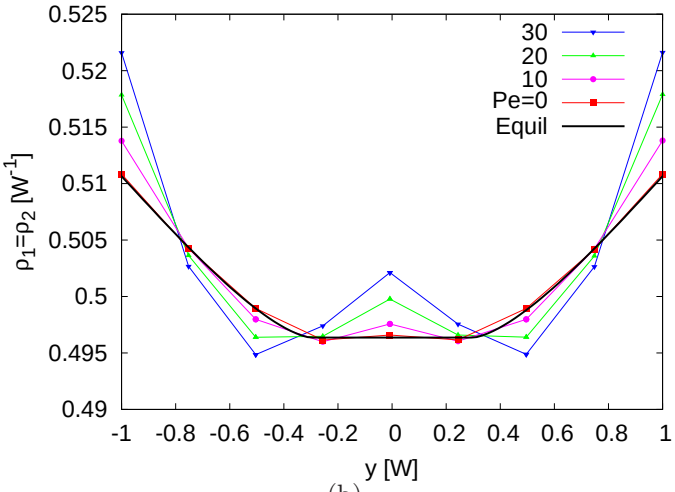

(b)

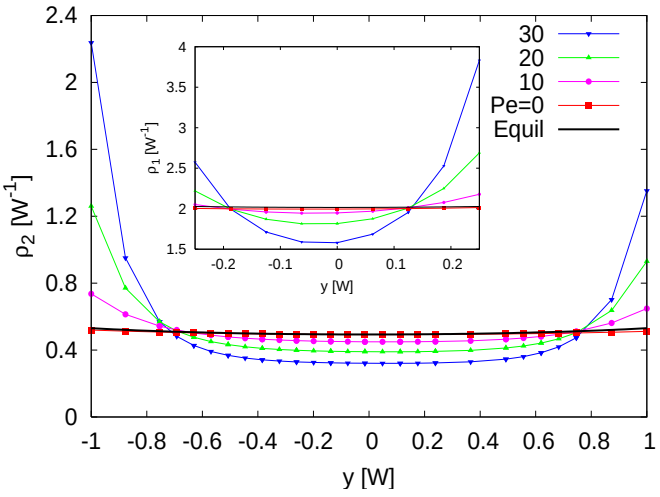

(c)

Figure 3.6: Normalized density profile for a) $W_1 = 0.25W$, $W_2 = W$, $d = 0.7W$ and $L = W$. The small particles are pushed towards the wall. b) $W_1 = W_2 = W$, $d = 0.7W$ and $L = 5W$. The particles will move at the center of the channel or near to the walls. c) $W_1 = 0.25W$, $W_2 = W$, $d = 1.4W$ and $L = 5W$.

towards the center of the channel and the small particle is pushed towards the wall (where the flow velocity is smaller than in the center). A stronger effect is observed for increasing flow velocity. We found a good agreement between our results and the basic picture of the mechanism underlying the hydrodynamic chromatography technique which is that larger particles move faster than smaller ones because large particles are more strongly confined to the center of the channel where the flow velocity is bigger.

For the symmetric case, $d_1 = d_2$, the influence of the flow on the particle distribution is much weaker. There one observes a tendency of the density to form two symmetrical regions of reduced density at both sides of the channel center due to the presence of the channel walls, as it is appreciated in the **Fig. 3.6 b**. The presence of the walls makes the flow tend to move the particles towards the center and the walls, resulting in a W-shaped distribution. A good agreement between the numerical data and the analytical prediction was also found for the equilibrium case.

If the particles cannot pass each other, see **Fig. 3.6 c**, an almost uniform distribution is observed in the regions far from the walls and the one-body density ρ_i increases at the channel walls. Both particles are pushed towards the wall by the flow, in contrast to the case when they can pass, where the big ones go to the channel center.

It is expected that besides increasing the flow, an increase of the separation of the particles inside the channel should take place. Therefore the next step was to analyze the throughput of each particle Q_i as a function of the flow u_0 for the same three cases, i.e., as a function of the Peclet number. We realize the same procedure as in section 3.1.2. The throughput of each particle Q_i is normalized by the solvent flow velocity u_0. The behavior of the throughput is shown in **Fig. 3.7**. We have represented Q_i/Pe as a function of Pe.

The results show an enhancement of the separation with flux. Without interaction, the flux is proportional to u_0, i.e., to the Peclet number. With interaction the flux increases more than linearly for the larger particles and less than linearly for the smaller particles as shown in **Fig. 3.7 a**. The variation of flux (variation between Q_1 and Q_2) increase with the increase of the flow velocity u_0. The bigger particles move towards the center of the channel where the flow is stronger while the smaller ones are pushed towards the wall where the flow is weaker. For the symmetric case, the flux for both particles is equal and for increasing u_0 and it increases almost linearly with u_0 **Fig. 3.7 b**. When the particles cannot pass each other **Fig. 3.7 c**, both particles have to have equal flux but it increases less than linearly with u_0. This is a consequence of both particles being pushed towards the wall, where the flow velocity

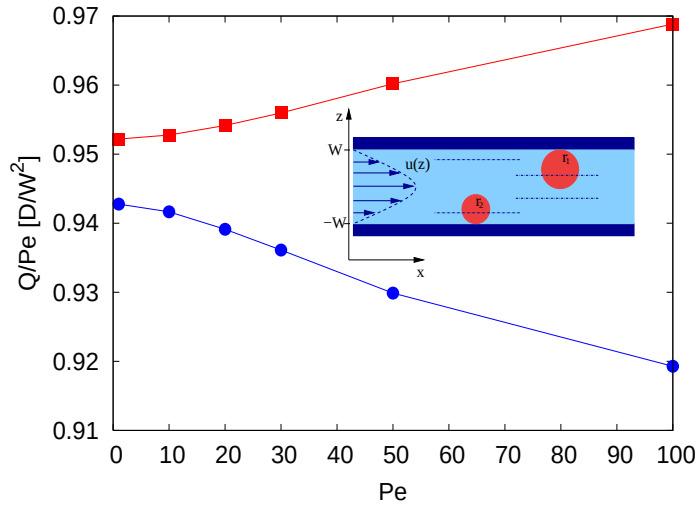

(a)

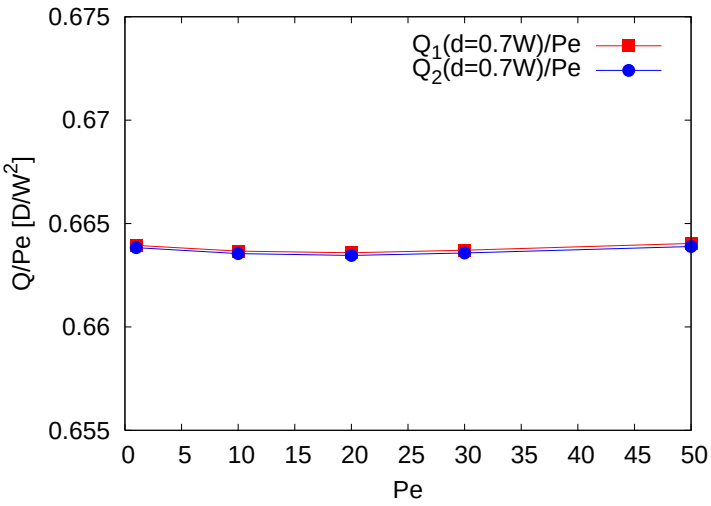

(b)

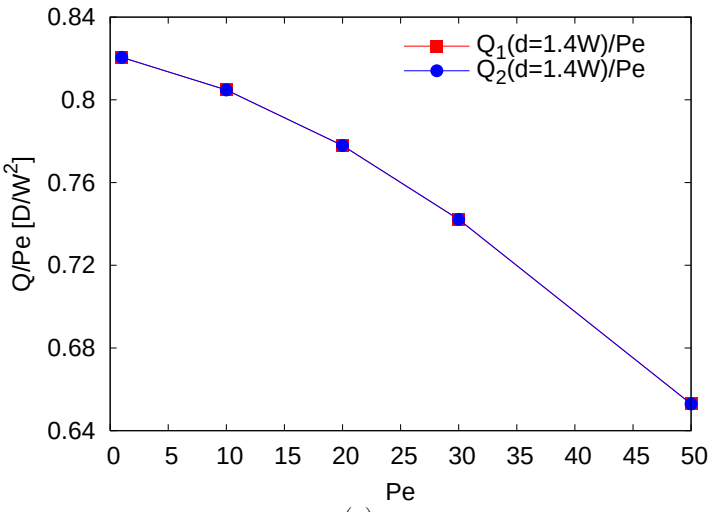

(c)

Figure 3.7: The throughput of each particle Q_i normalized to the solvent flow velocity as a function of the Pe number for: a) $W_1 = 0.25W$, $W_2 = 0.5W$, $d = 0.7$ and $L = 5W$ b) $W_1 = W_2 = W$, $d = 0.7$ and $L = 5W$ c) $W_1 = 0.25W$, $W_2 = W$, $d = 1.4$ and $L = 5W$

is smaller than at the channel center. The smaller particles are accelerated due to the fact that they travel together with the large particles and consequently, the large particles are decelerated for the same reason.

Let us now compare our model results with the dynamic density functional theory. As mentioned in section 2.2, since the velocity field depends only on the y-coordinate and is unidirectional in the x-direction the steady state solution of Eq. (2.1) is given by the equilibrium solution (i.e., the minimum of $\Omega[\rho_1, \rho_2]$ in Eq. (3.12)), which by symmetry only depends on y: the left hand side of Eq. (2.1) is equal to zero and the right hand side is zero for $\rho_{1/2} = \rho_{\mathrm{eq}_{1/2}}$. Therefore throughput through the channel is only generated by advection:

$$Q_{1/2}^{DDFT} = \int \rho_{\mathrm{eq}_{1/2}}(y)\, u_x(y)\, dx\, dy. \tag{3.13}$$

Within the framework of DDFT, the density distribution in the channel is independent of the solvent flow and the throughput is strictly linear in the flow velocity. In addition, the throughputs are not necessarily equal for particles that cannot pass each other.

3.2 Conclusions

In order to assess the effect of the direct interaction on the transport of suspended particles we have considered in Section 3.1.2 the particles in a simplistic model as hard spheres and hence the direct interactions among the particles and walls as a hard-sphere repulsion. This allows us to calculate out the throughputs and density distributions of each particle as a function of the particle size and flow velocity.

We have observed that the distribution of the particles through the channel changes as a function of the flow velocity u_0 and also depends on the size of the considered particles as expected. While at equilibrium the big particle is homogeneously distributed across the channel center, the small one is concentrated at the channel walls. When the solvent flow is switched on, it was observed how the larger particles push the smaller ones to the channel walls while remaining at the channel center. This effect is stronger as the solvent flow increases. This change on the density distribution across the channel induced by the solvent flow is not reproduced by the DDFT formalism. Why can DDFT not describe the distribution in the channel? Because the equilibrium assumption for two-point correlations $\rho^{(2)} = \rho_{eq}^{(2)}$ implies $\rho = \rho_{eq}$. Maybe this can be overcome by truncating the BGY-hierarchy at higher orders in the DDFT or by factorizing higher correlations functions.

With regards to the throughputs of each particle, for the case that the particles can pass each other we observed as the flux for the first particle increases the flux of the second one decreases and the variation of the flux increases with the particle size. For the last two considered cases — the symmetric and particles cannot pass each other cases — we observed that the fluxes of both particles are equal. The last result also can not be obtained with the DDF theory, because in this theory it is not possible to input that the particles cannot pass each other. That the throughputs of particles which cannot pass are not equal in DDFT might be related to the grand canonical character of the theory: particles can swith places by moving into a reservoir and back into the channel even if they cannot pass each other. But the main reason for the failure of the DDF theory is the equilibrium approximation for the correlation functions. The flow breaks the mirror symmetry of the system with respect to $x \to -x$ which is not reflected in the equilibrium correlation function used in the DDFT: the equilibrium correlation function is mirror symmetric. Marconi and Tarazona [83,84] put forward the discrepancies between their results with DDFT and Langevin simulations due to the interpretation of the density distribution in the grand-canonical ensemble in the DDFT and the interpretation of it in the canonical ensemble in the Langevin simulations.

In conclusion, we have used the hard sphere model in order to study the ideal case of suspended particles, which further allows for studying the role of the direct interactions.

Chapter 4

How hydrodynamic interactions influences colloidal particles' dynamics

In the previous chapter, we discussed the influence of direct interactions on the transport of colloidal particles ignoring hydrodynamic interactions (HI). Hydrodynamic interactions have to be taken into account — although up to now there is no agreement between the experimenters and theorists about the relevance of hydrodynamic interactions. In the present chapter, the effect of the second sphere and the effect of the walls in an bounded fluid — i.e., the hydrodynamic effect — will be discussed, and we will learn how the hydrodynamic interactions can influence the transport of colloidal particles. Upon considering the hydrodynamics interactions, the disturbance to the flow caused by the interaction with the other particles is taken into account.

In dilute systems, the hydrodynamic interaction has more influence on the particle motion, on the motion of the neighboring particles in particular, than the direct interaction. In addition to the hydrodynamic interaction between two particles, the interaction between three and more particles should be also considered for N-particles systems. The understanding of the resistance to motion felt by a sphere in a fluid in the presence of both a second sphere and two parallel walls can help us to understand the behavior of many particles systems.

The hydrodynamic interactions are capable of transferring local effects in a point of the fluid to very distant regions. Each particle in its motion creates a flow field in the solvent which will be felt by the other particles. The motion of one particle is affected by the motion of neighboring particles and by surfaces. As a result, each particle experiences a force which is related to hydrodynamics. The particles experience hydrodynamic interactions with each other and with the walls of the container. For

large separations, hydrodynamic interactions are the only interactions between suspended particles (electrostatic interactions are usually screened by the solvent). For very small distances, direct interactions should dominate. Hydrodynamic coupling is only possible if the particles are well-separated and move slowly through a viscous fluid [46]. Due to the hydrodynamic interactions and the confinement of the colloidal particles, the quantitative and qualitative description of the particle dynamics is a very complicated many-body problem. There are four factors that can influence HI: the distance between the walls and the particles, Reynolds number Re, surface shape and wall curvature. Calculating HI is a challenge in particular in confined systems where closed analytic forms are not available. In this thesis, we consider planar walls and low Reynolds number ($Re << 1$); therefore, the only factors that can influence the particle transport are the first two factors.

In Section 4.1 will be discussed the expected effect of the full hydrodynamic interactions and how they can be incorporated in the transport process. To assess the influence of the hydrodynamic interactions on the velocity of the particles and the particle distributions inside the channel, it is possible to study separately the particle-particle HI and the particle-wall HI. The influence of hydrodynamic interaction among the particles will be discussed in Section 4.2 and we will show that they affect the transport properties only weakly and therefore can be neglected. In Section 4.3, we will include the influence of HI between the particles and the walls as a diffusivity tensor and will discuss the necessity of achieving the expression for the diffusivity tensor in the case of many particles system.

4.1 Effect of hydrodynamic interactions

The effects of the hydrodynamic interactions between the particles should decrease with increasing separation distance. That means that hydrodynamic forces are a function of the separation between the particles. The expected effect of the hydrodynamic interactions is to retard the motion of the particles compared for the case without hydrodynamic interactions [63]. It is expected in confined systems that the effects of the surfaces on the particles will be similar to and stronger than those due to particle-particle interactions because the flow field is also affected by the channel walls. This implies that the flow field moves around the particle, i.e., the fluid passes between the particle and the wall. Therefore, there is a reduction of the hydrodynamic mobility of a particle diffusing close to a wall.

The hydrodynamic effect of the walls on a single particle is well known, but not so well known for many particles. Its influence was analyzed in a theoretical way by

Brenner [47]. Brenner establishes the basis of the influence of either other particles or a flat wall on the hydrodynamic drag force acting on a nearby isolated particle. The theory is based on the measure of the drag force acting between a sphere at certain distance to parallel walls at low Reynolds numbers and in the absence of walls and consequently the mobility and diffusion tensors. This formulation is very complicated to apply and is only applicable for some particle-wall configurations. Some authors have applied successfully both in the absence of walls like Crocker [25] and Meiners and Quake [89] and with walls like Lin *et al* [72], Faucheux *et al* [40] and Lobry *et al* [73], just to mention a few. However, for many particles systems, both in bulk and in confinement, there is still some theoretical uncertainty.

There are some other ways to incorporate the effect of the full hydrodynamic interactions on the transport process. One can include in the mobility tensor a term that depends on the density. This is only valid for low densities, for dilute fluid suspension which have a volume fraction of the sphere c much smaller than unity. This approximation was suggested by [8] for the case of spherical particles falling through a fluid. Batchelor studied the sedimentation of spherical particles. This can help us as a first estimation of the effect of these interactions. The relation between the mobility tensor Γ with the density probability function ρ can be obtained through the particles velocity and the interaction force. With this approximation, it is expected that the effect of the hydrodynamic interactions will be greater where there is more density.

Other ways to assess the influence of hydrodynamic interactions on transport properties are based on the calculation of the time dependent correlation function between two charged or neutral particles or between a particle with the confined walls using the Ornstein-Zernike equation and the Percus-Yevick approximation for hard spheres which has been demonstrated appropriate. This correlation function measures the influence of particle one on particle two at a certain distance. This formulation was applied successfully by Pesche and Nägele [97, 98] and more recently by Löwen *et al* [109]. Löwen introduces the hydrodynamics interactions among the particles on the DDFT considering the correlations among the particles using the Ornstein-Zernike equation and the Percus-Yevick approximation for the hard sphere case. For the last case, the calculation of the density function would be necessary, and hence the calculation of the N-body densities. For lack of time, it was not possible to perform the calculations and will not be used in this work. To give a little more clarity to the effects of the hydrodynamic interactions, we center on the study of these interactions for the case described in chapter 2, i.e., on two spherical particles diffusing through a narrow channel.

The most usual way to study the effect of the hydrodynamic interactions in the case as particle-wall interactions is including their effect on the mobility tensor as a function of the distance between the particles and the wall. This will be discussed in Section 4.3.

Most of the works on this subject are experimental or computational simulations, due to the difficulty in solving the Schmoluchowski equation. There are not many analytical studies on this subject. Lobry *et al* [73] used a semi-analytical treatment to calculate the diffusion coefficient for a single particle in the presence of two walls. Another analytically study by Bhattacharya is published in [11, 12].

Pesche [97] demonstrates that the effects of the HI on a confined system are enhanced in comparison with the case of an isolated colloid for charged colloidal particles. However, these kinds of effects are not expected for uncharged colloids for the case of HI between the particles and the walls.

4.2 Influence of hydrodynamic interactions among the particles

A particle that moves in a fluid induces a perturbation in the fluid flow velocity field whose magnitude decreases with the distance. The attenuation of the perturbation is slow, and when another particle is within reach of the above mentioned perturbation, the velocity of both particles diminishes.

The hydrodynamic interactions depend on the particle's size. The bigger the particle is, the greater amount of fluid will be displaced in their movement. Also, the resistance increases with size. The HI also depends on the distance between the particles l, the distance between the two walls W and the distance of the particles from the walls. For distance $l \ll W$, the particles behave as if they were isolated [11, 12]

The present Section presents the influence of the hydrodynamic interactions among the particles on the separation process, disregarding the particle-wall HI effects. To study this influence, one can make use of the method of reflections [30, 52, 63] or determine the time dependent correlation function. The use of the method of reflections implies an infinite number of images in the case of confinement of particles between two walls but it is not useful in more complex channel geometries. For this reason we solve the Stokes equation directly in order to assess their relevance for our system of interest.

Let us consider a simple spherical colloidal particle of radius R at the center of a three-dimensional channel of length $L_x = 200R$ and $L_y = 200R$ dragged through an incompressible viscous Newtonian solvent with velocity c in the x-direction at low

Reynolds number, see **Fig. 4.1**. We formulate the problem in a frame of reference co-moving with the sphere. Then the upper and bottom channel walls move in the

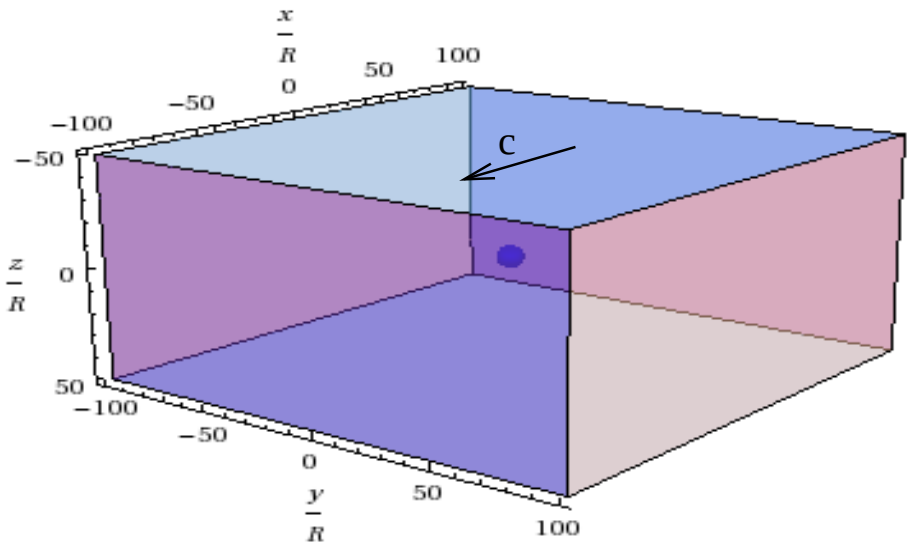

Figure 4.1: A simple spherical particle of radius $R = 1$ at the center of a three-dimensional channel of length $L_x = 200$ and $L_y = 200$ dragged through an unbounded incompressible viscous solvent with velocity c.

negative x-direction with velocity $-c$. We impose no-slip boundary conditions on the surface of the spherical particle and slip boundary condition on the side walls at $y = \pm L_y$. At the front and back wall at $x = \pm L_x$, we use an influx boundary condition with inflow velocity $-c\hat{e}_x$ and an outflow boundary condition with pressure $p = 0$, respectively. In the co-moving frame of reference, the no-slip boundary condition requires that the fluid velocity is zero on the surface of the sphere. The pressure of the fluid, the normal force per unit area, is greater in front of the sphere than on the back. As the particle is at the center of the channel, for every point where a force is experienced and hence a torque exerted, there will be a diametrically opposite point where the torque will be exerted in the opposite direction, and hence, there will be no net rotation. We put the sphere at the channel center to prevent the rotation, because at this position the momentum on the sphere is equal up and down of the sphere. For position away from the center, we would have to consider also the sphere rotation which is nummerically challenging.

The system is described well by the Stokes equation for very low Reynolds num-

bers:

$$\boldsymbol{\nabla} p - \mu \boldsymbol{\nabla}^2 \mathbf{u} = 0 \tag{4.1}$$

$$\boldsymbol{\nabla} \cdot \mathbf{u} = 0 \tag{4.2}$$

with the viscosity μ, the presure p, and the flow field $\mathbf{u}$.

In a 3D bulk system the flow field $\mathbf{u}(r)$, in a frame of reference commoving with the colloid at $\mathbf{r} =$, is given by the solution of the following Stokes equation [104]:

$$\mathbf{u}(\mathbf{r}) = \frac{3R}{4r}\left(1 + \frac{R^2}{3r^2}\right)\mathbf{c} + \frac{3R}{4r^3}\mathbf{r}(\mathbf{r}\cdot\mathbf{c})\left(1 - \frac{R^2}{r^2}\right) - \mathbf{c} \tag{4.3}$$

with c the solvent velocity. As we consider the flow on the x-axis, then the resulting flow field for a sphere of radius R in x-direction and y-direction will be

$$\mathbf{u}_x(x) = \left[\frac{3R}{2r}\left(1 + \frac{R^2}{3r^2}\right)\mathbf{e}_x - \mathbf{e}_x\right] c \tag{4.4}$$

$$\mathbf{u}_x(y) = \left[\frac{3R}{4r}\left(1 + \frac{R^2}{3r^2}\right)\mathbf{e}_x - \mathbf{e}_x\right] c \tag{4.5}$$

The force exerted over the sphere inside a channel should be bigger than for a sphere in bulk.

We perform a numerical solution of the incompressible Navier-Stokes equation

$$\rho(\mathbf{u}\cdot\boldsymbol{\nabla})\mathbf{u} = -\boldsymbol{\nabla} p + \mu\boldsymbol{\nabla}^2\mathbf{u} \tag{4.6}$$

$$\boldsymbol{\nabla}\cdot\mathbf{u} = 0 \tag{4.7}$$

using the COMSOL software, ρ being the fluid mass density within the above described channel geometry. To stay within the microfluidic regime $Re << 1$, we impose the density to be very small in comparison with the viscosity to obtain a $Re = 1 \cdot 10^{-7}$. We determine the flow field of the particle for different channel width from $W = 4R$ till $W = 200R$ for a fixed lateral channel dimensions $L_x = 200R$ and $L_y = 200R$ to see both the effect of the particle and the walls on the flow field. Later, these results were compared with the flow field in bulk Eq. (4.4). The results are presented in **Fig. 4.2**.

In a channel as a function of the distance from the sphere, the flow field decays more quickly to the limiting value $c\hat{e}_x$ than in a bulk system and the decay is faster for thinner channels. For intermediate distances larger than W and smaller than the size of the numerical box, we observe an approximate power law behaviour $u_x \propto x^{-2}$ along the channel axis, and in bulk we get $u_x \propto x^{-1}$. At the channel walls at $x = L_x$ and at $y = L_y$, the flow field goes to $-c$.

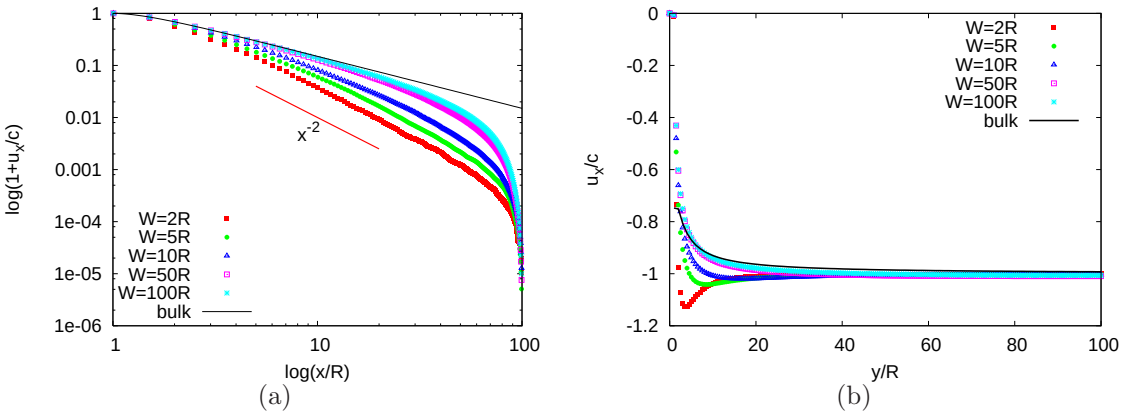

Figure 4.2: (a) Double-logarithmic graph of the x-component of the flow field as a function of x for different channel width from $W = 2R$ till $W = 100R$ and in the bulk. (b) Graph of x-component of the flow field as a function of y for different lateral walls width between $W = 2R$ and $W = 100R$. Also shown is the bulk solution from Eq. (4.3)

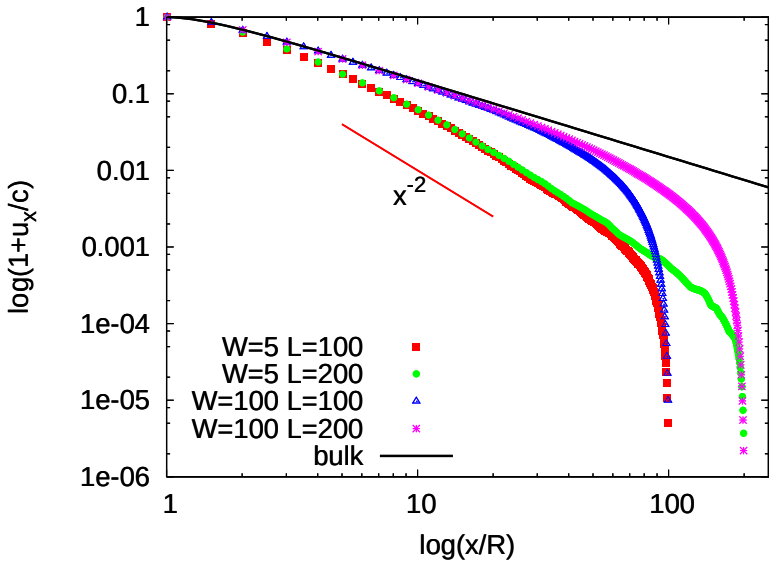

Figure 4.3: Double-logarithmic graph of the x-component of the flow field for the channel length $L = 100R$ and $L = 200R$ and for two different channel width $W = 5R$ and $W = 100R$.

We also assess the influence of the finite size of the numerical box by comparing the x-component of the flow field along the channel axis for two values $L_x = 100R$ and $L_x = 200R$ and for $W = 5R$ and $W = 100R$ as shown in **Fig. 4.3**. We found that the channel ends do not influence the flow field. In other words, the flow field is independent of the channel length.

We can conclude that neglecting hydrodynamic interactions among the particles in our two interacting particles model is better justified than in a bulk system because the flow field induced by the first particle decays with the second power of the distance rather with the first as in bulk. That is, each particle does feel the effect of the other particle on the solvent much less. Consequently, the influence of the hydrodynamic interactions among the particles is smaller than for the bulk case. Therefore, the hydrodynamic interactions among the particles are less important, and they will be neglected as compared to the direct interactions. So that the hydrodynamics forces are weak as compared to the direct forces.

4.3 Hydrodynamic interactions with channel walls

As we have found in the previous Section that the channel walls in the z-direction may affect the fluid motion, let us consider the case of particle-wall hydrodynamic interaction ignoring the particle-particle hydrodynamic interaction. To look in more detail at the effect of the particle-wall hydrodynamic interaction, this interaction will be incorporated in the diffusion coefficient which depends on the distance between the particle and the wall.

Due to the neglect of particle-particle hydrodynamic interactions, the diffusion tensor will not depend on the position of the other particle but depend on the relative distance of each particle with the wall. The mobility tensor decreases in the vicinity of the wall. As a consequence, the particles are accelerated or desaccelerated and the fluid is displace away from the walls.

Heretofore, all the analysis has always been carried out regarding the diffusion coefficient for each particle as a constant for reasons of simplicity. The hydrodynamic interactions with the channel walls can be introduced into the advection diffusion Eq. (3.4) as a wall-particle distance dependent diffusivity tensor $D_{ij}(r)$.

The influence of the hydrodynamic coupling on the transport properties of a particle in bulk or near a wall has been studied by many authors [10, 25, 47, 72], just to mention a few. The drag force, the hydrodynamic force, which is exerted on a hard sphere with radius R moving with velocity u in a quiescent fluid of viscosity η, is opposed to its direction of motion if there is no slip at the boundary between the

sphere and the fluid. This drag force was proposed by Stokes [47] and is given by

$$F_0 = -6\pi\eta R u \tag{4.8}$$

Consequently, the diffusion coefficient D_0 of the sphere is given by the Stokes-Einstein relation

$$D_0 = \frac{k_B T}{6\pi\eta R} \tag{4.9}$$

with k_B the Boltzmann constant and T the temperature of the system.

By contrast, if the particle is near a rigid wall or is confined between two walls, it is known that the drag force increases. The particle diffusion is hindered and depends on the distance to the wall y and varies with the distance to the wall like $D(y/R)$ [10,35]. In other words, the particle experiences a different diffusion coefficient at each height. When a particle is close to a wall, the force exerted on the particle is larger, and consequently, the diffusion coefficient is smaller than if the particle is far away from the wall. That could be due to the wall causing the fluid to flow around the particle away from the wall because the available space between the wall and the particles is very small and there the fluid cannot flow. It is expected that there are similar effects for the case of confined particles between two walls.

Fig. 4.4 displays the predicted value of the normal component $D_\parallel/D_0$ and the perpendicular component $D_\perp/D_0$ of the diffusion coefficient as a function of the related distance to the wall $(y-R)/R$ for an isolated sphere far from one flat wall. Nearness to the wall is expected to reduce both the sphere's hydrodynamic mobility and its diffusion coefficient [10]. Both are reduced by the same factor.

Coming back to the topic under discussion, for two confined particles diffusing through a narrow channel in two dimensions, the hydrodynamic coupling can not be studied. For a two-dimensional fluid flow (the particles and the flow moves in a plane), the flow field around a circle does not decay with distance. 2D hydrodynamics is ill defined[1]. However, the purpose of the 2D model presented in section 2.3 is to model the basic effects of direct and hydrodynamic interactions in 3D systems. In this spirit, we take the main result from [10] the reduced mobility of a sphere in the vicinity of a surface and transfer it to the simple 2D-model.

In two dimensions, there are two diffusion coefficients, one for each direction. These diffusivity tensors can be separated into two different and independent components, one related to the motion parallel to the walls $D_\parallel = D_{xx}$ and the other related to motions orthogonal to the walls $D_\perp = D_{yy}$. Both of these diffusion components

[1] Although there are some theoretical studies [39, 57, 99] and simulations [128, 131] on the 1970's and more recently [34, 49] about the transport coefficients in two dimensions, there is not yet a concluding theory.

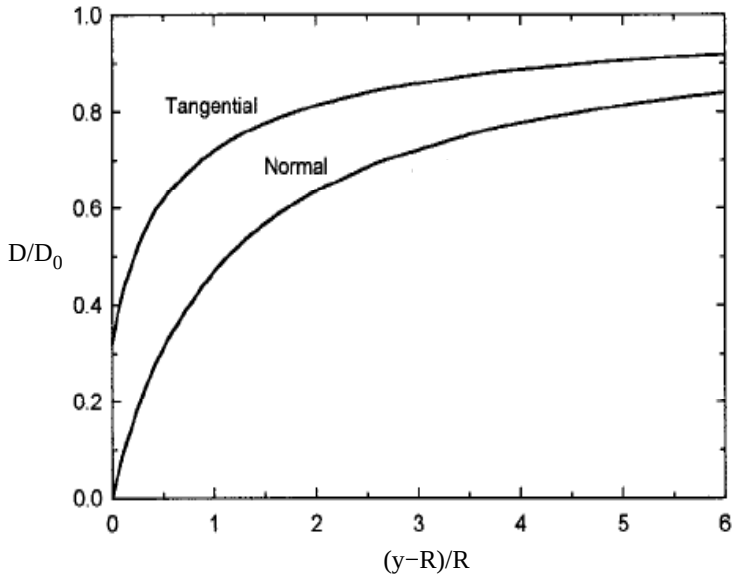

Figure 4.4: Dependence of the tangential and normal diffusivity on the distance to a no-slip wall [10]. The mobility is significantly reduced near the wall.

$D_{\parallel}$ and $D_{\perp}$ are a function of both the distance of the sphere from the walls and the separation of the walls for each other. They are given by

$$D_i(y) = \begin{pmatrix} D_{ixx}(y_i) & 0 \\ 0 & D_{iyy}(y_i) \end{pmatrix} \tag{4.10}$$

Brenner derived the exact solution for D_{iyy} for a sphere moving near a flat wall. Typically, one uses an approximation for the correction factors. In the 3D effective stationary problem Eq. (2.20) there is only one diffusivity tensor which will be a combination of both diffusivity tensors in the two-dimensional problem.

The orthogonal diffusion coefficient has been obtained experimentally both asymptotically [35] and by the method of reflections [10, 47, 70]. Experimentally, it is only possible to measure the normal diffusion coefficient. It is well known that the normal diffusion coefficient for a particle far from the wall reaches the bulk value, and when the particle is close to the wall, it reaches the zero value. Prieve *et al* [10] predict for the parallel component that it should reach the bulk value far from the wall and close to the wall should be approximately 30% of the bulk value.

Therefore, we approximate both components of the diffusion tensor for the case of a particle in a channel following the experimental data obtained for a particle near the wall and in bulk. The bulk value is assumed to be reached when the particle is in the middle of the channel. Close to the channel walls, the same values will be

achieved as in the case of one particle in the vicinity of a wall, i.e., 0.3 for the parallel component and 0 for the tangent component. As a result, the diffusion tensor will be given by Eq. (2.21)

$$\mathbf{D}(Y,Z) = \begin{pmatrix} D_{1xx}(Y) + D_{2xx}(Z) & 0 & 0 \\ 0 & D_{1yy}(Y) & 0 \\ 0 & 0 & D_{2yy}(Z) \end{pmatrix} \tag{4.11}$$

with the following parametrization

$$\frac{D_{ixx}(Y/Z)}{D_{i0}} = 0.3 + 0.7\frac{(W_i/2)^2 - y^2}{(W_i/2)^2} \tag{4.12}$$

$$\frac{D_{iyy}(Y/Z)}{D_{i0}} = \frac{(W_i/2)^2 - y^2}{(W_i/2)^2} \tag{4.13}$$

We are able to model the diffusion coefficient of both Brownian spheres in a channel. **Fig. 4.5** displays the assumed behavior for the tangential component $D_{ixx}(y_i)$ and for the normal components $D_{iyy}(y_i)$ normalized by D_{i0}. It shows the reduction of the diffusion coefficients close to the walls. As the particles approach the walls, their normal and parallel diffusion coefficient vanishes or goes to $0.3D_0$, respectively, and it reaches the bulk value at the channel center.

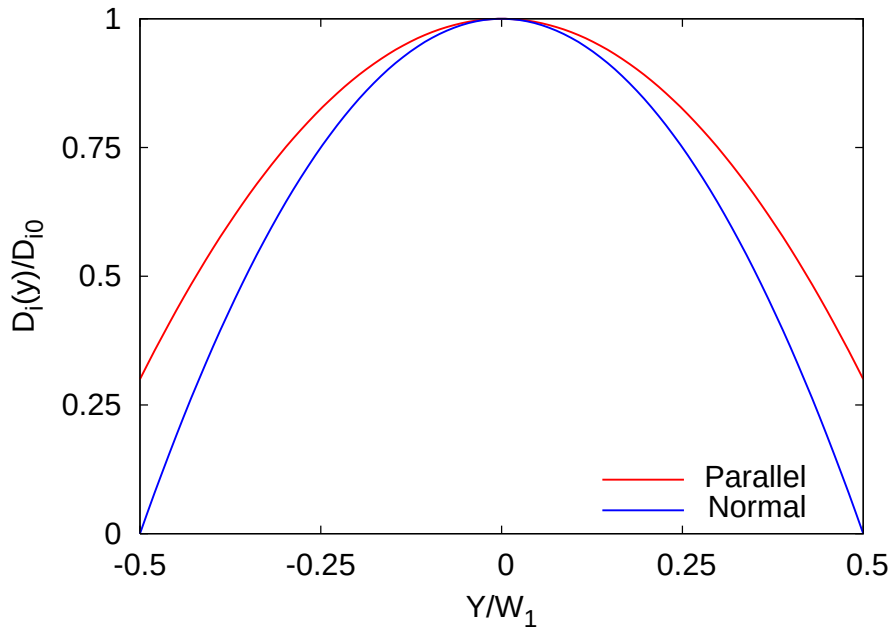

Figure 4.5: Parametrization of the tangential and normal components of the diffusion tensor $\mathbf{D}(y,z)$.

In order to measure the influence of the hydrodynamic interaction with the two confining planes, let us now determine the fluxes of each type of particle. The throughput Eq. (3.5) for hydrodynamically interacting particles with the walls leads to

$$Q_1 = \int_{-L}^{L}\int_{-W_1}^{W_1}\int_{-W_2}^{W_2} [u(Y)\, C(X,Y,Z) - D_{1xx}(Y)\, \partial_X C(X,Y,Z)]\ dY\, dZ\, dX. \tag{4.14a}$$

$$Q_2 = \int_{-L}^{L}\int_{-W_1}^{W_1}\int_{-W_2}^{W_2} [u(Z)\, C(X,Y,Z) + D_{2xx}(Z)\, \partial_X C(X,Y,Z)]\ dY\, dZ\, dX. \tag{4.14b}$$

in the effective 3D stationary problem.

The throughput with hydrodynamic interactions between the particles and the walls is compared with the corresponding result when particle-wall hydrodynamic interactions are disregarded. We perform the same procedure as in Section 3.1.3 using COMSOL for the symmetric cases from $W_1 = W_2 = 0.25W$ till $W_1 = W_2 = W$ for a channel length $L = 5W$ and a minimal distance between both center of mass $d = 0.7W$. We calculate the fluxes for each particle as a function of d_i. We impose the same boundary conditions as in Section 3.1 and we assume $D_{10} = D_{20} = 1$. This comparison is show in **Fig. 4.6**. As seen, in **Fig. 4.6**, the flux including particle-wall hydrodynamic interactions is slightly larger than without particle-wall hydrodynamic interactions, however, this difference is hardly significant as it is on the limit of numerical accuracy. This difference is very small independent of the minimal distance d of the center of mass; even the difference decreases for increasing d. We observe that a hard sphere system does not produce any hydrodynamic effect. Looking at the solution $C(X,Y,Z)$, we observed that the distribution of the particles through the channel is only weakly affected by the hydrodynamic interaction with the channel walls. The big one still moves in the channel center and the small one is pushed to the channel walls.

4.4 Conclusions

This chapter has presented analytical and numerical results for the hydrodynamic interactions on the separation process using the finite element software COMSOL. Our study has been focused on the influence, effect, and dependence of these hydrodynamic forces.

To provide a description of the hydrodynamic interactions, we have carried out a detailed study of their influence in Section 4.2. We have modeled the flow field corresponding to a Stokes flow for a single particle moving through a narrow channel.

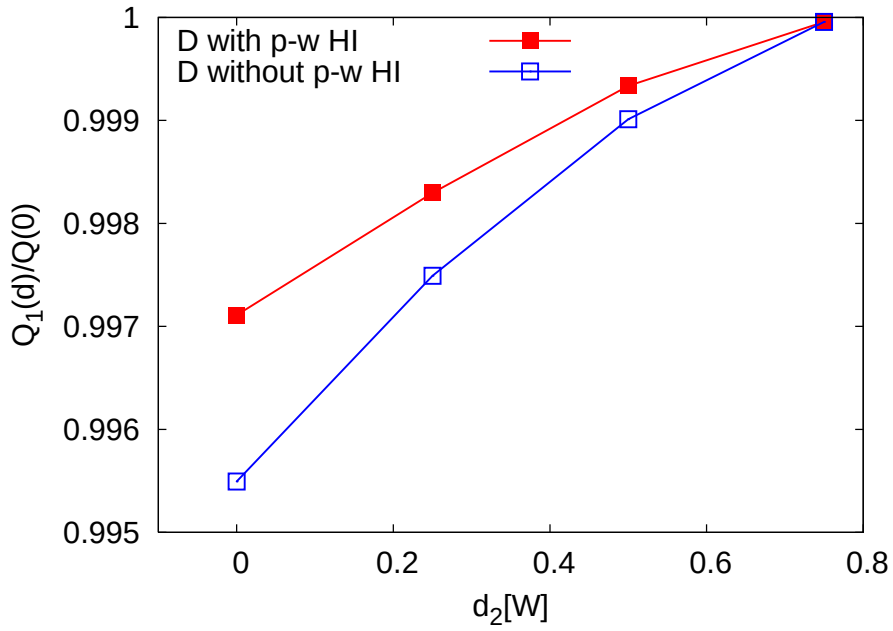

Figure 4.6: Comparison of the flux Q_i for the symmetric case normalized by $Q_i(d = 0)$ as a function of the width of the forbidden zone $d_1 = d_2$ for the diffusion coefficient with particle-wall hydrodynamic interactions (p-w HI) $\mathbf{D}(y, z)$ and without p-w HI.

We consider only two particles and neglect the hydrodynamic interactions among them. This is in contradiction with experimental works, which report an effect of the hydrodynamic interactions for non-confined particles. The reason for this difference is the confinement. However, even the effect of the hydrodynamic particle-wall interactions is weak as we have seen, maybe as weak as the hydrodynamic interactions among the particles. The next step would be to take into account the hydrodynamic interactions for N-particle systems where higher densities can be reached such that many-body hydrodynamic interactions can become relevant.

An important result of this chapter is that the hydrodynamic interactions between the particles are influenced by the lateral channel walls: they are significantly reduced.

An important result of this chapter is to demonstrate that the particles are affected by the lateral channel walls, both directly and hydrodynamically. This can be achieved including the hydrodynamic interactions on the diffusion tensor.

In order to assess the effect of hydrodynamic interactions with the walls on the transport of suspended particles, we have considered in Section 4.3 the diffusion tensor depending on the distance to the channel walls. This allows us to figure out the fluxes of each particle as a function of the particle size. We have shown how the hydrodynamic interactions with the walls hardly modify the behavior of the particles

inside the channel. Indeed, our numerical results for the diffusion tensor confirm that there is some kind of hydrodynamic effect due to the walls, and the effect is quite weak. It is also important to remark, however, that the dependence of the diffusion tensor on the distance to the wall should be calculated or measured more acurately for a better understanding of the hydrodynamic forces.

At the moment, the R. Weeber at the University of Stuttgart and A. Straube at the "Humboldt Universität" in Berlin are doing some simulations to obtain the dependence of the diffusion tensor with the distance to the wall. Up to now, the use of the Stockesian dynamics is not possible due to the impossibility to fix the no-slip at low Reynolds numbers.

Chapter 5

Soft particles

The present chapter concerns a more realistic case. A second kind of complex fluids will be discussed, those composed of polymers instead of colloids. The polymer fluid will be studied in confinement where the dynamic properties are strongly modified in the presence of walls in comparison to bulk systems. The hard sphere model, discussed in chapters 3 and 4, is a good model to describe compact colloidal particles, but it cannot model polymer coils due to the effective forces between soft particles. In this chapter, we model the polymer coils by soft particles, i.e., as penetrable spheres in which an effective interaction acts between the centers of mass of different polymer coils as shown in **Fig. 3.1 b**. Soft particles are a simplistic model for polymers in a good solvent. Many-body hydrodynamic effects arise from the disturbance of the flow field around one particle by neighboring particles and the walls. A polymer behaves quite differently in a flow field than a rigid sphere. However, in the soft particle model these differences are not taken into account.

As in colloidal suspensions, the impenetrable walls will exert an effective repulsion on the polymer coils, while with penetrable walls, the polymer chain can be fully or partially absorbed by the walls. The penetrable surface case lies beyond the scope of the present study. The study of this effective force between the polymer coils and the walls can give us a good initial description of the behavior of the polymers in a confined solution and on the transport process. The soft particle picture has been used before by other authors, among others Louis *et al* [16, 76].

Some polymer properties influence the transport process, such as the size of the polymer chain, which affects the chain mobility; the kind and goodness of the solvent; the interactions — between the polymers and the solvent, between the polymer and the walls of the confinement, and among the polymers —, various chemical properties such as the melting and boiling point; and also other properties that are beyond the scope of the present study.

There are two types of models to describe polymer chains. The simplest polymer model is a Gaussian random walk. In this model the interactions between monomers are neglected. A further simplification has been introduced by Asakura and Oosawa (AO) in 1958 who model the polymers as interpenetrable spheres [7]. Nevertheless, in real polymers two segments can interact even if they are separated by a long distance (inside the chain). The polymer chain cannot cross itself, which is a manifestation of the Pauli exclusion principle; therefore, the effect of excluded volume appears. This is named a "self-avoiding random walk" in which the size of the polymer is larger. The free energy increases, which is equivalent to a repulsive interaction. In this work, we focus our attention on real polymers, the Gaussian polymers, in a good solvent in particular. We neglect all chemical details of polymer systems except the excluded volume.

When polymers are in a bad solvent, the polymer chain has the tendency to be more compact, like a sphere. A poor solvent causes the polymer coil to shrink. The polymer in good solvents adopts the form of a coil and it is called a polymer coil. The solvent causes the polymer coil to swell because the solvent-polymer contacts are favored. When the polymer chain expands, it fluctuates and has a different behavior than when the polymer chain is compact. The behavior of polymers in a good solvent is more complex than in a bad solvent. For reasons of simplicity, in this work the polymers will be considered as an ideal chain in a good solvent. The effective interaction between the centers of mass of two polymer coils is well known and decays rapidly beyond the radius of gyration of the coils [75]. The radius of gyration is the average distance between the center of mass of the chain and the chain itself, and it expresses the space occupied by a polymer molecule, see **Fig. 3.1 b**. Also those changes in the coil dimension affect the viscosity.

In a good solvent, the attraction between the polymer and the solvent particles is stronger than the attraction between two segments of the polymeric chain. Consequently, the chain gains free energy upon expanding [94]. The polymer coil size is reduced due to monomer-monomer attraction. The effect of this attraction is greater at lower temperature, causing a reduction in the size of the coil.

As in hard spheres situation, the walls create a depletion layer due to the fact that the polymers have fewer possible configurations near the wall. A depletion zone is also created around the polymers: when two polymers are brought together at low densities, the polymers avoid the depletion layer (they cannot overlap). But for larger densities, the polymers can penetrate the depletion layer (they can overlap). Consequently, the accessible volume is greater than for spheres which do not overlap. In fact, the particles interact with a strong repulsion which does not generate an

excluded volume strictly speaking.

The resulting effective interaction among the particles is repulsive and it is well approximated by a Gaussian potential. There can also be attractive forces between polymers and walls. Then the polymers exhibit an absorption transition. It appears as if the qualitative behavior of the absorption transition does not strongly depend on the type of attractive surface interaction. In our simplification effort we have neglected the polymer wall attractions.

Polymer solutions have been studied by many authors in the last few decades. Louis *et al.* [77] studied a polymer solution in which a single hard sphere has been added and they reduced the number of configurations available to polymers. Krüger [64–66, 104] focused on a single hard sphere added to a polymer solution and studied the behavior of the flux when the particles travel together side by side or one before the other. Likos *et al.* [54] focused on the effective interactions between star polymers and a colloidal spherical particle in a good solvent. In contrast with the previous studies, we are interested to know how the dynamic properties of the polymers will be affected by the confinement walls on both the transport and separation process as in the case of hard spheres. We will look again at the density distributions and fluxes. In Section 5.1, we will discuss the interaction potential between the particles and the walls as a hard core type interaction and in Section 5.2 as a soft type interaction.

5.1 Particle wall potential as hard core repulsion

In polymers the excluded volume can be of a hard or soft core type. The choice of wall-particle potential influences the behavior of the polymer particles inside the channel. We have to choose the interaction potential in such away that it diverges such that the particles cannot penetrate the wall. In this section, as a first step will consider the excluded volume of the polymer both of a hard and soft core type. The hard core type will be used for the interaction potential between the particles and the channel wall and the soft core type will be for the interaction potential among the particles. Hence at this stage, the particle wall interaction repulsion Φ_i will be of the form of Eq (3.2), i.e., the polymer segments cannot penetrate the walls and then the polymers are repelled with a infinite intensity. In the next section 5.2, we will treat the excluded volume for this kind of interaction as a soft core type. The particle-wall interaction will be as thus for polymers in a good solvent. The hydrodynamic interactions will be neglected through this entire chapter.

This idealization of the direct interaction as hard type has already been discussed by other authors (see [66]) in the case of an interaction between a hard sphere particle

with a polymer. But they consider that the hydrodynamic radius can be smaller than the interaction radius.

Therefore, in this chapter the physical system considered consists of two polymers particles advected by a Poisseuille flow inside a narrow channel according to Eq. (2.6) [see **Fig. 5.1**]. As the relevant length scale in suspensions is the particle size, this

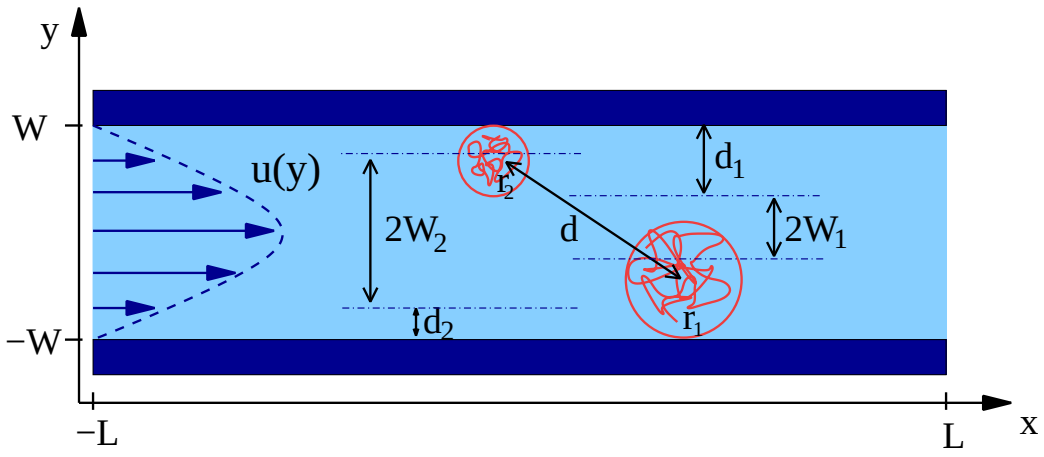

Figure 5.1: Two polymer coils of different size at positions r_1 and r_2 in a channel of width $2W$ and length $2L$, which is assumed to be longer than any other length in the system but finite; the region of each particle, where the particle can move through the channel, is denoted by $2W_1$ and $2W_2$; and the forbidden region for each particle near the wall is denoted by d_1 and d_2.

once more allows us to treat the solvent as a continuum. The statistical analysis of a system of many-body interactions is of significant physical interest.

Here the same parameters as in the preceding sections will be studied: the fluxes and the densities profiles. At this stage, we neglect the hydrodynamic interactions both with channel walls and among particles. According to direct interactions as mentioned above, the interaction potential of the polymer coils with the walls Φ_1 and Φ_2 will be a hard sphere repulsion potential [see Eq. (3.2) a]. The statistical description for the interaction potential between the center of mass of two polymers in a dilute solvent is well described by an interaction of a Gaussian form — the polymers interact via a Gaussian pair potential [95]. This potential has the form [see **Fig. 5.2**]:

$$\Psi(r) = \Psi_0 e^{-r^2/d^2} \tag{5.1}$$

where r is the interparticle distance and d determines the range of the pair interaction and is approximately the radius of gyration of the polymers. Thus the polymer-polymer interaction mimics the interaction among polymer coils in a good solvent

[103]. This Gaussian potential was proposed first by Flory and Krigbaum [43] and later was applied by Stillinger *et al.* [123].

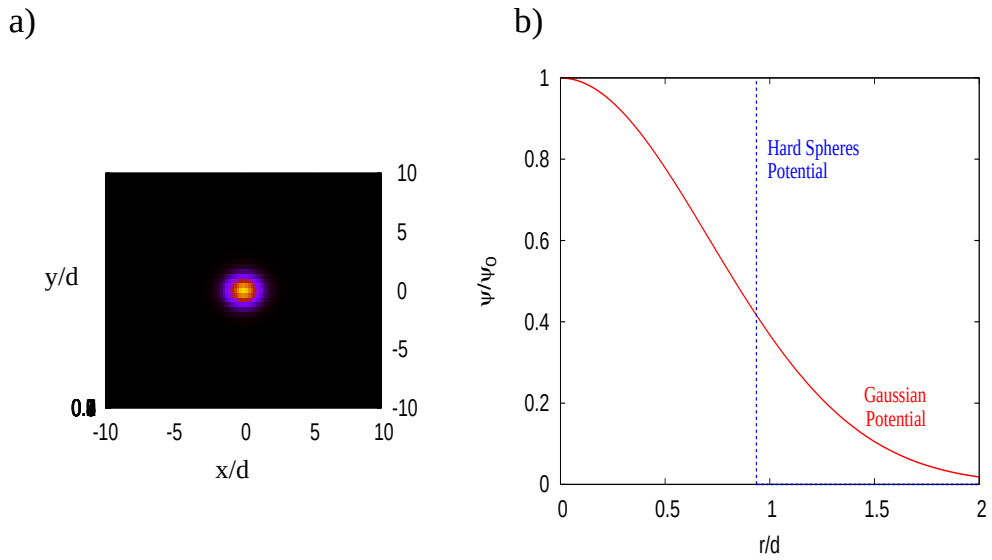

Figure 5.2: a) Normalized interparticle Gaussian Potential (Ψ/Ψ_0) as a function of r/d. The color scale encode the value of C ranging from a minimum value (black) to a maximum value (bright yellow).; b) Comparison of the interaction potential among the particles for colloid particles and for polymers as a function of the radius.

As the Gaussian potential (the interaction potential among the particles) depends on the temperature, the density distribution and the fluxes will also depend on the temperature through the narrow channel. Another aspect that changes with the temperature is the goodness of the solvent which lies beyond the scope of the present study. On the other hand, upon having increased the temperature of the system, the solvent viscosity decreases and therefore the friction of the particles. This leads to a larger diffusivity. Now, we turn our efforts to the temperature dependence, analyzing the equilibrium density [see Eq. (2.15)], $P_{eq} = \frac{1}{Z}e^{-\beta\Psi}$, with the potential given in Eq. (5.1). This dependence is shown in **Fig. 5.3**. With a smaller value of the interparticle interaction potential $\beta\Psi_0 = \Psi_0(k_BT)^{-1}$, the particles can pass each other and with larger value, they cannot pass each other. In other words, by increasing β (decreasing T) the difficulty for the particles to pass each other increases to the point where a value is reached at which it is no longer possible. For our study, the low temperature at which the particles can pass each other is $T = \Psi_0(10K_B)^{-1}$. Increasing T the particles can pass.

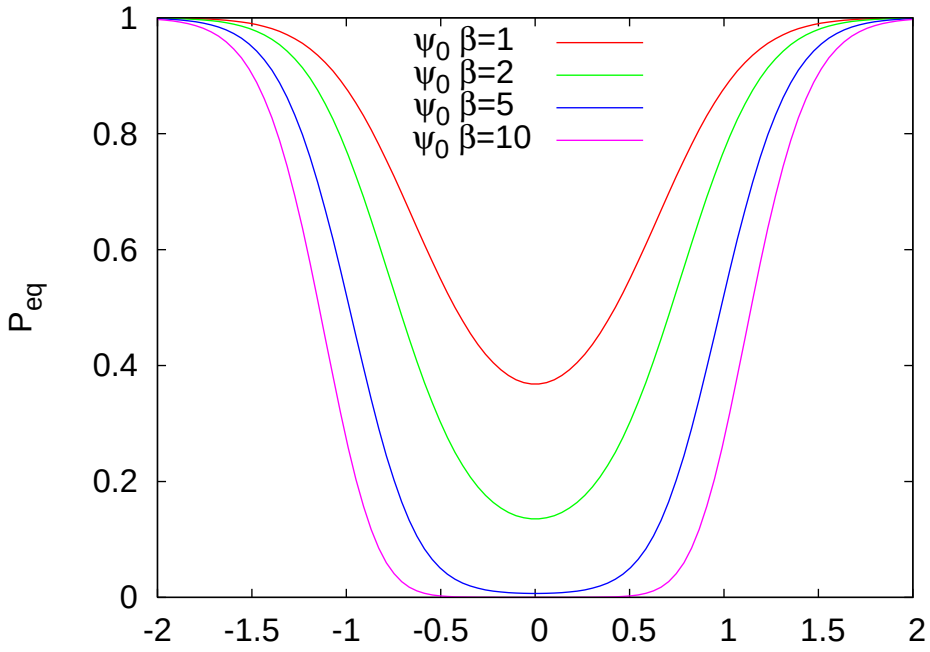

Figure 5.3: Behavior of the equilibrium density distribution as a function of the interparticle distance for $d = 0.7W$ at varies temperatures $\beta\Psi_0 = 1$ to $\beta\Psi_0 = 10$.

Throughput

Our starting point to study the throughput of the dilute polymers in a good solvent will be the advection diffusion equation Eq. (2.20). We consider the Brownian motion of the polymers. As the interaction with the channel walls will be treated as hard spheres, the total interaction potential V will be equal to the interaction potential between the polymers $V = \Psi$ and with a vertical and horizontal confinement coming from the interaction of the two particles with the channel walls, respectively. Then, Eq. (2.20) can be rewritten as

$$\boldsymbol{\nabla}_{\mathbf{R}} \cdot [-\mathbf{D}(Y,Z)\boldsymbol{\nabla}_{\mathbf{R}} C(\mathbf{R}) + (U(\mathbf{R}) - \beta\, \mathbf{D}(Y,Z)\, \boldsymbol{\nabla}_{\mathbf{R}} V(\mathbf{R})) \cdot C(\mathbf{R})] = 0 \qquad (5.2)$$

Due to the neglect of hydrodynamic interactions, the diffusion tensor $\mathbf{D}$ will be constant and given by Eq. (2.21) with $D_{ixx} = D_{iyy} = D$.

To study the throughput for each particle we solve Eq. (5.2) numerically using the finite element software COMSOL. In particular we use the steady-state convection and diffusion analysis. The geometry used is a rectangular channel where the walls in Y and Z are defined by the hard wall potentials ϕ_1 and ϕ_2 respectively [see **Fig. 5.4**] so that the polymer segments cannot penetrate the walls. To introduce the interparticle potential interaction $\Psi(R)$ in COMSOL, we have to define an effective flow velocity as

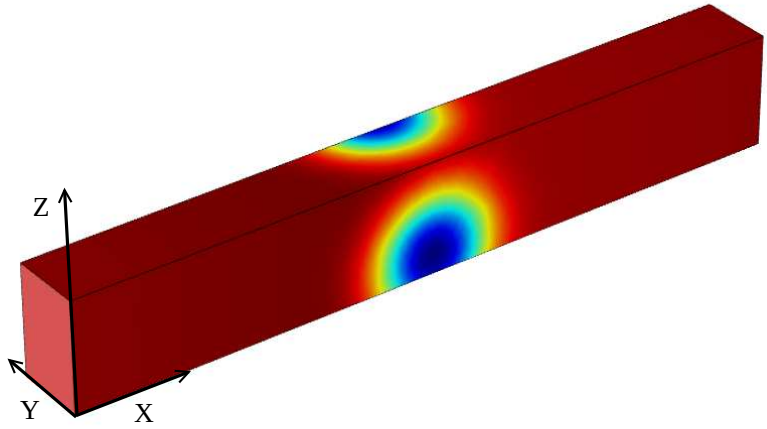

Figure 5.4: Rectangular channel of size $W_1 = 0.5W$, $W_2 = 0.75W$ and $L = 5W$ where the walls in Y and Z are defined by the infinitely repulsive potentials ϕ_1 and ϕ_2 respectively. The color scale encode the value of C ranging from a minimum value (dark blue) to a maximum value (dark red) for $Pe = 1$ and $\beta\Psi_0 = 1$.

$\mathbf{U}^*(R) = \mathbf{U}(Y,Z) - \beta\,\mathbf{D}(Y,Z)\cdot\boldsymbol{\nabla}_{\mathbf{R}}\Psi(\mathbf{R})$. We impose no-flux boundary conditions in the entire domain except in the two channel ends $X = \pm L$ where periodic conditions are imposed in order to allow for a steady state to develop.

Hence, to assess the throughput the potential term should be introduced in Eq. (3.6) which leads

$$Q_{1/2}(X,Y,Z) = \int_{\Omega} \left\{U(Y/Z)C(R) - D_{1/2}\left[\partial_X C(R) + \beta C(R)\partial_X \Psi(R)\right]\right\} dX dY dZ \tag{5.3}$$

with Ω the integration volume which corresponds with **Fig. 5.4**

At first we focus on the variation of the fluxes for each particle as a function of the thickness of the forbidden zone d_i on the channel for different particle sizes. We observe that the qualitative behavior of Q_i are the same as for hard spheres. That means the flux Q_i increases as d_i increases. In addition, if one increases d_1, Q_2 decreases and Q_1 decreases as d_2 is increased.

Next, we turn our attention to the variation of the fluxes with the solvent flow velocity u_0 (with the Pèclet number). The considered cases are the same as those for hard spheres: (a) one large particle $W_1 = 0.25W$ ($d_1 = 0.75W$) with a small particle $W_2 = 0.5W$ ($d_2 = 0.5W$) for a channel length $2L = 10W$ and a interparticle

interaction range $d = 0.7W$; (b) the second case named as symmetric case will be for two equal and small particles $W_1 = W_2 = W$ ($d_1 = d_2 = 0W$) with a channel length of $2L = 10W$ for the same d as the first case; and the last one (c) considering one big particle $W_1 = 0.25W$ and one small particle $W_2 = W$ with the same channel length as case (b) but with a interaction range of $d = 1.4W$. For all cases, we observed that the particles can pass each other or they can travel together for increasing velocity in contrast to hard particles where the particles cannot pass each other in some cases depending of the size of the hard spheres and/or the interaction distance d between them.

As the temperature can influence the behavior of the fluxes inside the channel through the Gaussian potential, we look at the fluxes Q_i as a function of the solvent flow velocity and for the same values of temperature used in **Fig. 5.3**. We are looking for different values of the solvent flow from $u_0 \geq 0$ till $u_0 = 50W/D$, i.e., for different values of the Pèclet number from $Pe = u_0 W/D = 0$ till $Pe = 50$. Upon increasing the flow solvent, we have different parabolic profiles, these profiles are sharper for increasing flow solvent. For example, we look at the case (a) in section 3.1.3 — two particle of size $W_1 = 0.25W$ and $W_2 = 0.5W$ — but now for a channel length of $2L = 40W$ and for a $d = 2W$. We solve numerically Eq. (5.3) using COMSOL due to the impossibility to solve analytically because of the dependence of the potential on X. The behavior of the throughput for different values of $\beta\Psi_0$ is shown in **Fig. 5.5**. The fluxes of each particle Q_i is normalized by the solvent flow velocity u_0. For increasing Pe the difference in throughputs decreases. This effect is most pronounced for $\Psi_0\beta = 5$ and least pronounced for $\Psi_0\beta = 1$. For $\Psi_0\beta = 10$ we expect to see the same effect at larger Pe. At this value the particles can hardly pass each other. In all cases the throughputs are larger than for the non-interacting case $\Psi_0\beta = 0$. We attribute this to the interplay between the flux and the interaction potential: The polymer particles are pushed together as the solvent flow increases. Looking these results, one can expect that in the middle of the channel at $Y = Z = 0$ the solution $C(X, Y, Z)$ will be inhomogeneous and on both sides of the channel homogeneous.

The comparison of the throughput for both cases, hard particles and soft particles, will be the next object for study. To be able to compare both cases, we have to look at the case $\beta\Psi_0 = 1$ in soft particles see **Fig. 5.6**. For soft particles, the separation efficiency, i.e., the differenc of Q_1 and Q_2, decreases as the Pèclet number increases inside the channel in contrast to hard spheres where the separation increases with the flow.

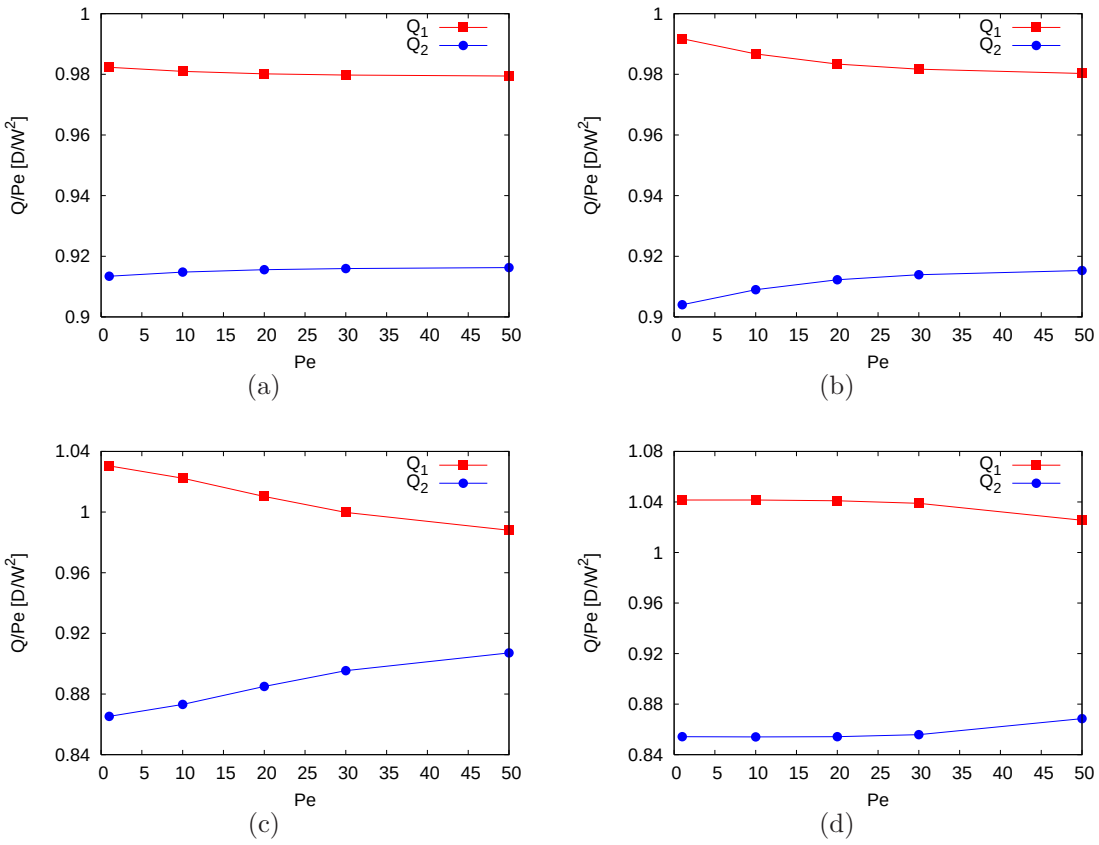

Figure 5.5: Throughput of each particle Q_i normalized to the solvent flow velocity as a function of u_0, i.e., as a function of the Pe number for the case of a big particle $W_1 = 0.25W$ with a small particle $W_2 = 0.5W$ for an interaction distance between both center of mass of $d = 2W$ and a channel length of $2L = 40W$ for different values of $\beta\Psi_0$ a) $\beta\Psi_0 = 1$, b) $\beta\Psi_0 = 2$ c) $\beta\Psi_0 = 5$ and d) $\beta\Psi_0 = 10$.

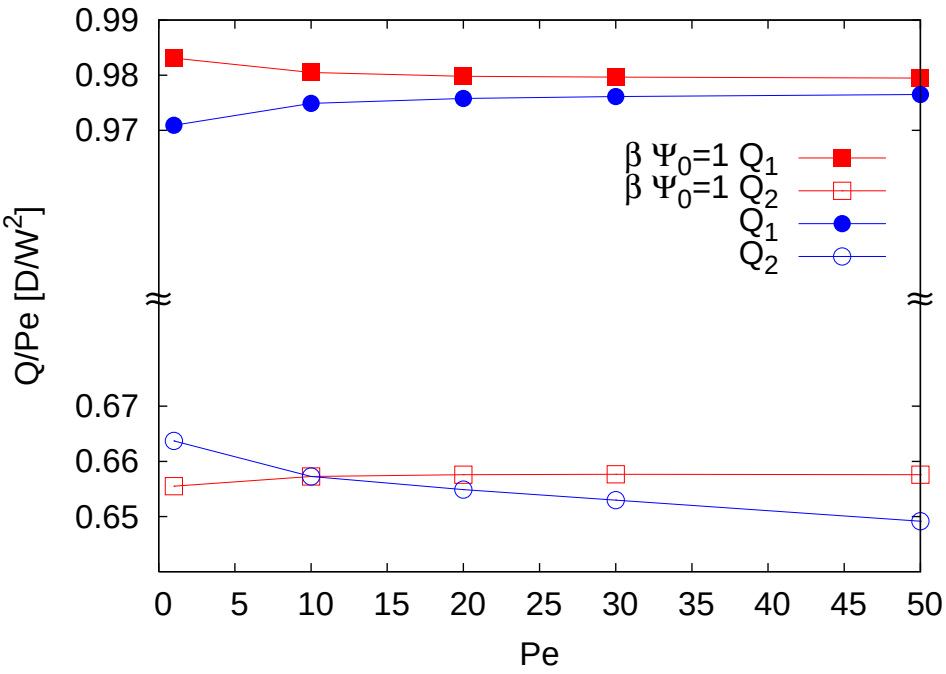

Figure 5.6: Behavior of the fluxes as a function of the solvent velocity both for hard spheres and soft spheres. We compare them for $W_1 = 0.25W$, $W_2 = W$, $d = 0.7W$ and $L = 5W$.

Density profiles

As we are interested on the separation process, the next step was to evaluate the density profiles of each particle ρ_i as a function of the solvent flow u_0 for the following case: two particle of size $W_1 = 0.25W$ and $W_1 = W$ for a channel length of $2L = 40W$ and for an interaction distance between both center of mass of $d = 2W$ and for three different values of the temperature $\beta\Psi_0 = 0.1, 1, 10$. We continue with the same analysis by COMSOL: the advection-diffusion model. We evaluate the density distribution profiles of particle 1 and 2 averaging along the X direction and the Y or Z direction of the variable C defined on some 3-dimensional domain in the yz-plane by calculating the integral on Eq. (3.8), respectively.

For the intermediate value $\beta\Psi_0 = 1$ [see **Fig. 5.7 (b)**], we observe that both particles —the smaller particle and the larger one — move closer to the channel walls. By increasing Pe, the modulation of the density profiles increase homogeneously and monotonously, and there is more probability of finding the particles at the channel walls than at the middle of the channel. For $\beta\Psi_0 = 10$ [see **Fig. 5.7 (c)**] (when particles can hardly pass each other), both particles are closer to the channel walls. The modulation of the density profiles now increase monotonic till $Pe = 10$ and then starts to decreases. The probability of finding the particles at the wall increases

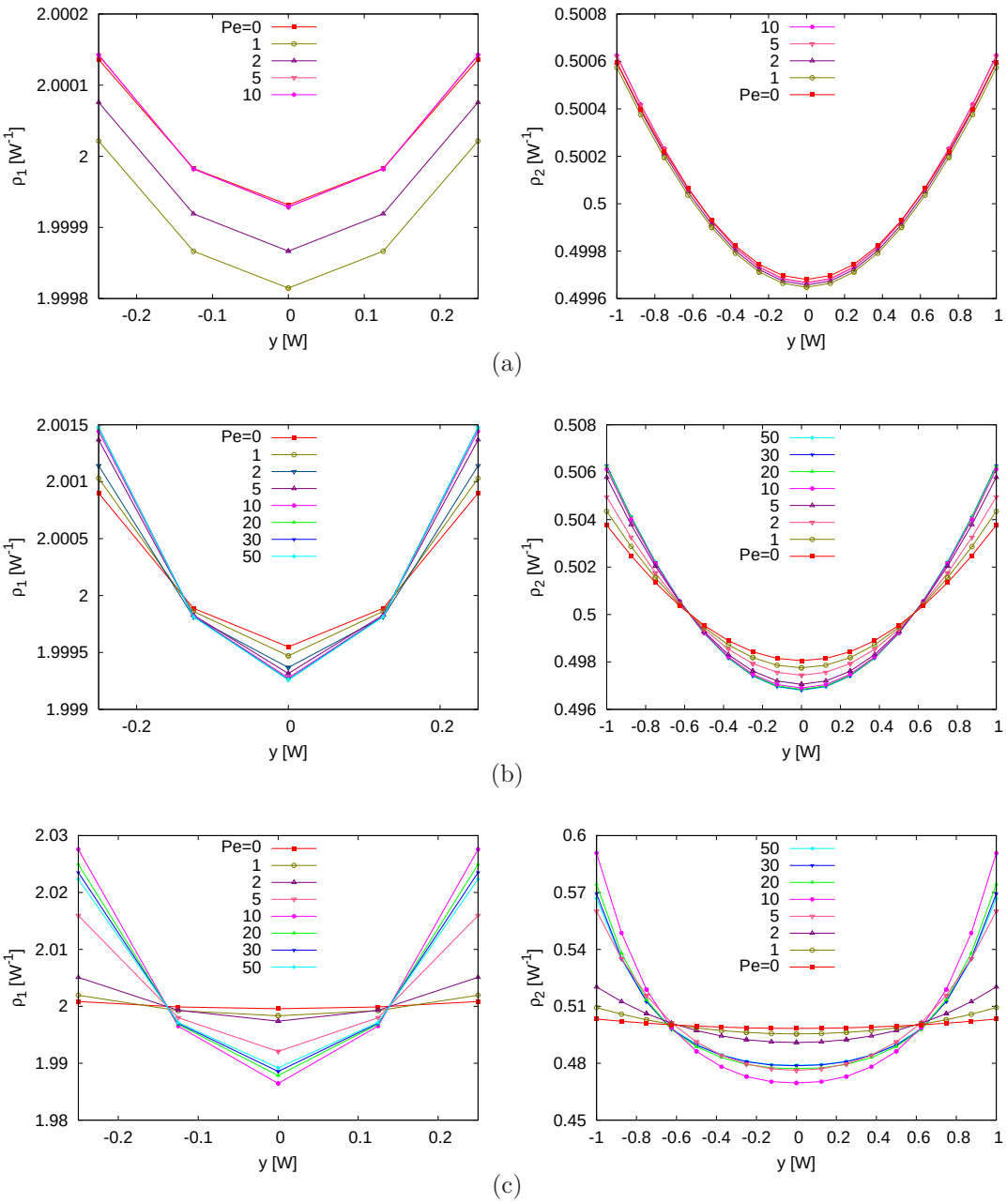

Figure 5.7: Normalized density profiles ρ_i for one big particle $W_1 = 0.25W$ with a small particle $W_2 = W$ for a distance between both center of mass $d = 2W$ and with a channel length of $2L = 40W$ for three increasing temperature cases: a) $\beta\Psi_0 = 0.1$; b) $\beta\Psi_0 = 1$; and c) $\beta\Psi_0 = 10$

with increasing u_0 until the value $Pe = 10$ is achieved, and then the probability starts to decreases very slowly. For the small value of $\beta\Psi_0 = 0.1$ (for larger T) [see **Fig. 5.7 (a)**], we observe that both particles move closer to the channel walls than at the middle of the channel. We observe the same modulation of the density profiles for all the values of Pe and therefore the probability densities ρ_i are independent of the Pèclet number Pe. This case corresponds with a weak interparticle interaction potential, i.e., with a high temperature.

We can conclude that independently of the temperature and the polymer size, the polymer particles tend to move closer to the channel walls in contrast with colloidal particles [see **Fig. 3.6**], of which only the smaller ones tend to move closer to the channel walls. Our result differs for those obtained in the group of Winkler in "Forschungszentrum Jülich" for the case of a flexible, single polymer in a channel. Winkler saw that the polymer was located in the central part of the channel. Maybe this difference is due to our neglecting of the hydrodynamic interactions with the walls, which were taken into account in the simulation by Winkler.

Louis *et al* [77] compare their results for polymer interactions with the polymers being modeled as polymers with that being modeled by the hard-sphere model. They found that the HS model is not a good model to describe the polymer interactions. Krüger [66] found that a particle is much less hindered in its motion by a suspension of equal sized polymers than by a suspension of equal sized spheres. The particle and the polymer interact less strongly via the solvent.

5.2 Soft wall potentials

The aim of this section is to model the interaction of the polymers with the channel walls as a soft type interaction. In order to compare the soft wall with the hard wall, we looked at the case of an ideal chain in a good solvent instead of a coil polymer. If we should treat it like a coil polymer, we would have to consider the interactions within the chain. In this case, the polymer can be described by a random walk. Although we neglect the solvent flow, we treat the interaction between the polymer and the walls as if this was in a good solvent but disregard the interaction between the solvent and the polymer and disregard the dependence of the type of solvent with the size of the polymer. As mentioned before, solvent goodness plays a role. If the polymer chain is in a good solvent, then a difficulty of bringing the polymers close exists due to the enthalpic repulsion caused by the solvent.

As discussed in the previous section, the interactions among the monomers will not be considered, only the interactions with the channel walls and among other

polymers. The interaction potential or energy will be independent of the polymer shape. The monomers will be reflected by the confinement walls.

First, we will introduce some basic concepts related to polymer physics, in particular to the ideal chain in a good solvent. A full statistical mechanics description of polymer physics is out of the scope of the thesis and can be found elsewhere [28,32,56,94].

An ideal chain trapped in a channel

The chain is captured in a cylindrical tube of diameter $h \ll R$ being R the end-to-end vector with hard nonabsorbing walls. In an ideal chain, the short range interactions between segments, which are located close to each other along the chain, are included but the long range interactions are ignored [32]. The free energy of a confined ideal chain squeezed between two walls for short distances between the walls is given by

$$\mathcal{F} \simeq k_B T \left(\frac{R}{h}\right)^2 \tag{5.4}$$

where $R^2 = Nb^2$ is the chain extension (the end-to-end distance) being b the segment length or Kuhn length, and h is the distance between the walls [28]. The channel walls will repel the chain strongly but will not affect the components of the random walk parallel to the channel axis [28]. Basically, one counts the number of encounters a random walk makes with the confining walls. One needs about g segments to reach the walls with $h^2 = gb^2$. Thus, there are N/g collisions with the wall, each of which contributes an amount of order $k_B T$.

The cut-off at large distances is given by the spatial distribution of the density, i.e., $e^{-ch/R}$ with c being a constant. Thus altogether one has

$$\mathcal{F} \simeq k_B T \left(\frac{R}{h}\right)^2 e^{-ch/R} \tag{5.5}$$

for the free energy. In a good solvent — real polymers — the monomers cannot intersect. The extension of the polymer is greater and one has to consider the excluded volume. The average size of an excluded volume chain is larger than that of an ideal chain. If one adds the restriction that no overlapping is permitted, one would expect the size distribution to be shifted to larger values, and so the excluded volume chain is larger than the ideal chain of the same length [32]. It is no longer a random walk, it is the so-called *self-avoiding walk*. Therefore, for three dimensions, the exponent 2 in Eq. (5.5) has to be replaced by $1/\nu$ with $\nu = 0.588$ being the *self-avoiding walk* (SAW) exponent. This ν parameter includes the excluded volume effects and it is related to chain size. The free energy increases, i.e., it is equivalent to a repulsive interaction. In the SAW, the walk can never intersect itself in contrast with the

random walk. The SAW model is the normal description of a dilute polymer coil in solution. The confinement energy for real polymers is larger than for ideal chains. Therefore, the free energy $\mathcal{F}$ for real polymers in confinement will be:

$$\mathcal{F} \simeq k_B T \left(\frac{R}{h}\right)^{1/\nu} \tag{5.6}$$

for short distances from the wall and

$$\mathcal{F} \simeq k_B T \left(\frac{R}{h}\right)^{1/\nu} e^{-ch/R} \tag{5.7}$$

for large distances.

The self-avoiding property reflects the fact that two monomers cannot occupy the same point in space. The SAW constraint causes the walk to spread out. The model of a self-avoiding walk (SAW) on a lattice has been widely used as a convenient representation of a polymer molecule in which the excluded volume is taken into account in a realistic manner.

The Gaussian character is already "used" in the leading factor and a Gaussian cut-off is not obviously worse or better. Louis and Hansen [15,16,76,77] have looked at the effective interaction between a polymer and a wall. They calculated numerically the polymer-wall interaction potential for polymers in a good solvent considering the SAW model and found that the effective wall-polymer repulsion increases with increasing concentration and becomes more repulsive with density.

Two polymers in a narrow channel

As we focus on a narrow channel, we don't need to know exactly the expression for the polymer-wall potential. We are interested only in the case that the polymers are close to the walls. We need only the qualitative behavior of this potential because for narrow channel we expect subtle differences not to induce a great difference on the density profiles or throughput. In the experiments one has to do a lot of measuring and refining of the measurements to obtain the exponential behavior.

For reasons of simplicity, we chose the interaction of the particles with the walls in such a way that it mimics the entropic repulsion from a solid wall. This interaction potential will correspond with the case that the particles are very close to the walls which is related to the free energy close from the walls Eq. (5.4). So the particle-wall interaction potential in the case of two polymers in a narrow channel will be given by:

$$\Phi_i(y, W) = \Phi_{0i}(W_i, W) \left[\frac{(W)^{1/\nu}}{(y - W)^{1/\nu}} + \frac{(W)^{1/\nu}}{(y + W)^{1/\nu}} - 2\right] \tag{5.8}$$

with the potential strengths Φ_{0i} choosed such that $\Phi_{0i}(W_i, W) = k_B T$. For simplicity we set $\nu = 0.5$. On the other hand, the polymer-polymer interaction potential will be the same as in preceding section, i.e., it will be a Gaussian pair potential. To allow us to compare with the hard spheres model, we set $\beta\Psi_0 = 1$.

Having deduced the expression of the polymer wall repulsion from the ideal chain interaction with the walls, we can now simulate the throughput using again the finite element software COMSOL. The analysis used is the advection-diffusion equation with the particle diffusivities assumed equal, and the flow velocity and the interactions potentials introduced in the effective flow velocity $\mathbf{U}^* = \mathbf{U}(Y,Z) - \beta\,\mathbf{D}(Y,Z) \cdot \boldsymbol{\nabla}_{\mathbf{R}}(\Psi(\mathbf{R}) + \Phi_1(Y) + \Phi_2(Z))$, see Section 5.1.

As the polymer-wall repulsion Φ_i is divergent on the walls, we are not able to solve numerically the advection-diffusion equation with COMSOL. The next step is to solve analytically. Our first attempt to eliminate the transport on the walls was to assume as a solution a convergence function $f(x,y,z) = Ce^{\Phi_1+\Phi_2}$ which only depends on the particle wall potentials and replacing C in Eq. (2.20). With this assumption, one arrives to the advection-diffusion equation for this convergent function f with a modified mobility tensor which depends on both particle wall potentials and therefore the diffusion tensor should also be modified and it is given by:

$$\mathbf{D}(y,z)/D = \begin{pmatrix} 2e^{-\Phi_1-\Phi_2} & 0 & 0 \\ 0 & e^{-\Phi_1-\Phi_2} & 0 \\ 0 & 0 & e^{-\Phi_1-\Phi_2} \end{pmatrix} \tag{5.9}$$

This modified diffusion tensor tends to zero on the walls. The same occurs when we attempt to solve with another convergence function like $f(x,y,z) = Ce^{\Phi_1+\Phi_2+\Psi}$, where $\mathbf{D}$ tends to zero on the walls. With this approximation we are also not able to solve numerically due to the singularity of the diffusion tensor. This is only possible if one moves the walls some quantity δ to eliminate the divergency in the region of interest.

Before doing the above approximation with COMSOL, we looked for another solution of the partial differential equation. We are interested to extend or expand the double layer near a wall. Then the new solution will be $C = f(x)e^{-\Phi_1-\Phi_2-\Psi}$. After some calculation we achieve that this is not a solution of the partial differential equation because the inhomogeneous solution depends on y and z and it should depend only on x. In conclusion, the advection-diffusion equation does not have an analytically solution.

We finally turn our attention to solve numerically the advection-diffusion equation Eq. (5.2). The analysis used with COMSOL is the steady-state convection and diffusion. We realize the following approximation: we reduce volume of integration,

i.e., we reduce the channel width and height by a small quantity δ to eliminate the divergence of the polymer-wall potential on the walls [see **Fig. 5.8 (a)**]. We solve

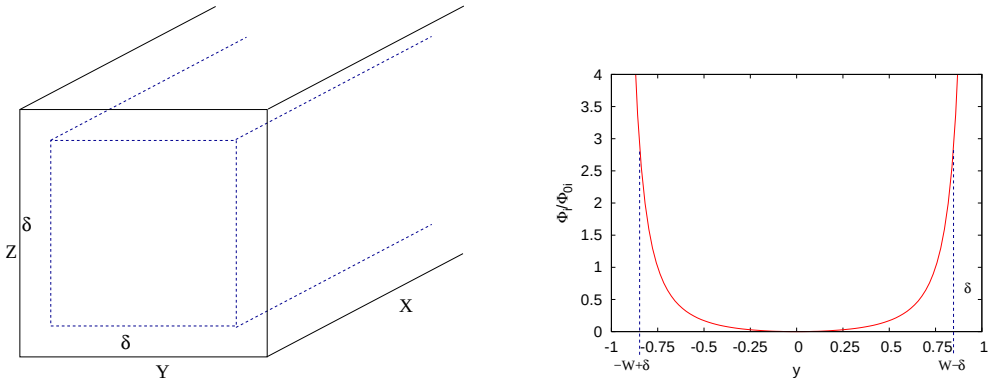

(a) (b)

Figure 5.8: (a) Reduction of the channel width and height (Y and Z direction) a quantity δ to eliminate the polymer-wall potential divergence; (b) Polymer-wall potential for the first particle as a function to the distance to the wall

with COMSOL being the walls now at $-W+\delta$ and $W-\delta$. We choose the smallest possible value of δ which allows for a numerical solution. We consider the diffusion coefficient of each particle equal $D_i = D_1 = D_2 = D$. We impose no-flux boundary conditions in the entire domain except in the two channel ends $X = \pm L/2$ where periodic conditions are imposed to allow for the motion of the particles.

We analyze the throughput for each particle Q_i as a function of the Pèclet number. The throughput of each particle Q_i is normalized by the Pèclet number. We consider four different cases with the channel length $2L = 10W$ and the interparticle interaction range $d = 2W$: (a) $W_1 = 0.25W$, $W_2 = 0.5W$ (b) $W_1 = 0.25W$, $W_2 = 0.75W$ (c) $W_1 = 0.5W$, $W_2 = 0.75W$ (d) $W_1 = 0.75W$, $W_2 = 0.75W$. We must vary δ for each case due to the dependence of the polymer-wall potential with the distance to the wall [see **Fig. 5.8 (b)**]. The behavior is shown in **Fig. 5.9**. We have represented Q_i/Pe as a function of Pe. The results show a reduction of the separation efficiency with flux in contrast with the HS model where flux enhanced the separation efficiency as shown in **Fig. 3.7 a**. This is the same behavior as for hard particle wall interaction potentials, see **Fig. 5.5**.

Hydrodynamic effect on polymers

As for colloidal suspensions, it is well-known the hydrodynamic interactions cannot be ignored in dilute solution and they contribute to the rheological behavior of these

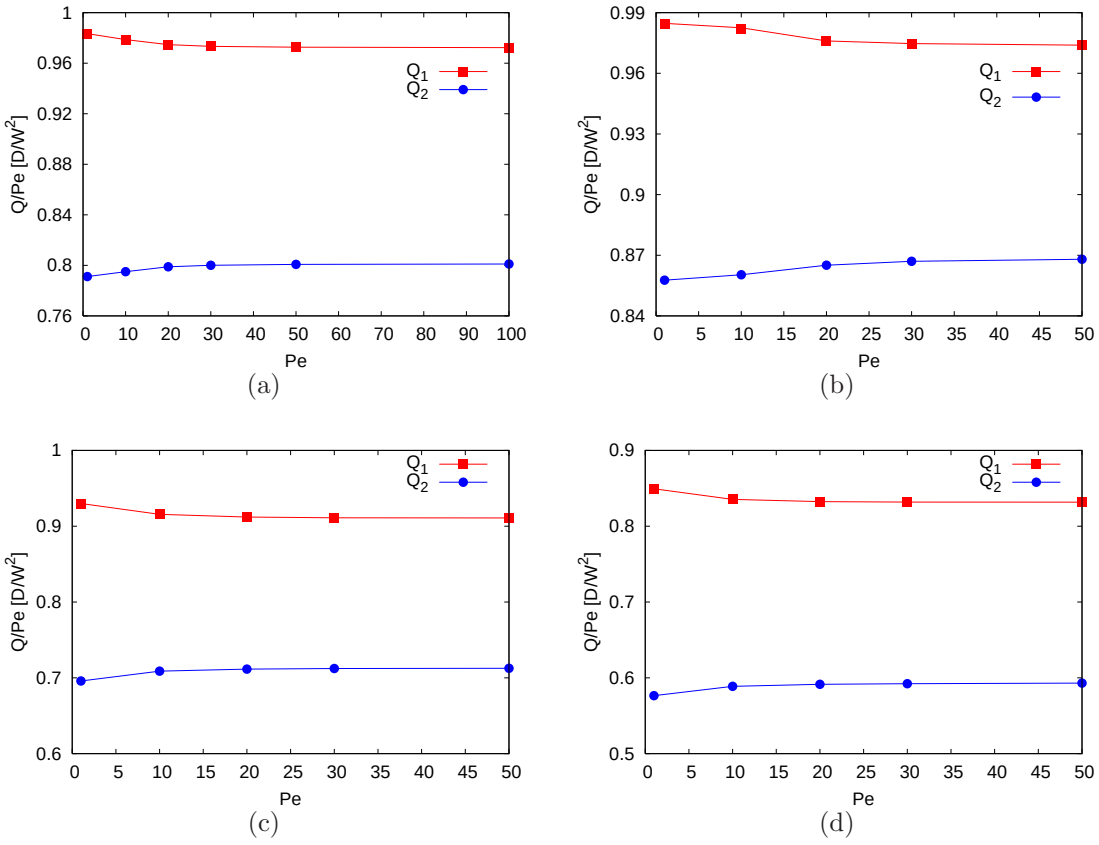

Figure 5.9: The throughput of each particle Q_i normalized to the Pèclet number as a function of Pe for a interparticle interaction range of $d = 2W$ and a channel length of $2L = 10W$: (a) $W_1 = 0.25W$, $W_2 = 0.5W$, $\delta = 0.4W$ (b) $W_1 = 0.25W$, $W_2 = 0.75W$, $\delta = 0.4W$ (c) $W_1 = 0.5W$, $W_2 = 0.75W$, $\delta = 0.22W$ (d) $W_1 = 0.75W$, $W_2 = 0.75W$, $\delta = 0.18W$

solutions. In polymer solutions, this is modelled by the Zimm model in good solvent which takes into account the hydrodynamic interactions between the polymer beads by using the Oseen tensor and predicts the dependency of the diffusion coefficient on the chain size as $D \sim R^1$ [33]. On the other hand, polymer-surface hydrodynamic interactions determine the polymer dynamics. But how is the form of the diffusion tensor for the case of two ideal chain polymers inside a channel? And which is the influence of HI in good solvents? At the moment these questions are still open.

The Zimm model has been already used to study the hydrodynamic interactions of DNA polymers in shear flow [51]. Previously the hydrodynamic interactions were studied for polymers immersed in a Newtonian flow with the method of induced forces [74]. More recently, Krüger [66] studied them for the case of a spherical particle in a polymer solution defining a time dependent diffusion coefficient $D(t)$ with two time limits, short and long corresponding with the short and long time diffusion coefficients respectively. He demonstrate that at time $t = 0$ the distribution of polymers around the sphere is still in equilibrium and the short time mobility is solely determined by the hydrodynamic force on the spherical particle. On the other hand, Winkler *et al* [20] have studied the hydrodynamic effect on a flexible polymer inside a channel and they saw how the hydrodynamic interactions are partially screened by the presence of the surfaces and there is still a pronounced migration.

As we have seen in Chapter 4, the hydrodynamic interactions between the particles and the walls alter the mobility tensor μ_{ij} and do not change the direct interactions potentials. Since we are neglecting the interaction among the beads or monomers, to take into account the hydrodynamic interactions between the polymer coils or between the polymer coil and the walls, we must choose an appropriate Oseen tensor. Once more we have to be sure about the dependence of the diffusion coefficient with R as in chapter 4. On the other hand, we are not able to study the influence and effect of the hydrodynamic interactions due to the impossibility at the moment of analytically solving the advection-diffusion equation and also due to the use of an uncontrolled numerically approximation.

5.3 Conclusion

This chapter focused on the understanding of the effect of direct interactions for polymers on the transport process. We have modeled the polymers as soft particles, but also as a hard core type for the case shown in Section 5.1

While for hard particles the only relevant parameters are the Pèclet number and the three lengths d_i and d, the situation is different for soft particles [103]. There,

the dimensionless potential strength $\Psi_o/(k_BT)$ is a fifth relevant parameter — the wall potential strengths Ψ_{0i} can be related to the lengths d_i. For hard particles, one only distinguishes between small Pèclet numbers $Pe \ll 1$, for which diffusion dominates over advection, and large Pèclet numbers $Pe \gg 1$, for which advection dominates. For soft particles, in addition one has to distinguish between weak and strong interactions potentials.

The dependence of the polymer-polymer interaction potential and the density profiles on the temperature was shown. By increasing $\beta\Psi_0$ the difficulty for the particles to pass each other increases till a value is reached at which it is no longer possible. Related to the density profiles, it was shown that independently of the value of $\beta\Psi_0$ both particles tends to move closer to the walls than at the middle of the channel.

We can conclude that independent of the temperature and the polymer size, the polymer particles tends to move closer to the channel walls in contrast to colloidal particles for which only the smaller ones tends to move closer to the channel walls. That is in contradiction with the results of Snook *et al* [119] for flexible polymers particles who find a greater probability of being in the centre of the channel than near the wall.

We have presented in Section 5.2 an approximation for the soft behavior in the case of the polymer-wall interaction potential. We have seen that it is not possible to analytically solve the advection-diffusion equation due to the divergence of the potentials. To have an idea of the throughput for each particle, we have realized an approximation of our integration volume to eliminate the divergence of the polymer wall potential on the walls. It was shown that the polymer separation efficiency is decreases with the flow.

Chapter 6

Summary and outlook

The purpose of this thesis has been to study the influence of the interactions and surface confinement on the transport process of suspended particles from a theoretical perspective. For the understanding of the transport process in the nano- and microscale, we focused on the dynamics of complex fluids, in particular colloidal suspensions and polymer solutions in a hydrodynamic chromatography setup. Since under confinement conditions the rheological properties of the complex fluids are affected both by the walls of the confinement as well as by the interactions present in the system, the focus of this work was mainly to assess the influence of interactions among the particles and between the particles and the channel walls.

Although the DDF formalism successfully describes mixtures of point particles with direct pair interactions and with many body interactions and advected in a solvent, we have showed how it fails when it comes to dense non-equilibrium steady states. In the first part of this thesis we discussed the failure of the dynamic density functional theory to describe a two dimensional problem: the non-equilibrium steady state of the transport properties of Brownian particles advected by a flowing solvent in a narrow channel. In particular for steady state systems, the solution of the DDFT equation is equal to the equilibrium density distribution and therefore the dynamics of the transport process are not described.

As a demonstration of the failure, we have analyzed the dynamics of a mixture of two colloidal suspended particles of different sizes diffusing and advected through a two dimensional narrow channel at low Reynolds numbers. We directly solved the Smoluchowski equation for two particles. We found that the DDFT fails to describe some aspects related to the transport properties. On the one hand we obtained a change of the density distribution across the channel induced by the solvent flow. This change cannot be detected by the DDF formalism due to the independency of the density distribution of the solvent flow in this theory. Additionally we observed

that the flux must be equal in the case that the particles cannot pass each other which is no attainable in the DDF formalism since it is impossible to input that the particles cannot pass each other. We related these discrepancies between our results and the DDF formalism to the grand canonical character of the density functional and to the equilibrium assumption for the correlations functions (the local equilibrium) within the framework of DDFT.

For further studies, it would be interesting to think about the limit of the DDFT. One has to think about how to overcome this problem, perhaps by truncating the BGY-hierarchy in the DDFT at higher orders or by factorizing higher correlation functions.

For these reasons, we resorted to a simple two-dimensional two-particle system in order to get insight into the transport of colloidal suspensions in thin channels. In order to study the transport phenomena, we start with the Smoluchowski equation for the non-equilibrium density probabilities also called drift-diffusion equation. On the other hand we focused on the understanding of the hydrodynamic chromatography mechanism and the transport process. For that purpose we calculated the fluxes and density profiles for each particle. We found a good agreement between our results and the basic picture of the mechanism underlying the hydrodynamic chromatography technique when we took only the direct interactions into account. The separation process is achieved because large particles are confined to channel center where the velocity is bigger such that they travel faster than smaller ones. An enhancement of the particles separation with solvent flux was observed. The reason is that smaller ones are pushed to the channel walls by larger ones. However, the separation efficiency is reduced by direct interactions: smaller ones are accelerated and bigger ones are decelerated in collisions.

Given that the hydrodynamic interactions are most important in dilute bulk systems and have more influence on the particle motion, it is significant to assess the effect of these solvent mediated interactions. First we looked at the influence of the hydrodynamic interaction among the particles. We solved the Stokes equation for a sphere fully immersed in a channel. In comparison with the bulk, we found that the flow field decays proportionally to $1/x^2$ with x being the distance along the channel axis. Therefore the effect on the other particles is smaller than in a bulk system where the flow field decays proportional to $1/x$. We also observed a faster decay for thinner channels. An important result for particle-particle hydrodynamic interactions is that they are significantly reduced by the lateral channel walls.
Finally we studied the hydrodynamic interactions with the confinement surface. As the two dimension hydrodynamics is ill defined, we modeled the basic effects of the

particle surface hydrodynamic interaction in a three dimensional problem: the diffusivity near the channel walls is reduced. In accordance with the corresponding results for a three-dimensional sphere near a wall, we take the diffusivity normal to the wall to vanish at contact and the diffusivity parallel to the wall to be reduced to 1/3 of the bulk diffusivity. The influence of the reduced mobility on the particle distribution within the channel as well as on the throughput and the separation efficiency is very small.

At this moment we do not have information about experimental investigations for two particles between parallel walls, and consequently we cannot do comparisons with experimental results. For further studies, it would be interesting to know exactly the dependence of the particle mobilities on the distance to the wall and on the distance to other particles for a better understanding of the hydrodynamic forces. It is well known that the separation of the hydrodynamic effect on the particles into particle-wall and particle-particle interactions is rather ambiguous.

Many colloidal particles are non-spherical. For these kinds of particles, it would be interesting to see the relevance of the hydrodynamic interactions. For a better understanding of the dynamics of real suspended particles, one can include in further studies their rotational motion. In our model we neglected the rotational motion because it is not relevant for spherical particles. If one considers asymmetric particles, it is well known that translational and rotational motion can induce a fluid flow velocity that affects other particles in their motion. One has to add a term depending of the rotational diffusion coefficient in the Smoluchowski equation (2.5) as shown in [110]. Hydrodynamic torque induced by hydrodynamic interactions has been calculated for hard spheres in [50].

It would be also interesting to consider charged particles instead of uncharged particles. If the particles are charged then the electrostatic interaction between the charged spheres and the walls must be taken into account. One have two cases to analyze: a) when the suspended particles and the surface confinement have different electric charges, then an attractive force between them exists, and b) when both — particles and wall — have the same charge, then the particles would be repelled by the surface. This phenomenon is generated by a double layer near the particles and the wall. The main challenge here is to take into account the dynamics of this double layer in the solvent flow.

In the last part of this thesis, we draw special attention to a more realistic case: the transport of polymer solutions in narrow channels. For that purpose we modeled the polymers as soft point particles. While for hard particles the only relevant parameters are the Peclet number and the hard core interaction distances between the

particles and the wall as well as among the particles, the situation is different for soft particles [103]. There, the dimensionless inter-particle interaction potential strength (normalized by the thermal energy) is a fifth relevant parameter — the wall potential strengths can be related to particle-wall hard core distances. For hard particles, one only distinguishes between small Peclet numbers $Pe \ll 1$, for which diffusion dominates over advection, and large Peclet numbers $Pe \gg 1$, for which advection dominates. For soft particles, in addition one has to distinguish between weak and strong interactions potentials.

First, we analyzed the dependence of the system on the interaction potential between the polymers, which we model as a Gaussian. By increasing the interaction strength, the difficulty for the particles to pass each other increases and for large enough values it is hardly possible for them to pass each other. Additionally, by increasing the interaction strengh both particles — the smaller particle and the larger one — move closer to the channel walls. But for weak potentials, we observed that the large particle is homogenously distributed across the channel while the small particle tends to move closer to the channel walls. The last result is inconsistent with the simulation by Winkler. The explanation for this discrepancy can come from our disregarding of the hydrodynamic interactions and of the internal structure of the polymer coil.

Concerning to the interaction potential of the polymers with the walls, we analyzed two cases. The first case considered the interaction potential as a hard core type. We observed that the behavior of the polymer is quite different than the behavior of hard spheres. The particles were found to be closer to each other in comparison with colloidal particles and this effect is strong as the flow velocity increases. Finally, we considered the interaction potential as a soft type. We modeled the wall interactions as that of an ideal chain diffusing in a good solvent and neglecting the dependency of the solvent on the temperature. We chose this potential so that it mimicked the entropic repulsion from a solid wall. We found some problems to solve the corresponding Smoluchowski equation both analytically and numerically due to the divergence of this potential at the walls. We used an uncontrolled approximation to eliminate the divergence on the walls by reducing the volume of integration. We observed the same behavior on the separation of particles as in the case of hard core type interaction potential.

Once the understanding of the transport process corresponding to a mixture of two suspended particles is achieved, another interesting thing would be to extend the studies to N-body systems and to time dependent problems, i.e., to transient states. To take a step forward in the understanding on the transport process, one can study

a mixture of particles (colloids and polymers).

Zusammenfassung

Die vorliegende Arbeit behandelt den Bereich der statistischen Mechanik der komplexen Flüssigkeiten. Die Motivation war es den Einfluss von Wechselwirkungen und den Effekt der Einschreibung der Geometrie auf dem Transportprozess von suspendierten Partikeln aus theoretische Sicht zu studieren. Für das Verstehen des Transportprozesses auf der Nano- und der Mikroskala wurde sich auf die Dynamik von Weicher Materie, insbesondere die kolloidale Suspensionen und Polymer-Lösungen durch die hydrodynamischen Chromatographie konzentriert. In eingeschränkten Geometrien werden die rheologischen Eigenschaften der komplexe Flüssigkeiten beide durch die Wände sowie durch die Wechselwirkungen im System beeinflusst. Diese Arbeit ist fokussierte darauf, den Einfluss von Wechselwirkungen zwischen den Partikeln und den Kanalwänden ebenso wie die Wechselwirkung zwischen Partikeln abzuschätzen.

Obwohl die dynamische Dichtefunktionaltheorie (DDFT) erfolgreiche Mischungen von Punktteilchen mit direkten Wechselwirkungen und advektiert in einem Lösungsmittel beschreibt, haben wir den Misserfolg der DDFT beim dichtem Nichtgleichgewicht des stationären Zustandes aufgezeigt. In dem ersten Teil der Arbeit erläutern wir den Misserfolg der DDFT am Beispiel eines zweidimensionalen Problems: der Stationäre Nichtgleichgewichtszustand von Brownschen Teilchen advektiert durch ein Lösungsmittel im schmalen Kanal. Insbesondere für den stationären Zustand, ist die Lösung von der DDFT Gleichung durch die Gleichgewichtslösung beschrieben. Die Dynamik des Transportprozesses wird nicht dargestellt.

Wie der Nachweis von dem Misserfolg zeigt, haben wir die Dynamik von einer Mischung aus zwei Kolloidteilchen verschiedener Größe welche durch einen zweidimensional schmalen Kanal bei niedrigen Reynolds-Zahlen diffundieren analysieren. Wir lösten direkt die Smoluchowski Gleichung für zwei Teilchen. Wir fanden dass die DDF Theorie manche Aspekte des Transportes nicht beschreibt. Einerseits erhielten wir eine Strömungsinduzierte Änderung der Dichteverteilung ins Kanal. Diese Änderung kann der DDF Formalismus aufgrund der Unabhängigkeit der Dichteverteilung von Lösungsmittelfluss in dieser Theorie nicht reproduzieren. Zusätzlich beobachteten wir, dass die Transportrate gleich sein muss in dem Fall, dass die Partikeln

einander nicht überholen können. Dieses ist im DDF Formalismus nicht erreichbar da es unmöglich ist, die Tatsache, dass Teilchen sich nicht überholen können zu implementieren. Wir brachten diese Diskrepanzen zwischen unseren Ergebnissen und dem DDF Formalismus in Verbindung mit den großkanonischen Charakter des Funktionals und mit der lokalen Gleichgewichtsannahme für die Korrelationsfunktionen (das lokale Gleichgewicht) innerhalb der DDFT.

Aus diesen Gründen beschränkten wir uns auf ein einfaches zweidimensionales Zwei-Teilchen-System, um den Transport von den kolloidalen Suspensionen in dünnen Kanälen zu verstehen. Um die Transportphänomene zu studieren, fingen wir mit der Smoluchowski Gleichung für die Wahrscheinlichkeitsdichte im nicht-Gleichgewicht, auch Advektions-Diffusions-Gleichung genannt, an. Andererseits konzentrierten wir uns auf das Verstehen des Mechanismus der hydrodynamischen Chromatographie und des Transportprozesses. Für dieses Ziel berechneten wir die Transportrate und die Dichte Verteilungen für jeden Teilchen. Wir fanden eine gute Übereinstimmung zwischen unseren Ergebnissen und dem grundlegenden Bild des Mechanismus der hydrodynamischen Chromatographie wenn wir nur die direkten Wechselwirkungen betrachteten. Die Auftrennung nach Teilchengröße wird erreicht, weil die großen Partikel auf das Zentrum des Kanals eingeschränkt sind, wo die Lösungsmittel-Geschwindigkeit größer ist so dass sie sich schneller bewegen als die kleineren. Eine Verbesserung der Auftrennung mit den Lösungsmittelfluss wurde beobachtet. Der Grund ist, dass die kleineren durch die größen Teilchen an die Kanalwänden gedrückt werden. Allerdings wird die Trennungseffizienz durch direkte Wechselwirkungen reduziert: kleinere Teilchen werden beschleunigt und größere werden in Kollisionen verlangsamt.

Hydrodynamische Wechselwirkungen sind in verdünnten Lösungen und für von Wänden sehr wichtig. Da sie Einfluss auf die Teilchenbewegungen haben, es ist wichtig den Effekt von diesen Lösungsmittelinduzierten Wechselwirkungen zu berechnen. Erst betrachten wir den Einfluss von hydrodynamischen Wechselwirkungen zwischen Partikeln. Wir lösten die Stokes Gleichung für eine Kugel in einem Kanal. Im Vergleich zum Volumen, fanden wir, dass das Strömungsfeld proportional zu $1/x^2$ abfällt, wobei x der Abstand entlang der Kanalachse ist. Deshalb ist der Einfluss auf die anderen Partikel kleiner als im Volumen wo das Strömungsfeld proportional zum $1/x$ abfällt. Außerdem beobachteten wir einen schnelleren Abfall bei dünneren Kanälen. Ein wichtiges Ergebnis in Bezug auf die hydrodynamischen Wechselwirkungen zwischen den Teilchen ist, dass sie durch die Kanalwände signifikant reduziert werden.
Am Ende studierten wir die hydrodynamischen Wechselwirkungen mit den Kanalwänden. Weil die zweidimensionale Hydrodynamik schlecht definiert ist, wählten wir für die grundlegenden Effekte der hydrodynamischen Wechselwirkung zwischen den

Teilchen und der Kanalwand in einem dreidimensionalen Problem eines phänomenologischen Ansatz: Die Diffusivität in der Nähe der Kanalwände wurde reduziert. In Übereinstimmung mit den entsprechenden Ergebnissen für ein dreidimensionales System in der Nähe von einer Wand nehmen wir an, dass die Diffusivität normal zur Wand am Kontakt verschwindet und dass die Diffusivität parallel zur Wand auf 1/3 des Volumenwertes reduziert wird. Der Einfluss der reduzierten Mobilität auf die Verteilung der Teilchen innerhalb des Kanals sowie auf die Transportrate und Effizienz der Trennung ist sehr klein.

In dem letzten Teil dieser Arbeit lenkten wir die spezielle Aufmerksamkeit auf einen realistischeren Fall: den Transport von Polymerlösungen in schmalen Kanälen. Zu diesem Zweck modellierten wir die Polymere als weiche Punkt-Teilchen. Während für harte Teilchen die einzigen relevant Parameter die Pèclet-Zahl und die harten Wechselwirkungsabstände zwischen den Teilchen und der Wand sowie zwischen den Teilchen sind, ist die Situation anders für weiche Teilchen. Dort ist, die dimensionlose Stärke der Wechselwirkung zwischen den Teilchen (bezogen auf die thermische Energie) ein fünfter relevanter Parameter — die Wandpotenzialstärken ergeben sich aus den Teilchen-Wand-Wechselwirkungsabständen. Für harte Partikel unterscheidet man nur zwischen kleiner Pèclet-Zahlen $Pe << 1$, wo die Diffusion über Advektion dominiert, und grosser Pèclet-Zahl $Pe >> 1$, wo die Advektion dominiert. Für weiche Partikeln muss man außerdem zwischen schwachen und starken Wechselwirkungspotenzialen unterscheiden.

Zunächst analysierten wir die Abhängigkeit des Systems von Wechselwirkungspotenzial zwischen den Polymern, welches wir als Gauß'sch modellieren. Bei steigender Wechselwirkungskraft steigt die Schwierigkeit für die Partikel einander zu passieren und für große genug Werte ist es für diese kaum möglich um einander zu passieren. Zusätzlich, bei größerer Wechselwirkungskraft bewegen sich beide Partikel — die kleineren Partikel und die größere — näher bei den Kanalwänden. Aber für schwache Potenziale bemerkten wir, dass das große Partikel über den Kanal homogen verteilt wird, während das kleiner Partikel dazu tendiert sich näher zu den Kanalwänden zu bewegen. Das letzte Ergebnis war mit der Simulation durch Winkler inkonsequent. Ein Erklärung dieses Unterschieds kann sein, dass wir die hydrodynamischen Wechselwirkungen und der innere Struktur des Polymerknäuels vernachlässigt haben.

In Bezug auf das Wechselwirkungspotenzial des Polymers mit den Wänden analysierten wir zwei Fälle. Der erste Fall betrachtete das Wechselwirkungspotenzial als das einer harten Wand. Wir beobachten, dass das Verhalten des Polymers sehr verschieden von das Verhalten von harten Kugeln ist. Man hat gefunden, dass die Polymerteilchen einander näher waren als die kolloidalen Teilchen und dieser Effekt

ist stärker je höher die Strömungsgeschwindigkeit des Lösungsmittel ist. Schließlich betrachteten wir ein weiches Wechselwirkungspotenzial. Wir modellierten die Wandwechselwirkungen als die einer idealen Kette, die sich in einem guten Lösungsmittel befindet und wir vernachlässigen die Abhängigkeit des Lösungsmittels von der Temperatur. Wir wählten dieses Potenzial, so dass es die entropische Abstoßung von einer festen Wand imitiert. Wir fanden einige Probleme bei der Lösung der Smoluchowski Gleichung, sowohl analytisch als auch numerisch, aufgrund der Divergenz dieses Potenzials an den Wänden. Wir benutzen eine nicht kontrollierte Näherung, um die Divergenz an den Wänden zu eliminieren, indem wir das Integrationsvolumen reduzierten. Wir beobachteten den selben Einfluss des Wandpotentials auf die Trennung von Teilchen wie im Fall des harten Wandpotentials.

Resumen

El presente trabajo esta enmarcado en el ámbito de la Mecánica Estadística de fluidos complejos confinados. El propósito fue estudiar la influencia de las interacciones y el efecto del confinamiento en el proceso de transporte de partículas suspendidas desde un punto de vista teórico. Para comprender el proceso de transporte a escala nano y micro, nos concentramos en la dinámica de fluidos complejos, en particular suspensiones coloidales y soluciones poliméricas mediante cromatografía hidrodinámica. Como bajo condiciones de confinamiento las propiedades reológicas de los fluidos complejos se ven afectadas tanto por las paredes que confinan el sistema así como por las interacciones presentes dentro del sistema, este trabajo se enfocó principalmente en evaluar la influencia de las interacciones entre partículas así como la influencia de las interacciones entre las partículas y las paredes de canal.

Aunque la teoría del funcional de la densidad dinámico (DDFT) describe con éxito mezclas de partículas con interacciones directas entre dos partículas puntuales y entre varias partículas y transportadas (adveccionadas) en un disolvente, mostramos como esta teoría falla a la hora de describir estados estacionarios densos fuera del equilibrio. En la primera parte de esta tesis explicamos el fracaso de la teoría del funcional de la densidad dinámico para describir un problema bidimensional: las propiedades de transporte de partículas brownianas disueltas y transportadas por un disolvente en un canal estrecho y en un estado estacionario fuera del equilibrio. En particular para sistemas estacionarios, la solución de la ecuación DDFT es igual a la distribución de densidad de equilibrio y por lo tanto la dinámica del proceso de transporte no esta descrita.

Como demostración del fracaso de la teoría, hemos analizado la dinámica de una mezcla de dos partículas coloidales de diferentes tamaños suspendidas y transportadas en un canal estrecho en dos dimensiones para números de Reynolds bajos. Resolvimos directamente la ecuación de Smoluchowski para dos partículas. Encontramos que la DDFT no describe algunos aspectos relacionados con las propiedades de transporte. Por una parte obtuvimos un cambio de la distribución de densidad a través del canal inducido por el flujo del disolvente. Este cambio no puede ser descrito por el

formalismo DDF debido a la independencia de la distribución de densidad del flujo del disolvente en esta teoría. Además, observamos que el flujo debe ser igual en el caso de que las partículas no se pueden adelantar lo cual no es alcanzable en el formalismo del DDF debido a la imposibilidad de introducir que las partículas no se pueden adelantar. Nosotros relacionamos estas discrepancias entre nuestros resultados y los resultados dados por la teoría DDF con el carácter canónico del funcional de la densidad y con la aceptación de equilibrio local para las funciones de correlación (equilibrio local) dentro del marco de la DDFT.

Por estos motivos, nos circunscribimos a un sistema simple bidimensional de dos partículas con la finalidad de entender el transporte de suspensiones coloidales en canales estrechos. Para estudiar los fenómenos de transporte preferimos partir de la ecuación de Smoluchowski para las probabilidades fuera de equilibrio denominada también ecuación de difusión advección. Por otra parte, nos concentramos en el entendimiento del mecanismo hidrodinámico de cromatografía y el proceso de transporte. Para dicho propósito calculamos el porcentaje de particulas transportadas y las distribuciones de densidad para cada partícula. Encontramos concordancia entre nuestros resultados y la descripción básica del mecanismo de la técnica de cromatografía hidrodinámica cuando tomamos solamente en cuenta las interacciones directas. El proceso de separación se logra porque las partículas grandes están confinadas en el centro del canal donde la velocidad del flujo es mayor por lo cual estas viajan más rápido que las partículas pequeñas. Se observó un aumento de la separación entre partículas dentro del canal al aumentar el flujo. Esto es debido a que las partículas pequeñas son empujadas hacia las paredes del canal por las partículas grandes. Sin embargo, la eficacia de separación se ve reducida por las interacciones directas: las partículas más pequeñas son aceleradas y las más grandes son desaceleradas en las colisiones.

Considerando que las interacciones hidrodinámicas son las más importantes en sistemas diluidos en bulto y tienen más influencia en el movimiento de partículas, esto es significativo para evaluar el efecto de estos disolventes mediante interacciones. Primero nos fijamos en la influencia de la interacción hidrodinámica entre las partículas. Resolvimos la ecuación de Stokes para una esfera totalmente sumergida en un canal. En comparación con el bulto, encontramos que el campo de flujo disminuye proporcionalmente como $1/x^2$ siendo x la distancia a lo largo del eje del canal. Por lo tanto, la influencia en las otras partículas es más pequeña que en un sistema de bulto dónde el campo de flujo decae proporcional al $1/x$. Además observamos una disminución más rápida para canales más estrechos. Un resultado importante para las interacciones hidrodinámicas entre partículas consiste en que estas son reducidas

considerablemente por las paredes laterales del canal.
Finalmente, estudiamos las interacciones hidrodinámicas con las paredes del canal. Como la hidrodinámica en dos dimensiones no esta bien definida, modelamos los efectos básicos de la interacción hidrodinámica entre la partícula y la pared en un problema tridimensional: la difusividad en las proximidades de las paredes de canal es reducida. De acuerdo con los resultados correspondientes para una esfera tridimensional cerca de una pared, tomamos la componente normal de la difusividad con la pared de tal forma que desaparezca al contacto y la componente paralela de la difusividad con la pared de tal forma que se ve reducida a 1/3 de la difusividad correspondiente al bulto. La influencia de la movilidad reducida en la distribución de las partículas dentro del canal así como en el rendimiento de transporte y en la eficacia de separación es muy pequeña.

En la última parte de este trabajo, dirigimos nuestra atención hacia un caso más realista: el transporte de soluciones poliméricas en canales estrechos. Para dicho objetivo modelamos los polímeros como partículas de punto blandas. Mientras que para partículas duras los únicos parámetros relevantes son el número de Pèclet y las distancias de interacción entre las partículas y la pared así como entre las partículas, la situación es diferente para partículas blandas. Allí, la intensidad de la interacción entre partículas (que es una magnitud adimensional) normalizada por la energía termica es un quinto parámetro relevante—las intensidades del potencial con la pared pueden estar relacionadas con la distancia entre la pared y la partícula de esferas duras. Para partículas duras, se distingue únicamente entre números de Pèclet pequeños $Pe << 1$, donde la difusión domina sobre la advección, y números de Pèclet grandes $Pe >> 1$, donde la advección predomina. Para partículas blandas, además se tiene que distinguir entre potenciales de interacciones débiles y fuertes.

En un primer lugar, analizamos la dependencia del sistema con el potencial de interacción entre los polímeros, que modelamos como gaussiano. Aumentando la fuerza de interacción, la dificultad de que las partículas se puedan adelantar entre ellas aumenta y para valores bastante grandes apenas es posible que las partículas puedan adelantarse. Además, aumentando la intensidad de las interacciones, ambas partículas—la partícula pequeña y la grande—se aproximan a las paredes del canal. Pero para potenciales débiles, observamos que la partícula grande se encuentra distribuida homogéneamente a través del canal mientras la partícula pequeña tiende a aproximarse a las paredes del canal. El último resultado es inconsecuente con la simulación realizada por Winkler. La explicación de esta discrepancia puede venir por haber despreciado las interacciones hidrodinámicas y la estructura interna del ovillo polimérico en nuestro análisis.

En relación al potencial de interacción de los polímeros con las paredes, analizamos dos casos. En el primer caso consideramos el potencial de interacción como una interacción dura de exclusión. Observamos que el comportamiento del polímero es completamente diferente al comportamiento de las esferas duras. Se encontró que las partículas se encuentran más próximas entre sí en comparación con las partículas coloidales y este efecto es más fuerte según aumentamos la velocidad de flujo. Finalmente, consideramos un potencial de interacción blando. Modelamos las interacciones con la pared como las de una cadena ideal difundiéndose en un buen disolvente y despreciamos la dependencia del disolvente con la temperatura. Elegimos este potencial de modo que imitara la repulsión entropica de una pared sólida. Encontramos algunos problemas para resolver la ecuación de Smoluchowski tanto analíticamente como numéricamente debido a la divergencia del potencial en las paredes. Usamos una aproximación incontrolada para eliminar la divergencia en las paredes reduciendo el volumen de integración. Observamos el mismo comportamiento sobre la separación de partículas como en caso del potencial de interacción de tipo duro.

Bibliography

[1] *Comsol Multiphysics*, COMSOL AB (2008), URL `file:///server/systems/Linux/femlab3.5/doc/plain/helpdesk.htm`.

[2] L. Almenar and M. Rauscher (2010), in preparation.

[3] A. J. Archer, J. Phys.: Condens. Matter **18**, 5617 (2006).

[4] A. J. Archer and R. Evans, J. Phys.: Condens. Matter **14**, 1131 (2002).

[5] A. J. Archer and R. Evans, J. Chem. Phys. **121**, 4246 (2004).

[6] A. J. Archer, P. Hopkins, and M. Schmidt, Phy. Rev. E **75**, 040501(R) (2007).

[7] S. Asakura and F. Oosawa, J. Polym. Sci. **33**, 183 (1958).

[8] G. Batchelor, J. Fluid Mech. **52**, 245 (1972).

[9] G. Batchelor, *An introduction to fluid dynamics* (Cambridge university press, Cambridge, UK, 2000).

[10] M. A. Bevan and D. C. Prieve, J. Chem. Phys. **113**, 1228 (2000).

[11] S. Bhattacharya, J. Blawzdziewicz, and E. Wajnryb, J. Fluid Mech. **541**, 263292 (2005).

[12] S. Bhattacharya, J. Blawzdziewicz, and E. Wajnryb, Phy. Fluids **18**, 053301 (2006).

[13] R. B. Bird, W. E. Stewart, and E. N. Lightfoot, *Transport phenomena* (Wiley, New York, 2007).

[14] M. T. Blom, E. Chmela, J. G. E. Gardeniers, R. Tijssen, M. Elwenspoek, and v. A, Sensors and Actuators B **82**, 111 (2002).

[15] P. Bolhuis and A. Louis, Macromolecules **35**, 1860 (2002).

[16] P. Bolhuis, A. Louis, J. Hansen, and E. Meijer, J. Chem. Phys. **114**, 4296 (2001).

[17] W. Briels (1998), theory of polymer dynamics. Lecture notes.

[18] I. N. Bronštejn and K. A. Semendajaev, *Taschenbuch der Mathematik* (Teubner Verlagsgesellschaft, Stuttgart, Leipzig, 1991), 25th ed.

[19] H. Bruus, *Theoretical Microfluidics* (Oxford University Press, New York, 2008).

[20] L. Cannavacciuolo, R. Winkler, and G. Gomper, Europhys. Lett. **83**, 34007 (2008).

[21] A. Casanovas Vázquez (2002–2003), lecture Notes. Universidad de Valencia.

[22] E. F. Casassa, Macromolecules **17**, 601604 (1984).

[23] G.-L. Chan and R. Finken, Phy. Rev. Lett. **94**, 183001 (2005).

[24] R. Chelakkot, R. Winkler, and G. Gompper (2010), arXiv:1006.4485v1.

[25] J. Crocker, J. Chem. Phys. **106**, 2837 (1997).

[26] J. Cuesta, Revista Española de Física **20**, 13 (2006).

[27] N. de Bruijn, *Asimptotic methods in analysis* (North-Holland Publ., 1961), 2nd ed.

[28] P.-G. de Gennes, *Scaling Concepts in Polymer Physics* (Cornell University Press, London, United Kingdom, 1979).

[29] B. Derrida, S. Janowsky, J. Lebowitz, and E. Speer, J. Stat. Phys. **73**, 813 (1993).

[30] J. K. Dhont, *An Introduction to Dynamics of Colloids*, vol. II of *Studies in Interface Science* (Elsevier, Amsterdam, 1996).

[31] G. Doetsch, *Handbuch der Laplace-Transformation*, vol. I, II and III (Birkhäuser Verlag Basel, Basel, 1971).

[32] M. Doi, *Introduction to polymer physics* (Oxford University Press, New York, 1996).

[33] M. Doi and S. Edwards, *The Theory of Polymer Dynamics* (Oxford University Press, Oxford, 1986).

[34] Z. Donkó, J. Goree, P. Hartmann, and B. Liu, Phys. Rev. E **79**, 026401 (2009).

[35] E. R. Dufresne, D. Altman, and D. G. Grier, Europhys. Lett. **53**, 264 (2001).

[36] E. R. Dufresne, T. M. Squires, M. P. Brenner, and D. G. Grier, Phy. Rev. Lett. **85**, 3317 (2000).

[37] J. Dzubiella and C. N. Licos, J. Phys.: Condens. Matter **15**, L147 (2003).

[38] J. Dzubiella, H. Löwen, and C. N. Likos, Phy. Rev. Lett. **91**, 248301 (2003).

[39] M. H. Ernst, B. Cichocki, J. R. Dorfman, J. Sharma, and H. van Beijeren, Journal of Statistical Physics **18**, 237 (1978).

[40] L. Faucheux and A. Libchaber, Phy. Rev. E **49**, 5158 (1994).

[41] B. U. Felderhof, J. Phys. A: Math. Gen. **11**, 929 (1978).

[42] B. U. Felderhof, J. Phys. A: Math. Gen. **11**, 921 (1978).

[43] P. Flory and W. Krigbaum, J. Chem. Phys. **18**, 1086 (1950).

[44] L. D. Fosdick, *Molecular Dynamics: An Introduction*, High Performance Scientific computing. University of Colorado at Boulder (1995).

[45] Fundación Telefónica.

[46] D. G. Grier and S. H. Behrens, in *Electrostatic Effects In Soft Matter And Biophysics*, edited by P. K. C. Holm and R. Podgornik, The Nato Advanced Study Institute, Les Houches (Kluwer, Dordrecht, 2001).

[47] J. Happel and H. Brenner, *Low Reynolds number hydrodynamics* (Noodhoff International Publishing, The Netherlands, 1973), second revised ed.

[48] R. Hunter, *Foundations of Colloid Science* (Oxford University Press, 2001), 2nd ed.

[49] M. Isobe, Phys. Rev. E **77**, 021201 (2008).

[50] D. Jeffrey and Y. Onishi, J. Fluid Mech. **139**, 261 (1984).

[51] R. M. Jendrejack, J. J. de Pablo, and M. D. Graham, J. Chem. Phys. **116**, 7752 (2002).

[52] R. Jones, Physica A **92A**, 545 (1978).

[53] R. A. Jones, *Soft Condensed Matter* (Oxford University Press, New York, 2002).

[54] A. Jusufi, J. Dzubiella, C. Likos, C. von Ferber, and H. Löwen, J. Phys.: Condens. Matter **13**, 6177 (2001).

[55] G. Karniadakis, A. Beskok, and N. Aluru, *Interdisciplinary applied mathematics. Microflows and Nanoflows: Fundamentals and Simulation*, vol. 29 (Springer, New York, 2005).

[56] T. Kawakatsu, *Statistical Physics of Polymers* (Springer-Verlag, Germany, 2001).

[57] K. Kawasaki, Physics Letters A **34**, 12 (1971).

[58] K. Kawasaki, Physica A **208**, 35 (1994).

[59] K. Kawasaki, J. Phys.: Condens. Matter **12**, 6343 (2000).

[60] K. Kawasaki, J. Phys.: Condens. Matter **14**, 6343 (2002).

[61] K. Kawasaki, J. Stat. Phys. **110**, 1249 (2003).

[62] K. Kawasaki and K. Fuchizaki, J. Phys.: Condens. Matter **14**, 12203 (2002).

[63] S. Kim and S. J.Karrila, *Microhydrodynamics: Principles and Selected Applications* (Dover Publications, Inc, Mineola, New York, 2005).

[64] M. Krüger, Master's thesis, Universität Stuttgart (2006).

[65] M. Krüger and M. Rauscher, J. Chem. Phys. **127**, 034905 (2007).

[66] M. Krüger and M. Rauscher, J. Chem. Phys. **131**, 094902 (2009).

[67] D. Langbein, J. Phys. A:Math. Nucl. Gen. **6**, 1149 (1973).

[68] D. Langbein, *Theory of Van der Waals Attraction* (Springer-Verlag, New York, 1974).

[69] D. Langbein, Advances in Colloid and Interface Science **46**, 91 (1993).

[70] E. Lauga and T. M. Squires, Physics of Fluids **17**, 103102 (2005).

[71] C. N. Likos, Phys. Rep. **348**, 267 (2001).

[72] B. Lin, J. Yu, and S. Rice, Phy. Rev. E **62**, 3909 (2000).

[73] L. Lobry and N. Ostrowsky, Phy. Rev. B **53**, 12050 (1996).

[74] M. López de Haro, A. Pérez-Madrid, and J. Rubí, J. Chem. Phys. **88**, 7964 (1988).

[75] A. Louis, P. Bolhuis, and J. Hansen, Phy. Rev. E **62**, 7961 (2000).

[76] A. Louis, P. Bolhuis, J. Hansen, and E.J.Meijer, Phy. Rev. Lett. **85**, 2522 (2000).

[77] A. Louis, P. Bolhuis, E. Meijer, and J. Hansen, J. Chem. Phys. **116**, 10547 (2002).

[78] H. Löwen and J. Dzubiella, Faraday Discuss. **123**, 99 (2003).

[79] J. Lyklema, *Fundamentals of Interface and Colloid Science*, vol. I: Fundamentals (Academic Press, London, San Diego, 1991).

[80] J. Lyklema, *Fundamentals of Interface and Colloid Science*, vol. II: Solid-Liquid Interfaces (Academic Press, London, San Diego, 1995).

[81] S. Mafé and J. de la Rubia, *Manual de Física Estadística* (Publicacions Universitat de València, Valencia, Spain, 1998).

[82] U. M. B. Marconi and S. Melchionna, J. Chem. Phys. **131**, 014105 (2009).

[83] U. M. B. Marconi and P. Tarazona, J. Chem. Phys. **110**, 8032 (1999).

[84] U. M. B. Marconi and P. Tarazona, J. Phys.: Condens. Matter **12**, A413 (2000).

[85] U. M. B. Marconi and P. Tarazona, J. Chem. Phys. **124**, 164901 (2006).

[86] U. M. B. Marconi and P. Tarazona, J. Chem. Phys. **128**, 164704 (2008).

[87] U. M. B. Marconi, P. Tarazona, F. Cecconi, and S. Melchionna, J. Phys.: Condens. Matter **20**, 494233 (2008).

[88] R. M. Mazo, *Brownian Motion: Fluctuations, Dynamics and Applications* (Clarendon Press, Oxford, 2002).

[89] J. Meiners and S. Quake, Phy. Rev. Lett. **82**, 2211 (1999).

[90] R. Mukhopadhyay, Analytical Chemestry **78**, 73797382 (2006).

[91] M. Müller, in *Comprehensive Polymer Science* (Elsevier, Oxford, UK, 2010).

[92] J. Ortiz de Zárate, R. Pérez Cordón, and J. Sengers, Physica A **291**, 113 (2001).

[93] J. Ortiz de Zárate and J. Sengers, Physica A **300**, 25 (2001).

[94] P. C. Painter and M. M. Colema, *Fundamentals of Polymer Science: An Introductory Text* (CRC Press, Florida, 1997), 2nd ed.

[95] F. Penna, J. Dzubiella, and P. Tarazona, Phy. Rev. E **68**, 061407 (2003).

[96] F. Penna and P. Tarazona, J. Chem. Phys. **119**, 1766 (2003).

[97] R. Pesché and G. Nägele, Europhys. Lett. **51**, 584 (2000).

[98] R. Pesché and G. Nägele, Phy. Rev. E **62**, 5432 (2000).

[99] Y. Pomeau and P. Rsibois, Physics Reports **19**, 63 (1975).

[100] Portal für Organische Chemie (2008), www.organische-chemie.ch.

[101] S. Prakash, A. Piruska, E. N. Gatimu, P. W. Bohn, J. V. Sweedler, and M. A. Shannon, IEEE Sensors Journal **8**, 441 (2008).

[102] A. Pralle, E.-L. Florin, E. Stelzer, and J. Hörber, Appl. Phys. A **66**, S71 (1998).

[103] M. Rauscher and L. Almenar, J.Phys.: Condens. Matter. in print (2010).

[104] M. Rauscher, A. Domínguez, M. Krüger, and F. Penna, J. Phys.: Condens. Matter **127**, 244906 (2007).

[105] M. Reichert and H. Stark, Phy. Rev. E **69**, 031407 (2004).

[106] P. Reuland and B. U. Felderhof, **93A**, 465 (1978).

[107] M. Rex, C. N. Likos, H. Löwen, and J. Dzubiella, Mol. Phys. **104**, 527 (2006).

[108] M. Rex and H. Löwen, Phy. Rev. Lett. **101**, 148302 (2008).

[109] M. Rex and H. Löwen, Eur. Phys. J. E **28**, 139 (2009).

[110] M. Rex, H. H. Wensink, and H. Löwen, Phy. Rev. E **76**, 021403 (2007).

[111] K. Riley, M. Hobson, and S. Bence, *Mathematical Methos for Physics and Engineering: A Comprehensive Guide.* (Cambridge University Press, Cambridge, 2006), 3rd ed.

[112] H. Risken, *The Fokker-Planck equation: methods of solution and applications*, vol. 18 of *Springer Series in Synergetics* (Springer, Berlin, 1984), 2nd ed.

[113] Y. Rosenfeld, Phy. Rev. A **42**, 5978 (1989).

[114] Y. Rosenfeld, Phy. Rev. Lett. **63**, 980 (1989).

[115] C. P. Royall, J. Dzubiella, M. Schmidt, and A. van Blaaderen, Phy. Rev. Lett. **98**, 188304 (2007).

[116] E. Runge and E. Gross, Phy. Rev. Lett. **52**, 997 (1984).

[117] B. Schmittmann and R. K. P. Zia, in *Phase Transitions and Critical Phenomena*, edited by C. Domb and J. L. Lebowitz (Academic Press, London, 1995), vol. 17.

[118] E. G. Sinaiski and L. I. Zaichik, *Statistcal Microhydynamics* (Wiley-VCH, Weinheim, 2008).

[119] I. Snook, P. Daivis, and T. Kairn, J. Phys.: Condens. Matter **20**, 404211 (2008).

[120] W. Sparreboom, A. van den Berg, and J. Eijkel, New Journal of Physics **12**, 015004 (2010).

[121] H. Spohn, J. Phys. A: Math. Gen. **16**, 4275 (1983).

[122] G. Stegeman, A. C. van Asten, J. C. Kraak, H. Poppe, and R. Tijssen, Anal. Chem. **66**, 1147 (1994).

[123] F. H. Stillinger, J. Chem. Phys. **65**, 3968 (1976).

[124] R. Tijssen, J. P. A. Bleumer, and M. E. Van Kreveld, Journal of Chromatography **260**, 297 (1983).

[125] R. Tijssen, J. Bos, and M. van Kreveld, Anal. Chem. **58**, 3036 (1986).

[126] J. Toro-Mendoza, G. Urbina-Villalba, and M. García-Sucre, Revista Mexicana de Física **52**, 72 (2006).

[127] T. Uneyama, J. Chem. Phys. **126**, 114902 (2007).

[128] M. A. van der Hoef, D. Frenkel, and A. J. Ladd, Phy. Rev. Lett. **67**, 3459 (1991).

[129] E. Velasco, *Física Estadística de Sistemas Complejos: Fases Blandas de la Materia*, Universidad Autonoma de Madrid (2005-06).

[130] J. Vilar and J. Rubi, PNAS **98**, 11081 (2001).

[131] T. Wainwright, B. Alder, and D. Gass, Phy. Rev. A **4**, 233 (1971).

[132] J. Wu, AIChE J. **52**, 1169 (2006).

[133] K. Zahn, J. Méndez-Alcaraz, and G. Maret, Phy. Rev. Lett. **79**, 175 (1997).

[134] M. E.-J. Zewska, Phy. Rev. E **59**, 3182 (1999).

[135] W. Zimmerman (2010), concluding Conference Nano- and Microfluidics.

Acknowlegements

This thesis could not have been accomplished without the help and support of many people around me, to only some of whom I give particular mention here.

The greatest thanks go to Prof. Dr. S. Dietrich for giving me the opportunity to carry out my doctoral studies at his department at the Max-Planck-Institute for Metals Research in Stuttgart.

I would like to thank Prof. Dr. J. Main for kindly accepting to co-referee this thesis.

I am heartily thankful to my direct supervisor, Dr. Markus Rauscher, whose encouragement, guidance and support from the initial to the final level enabled me to develop an understanding of the subject.

I wish to thank my present and former colleagues at Prof. Dietrich's department for the nice atmosphere.

I thank the German Research Foundation for financial support of this work within the priority program "Nano-and Microfluidics".

Outside the physics, I would like to express my personal gratitude to some special friends for their support despite the distance during these last few years and for being there in the most difficult moments, Pedro and Esther. Also especially, I would like to mention my friends of the "Hispanoalemán Stammtisch" for distracting me from physics and for making my stay in Stuttgart easier.

This thesis would not have been possible without the love and unconditional support from my family. My very special gratitude to my father whom I owe everything I am today and who I want to dedicate this thesis.